DYNAMIC BALANCING OF ROTORS SUPPORTED ON FLUID FILM BEARINGS USING FINITE ELEMENT ANALYSIS

SUNIL AHUJA

DYNAMIC BALANCING OF ROTORS SUPPORTED ON FLUID FILM BEARINGS USING FINITE ELEMENT ANALYSIS

BY

© Sunil Ahuja, B. Eng.

A thesis submitted to the School of Graduate Studies in partial fulfillment of the requirements for the degree of Master of Engineering

Faculty of Engineering and Applied Science
Memorial University of Newfoundland

May 1984

St. John's Newfoundland Canada

Author

Sunil Ahuja, B. Eng.

Approved by:
Supervisor

Dr. Anand M. Sharan, Associate Professor
Faculty of Engineering and Applied Science

Internal Examiner

Dr. Michael Booton, Associate Professor
Faculty of Engineering and Applied Science

Dr. Jim L. Lever, Assistant Professor
Faculty of Engineering and Applied Science

External Examiner

Dr. R. B. Bhat, Associate Professor
Department of Mechanical Engineering
Concordia University

ABSTRACT

This thesis presents a comprehensive analysis of a multi-rotor bearing system, that includes realistic end support conditions. It provides a design engineer with the present day technology available in carrying out a balancing analysis. The design is based on minimizing the flexural response, due to mass unbalance.

The model is developed based on the finite element approach which provides a convenient and accurate means of balancing a rotor-bearing system. The model incorporates the effects of translational, and rotational inertia, and gyroscopic moments, using the consistent matrix approach in conjunction with dynamic matrix reduction technique, modal analysis, and least-square balancing technique. The use of matrix reduction technique for determining a equivalent reduced system, provides subsequent saving of both computational time and space on the digital computer. This allows modelling of complex rotor system conveniently, while retaining only those degree of freedom essential to the solution of the problem. The modal analysis used is an effective means of determining the unbalance force response, for systems with unsymmetric stiffness and damping matrices. The least-square method for balancing, is used to include balancing cases where the number of measuring planes exceeds the number of balancing planes. This represents most actual

balancing situations, and allows an increase in the input data, whereby the consequence of a single error in data tends to decrease. The balancing at one speed is usually sufficient to bring the rotor amplitude down over its entire speed range. Further, flexibility in rotor balancing is provided by including the effect of varying the location, and number of balancing planes.

ACKNOWLEDGEMENTS

I would like to thank Dr. Anand M. Sharan for his supervision and encouragement during the period of research. His contribution of time and technical expertise have helped me immensely.

A special word of thanks to Dr. F. A. Aldrich, Dean of Graduate Studies, and Dr. G. R. Peters, Dean of Engineering, at Memorial University, for the opportunity and financial assistance provided during the program.

The VAX. 11/780 computing facilities of Memorial University are acknowledged. And the care and patience taken by Levinia Vatcher in typing this thesis.

To my Parents and Wife

Hira
Kamal
Anshu

TABLE OF CONTENTS

LIST OF FIGURES

LIST OF TABLES

NOMENCLATURE

$[\,]$	matrix
$'$	differentiation with respect to position
$\cdot$	differentiation with respect of time
$\mathbb{H}$	fixed reference frame (XYZ)
$\mathbb{T}$	rotating reference frame (xyz)
$(B,\ \Gamma)$	small angle rotations about (Y, Z)
θ	trial weight addition angle
ϕ_j	j-th complex eigenvector of the original system
ϕ_j^*	j-th complex eigenvector of the transposed system
η_j	j-th modal displacement
Ω	spin speed
$\{\sigma\}$	generalized force vector
$[\mu]$	generalized mass matrix
$[\kappa]$	generalized stiffness matrix
$[\Psi]$	matrix of translation displacement functions; $\phi_i(s)$, i=1,2,3,4
$[\Phi]$	matrix of rotation displacement function: ϕ_i^1 (s), i=1,2,3,4,
ω	speed of rotation of shaft
$\eta_d,\ \zeta_d$	location of disk mass centre relative to $\mathbb{T}$
$\eta(s)\ \zeta(s)$	distributed location of element cross section mass centre relative to $\mathbb{T}$
α	complex influence coefficient
μ	element mass per unit length
ℓ	element length
$\{q\}$	displacement vector relative to $\mathbb{H}^1$

$\{q_c\}\{q_s\}$	unbalance response associated with cos Ωt, sin Ωt[1]
s	axial position along an element
t	time
$[A]$	matrix of complex influence coefficient
$[\bar{A}]$	conjugate of the complex influence coefficient matrix
$[C]$	system damping matrix
$[D]$	dynamical matrix
E_j	forward component of the j-th modal force vector
$\bar{E}_j$	backward component of the j-th modal vector
$\{F\}$	overall exciting force vector
$[G]$	system gyroscopic matrix
$[I]$	identify matrix
$\bar{I}_D$, $\bar{I}_p$	elemental diametral and polar inertia per unit length
$[K]$	system stiffness matrix
$[M]$	system mass matrix
$\bar{P}$	potential energy[1]
$\{Q_c\}$, $\{Q_s\}$	unbalance force associated with cos Ωrt, sin Ωt
R_1, R_2	major and minor diameters of the elliptical response orbital
S_1	Sommerfeld number
T	trial weight
$\bar{T}$	kinetic energy[1]
$[T]$	reduction transformation matrix
$\{U\}$	is a complex vector defining the correction weights

$\bar{U}$	is a complex conjugate of the elements of vector u.
(V, W)	translations in (Y,Z)
{X}	overall displacement vector
M_d, I_D, I_p	disk mass, diametral inertia, and polar inertia
$[M^d]$, $[G^d]$	disk mass, gyroscopic, matrices[1]
$[M^e]$,$[G^e]$,$[K^e]$	elemental mass, gyroscopic, stiffness matrices[1].
$[C^b]$, $[K^b]$	bearing damping and stiffness matrices
$C_{VV}{}^b$, $C_{VW}{}^b$, $C_{WV}{}^b$, $C_{WW}{}^b$	elements of $[C^b]$
$K_{VV}{}^b$, $K_{VW}{}^b$, $K_{WV}{}^b$, $K_{WW}{}^b$	elements of $[K^b]$

[1] Where appropriate the superscripts d, e, b, s refer to disk, element, and bearing respectively, and subscripts T, R, B refer to translational, rotational, and bending respectively.

CHAPTER 1

INTRODUCTION AND LITERATURE SURVEY

1.1 The Unbalance Forces in Rotating Machinery

There has always been a demand for greater power output per unit weight in the design of turbo-machinery. This requires higher operating speeds. One key factor in achieving this objective is the control of vibrations of the rotor as it goes through its critical speeds; others include aeroelastic problems, aerodynamic problems, etc. The need for higher speeds, yet reliable operation, requires that the rotor shaft be considered as a flexible element. Because of this, an accurate dynamic analysis of rotor-bearing systems has to be carried out.

The turbo-machinery can be modelled as several disks mounted on hydrodynamic bearings as shown in Fig. 1.1. The stiffness and damping coefficients of such bearings are speed dependent, hence the analysis is much more involved as compared to systems which are supported on ball bearings, where these coefficients can be considered as isotropic. The response orbitals in case of a ball bearing, are circular; whereas for hydrodynamic bearings, they are elliptical.

Naturally all effort is made to reduce the unbalance response and make the rotor perfectly symmetrical with respect to stiffness and inertia of the system. Unfortunately, there are unbalance forces present in these

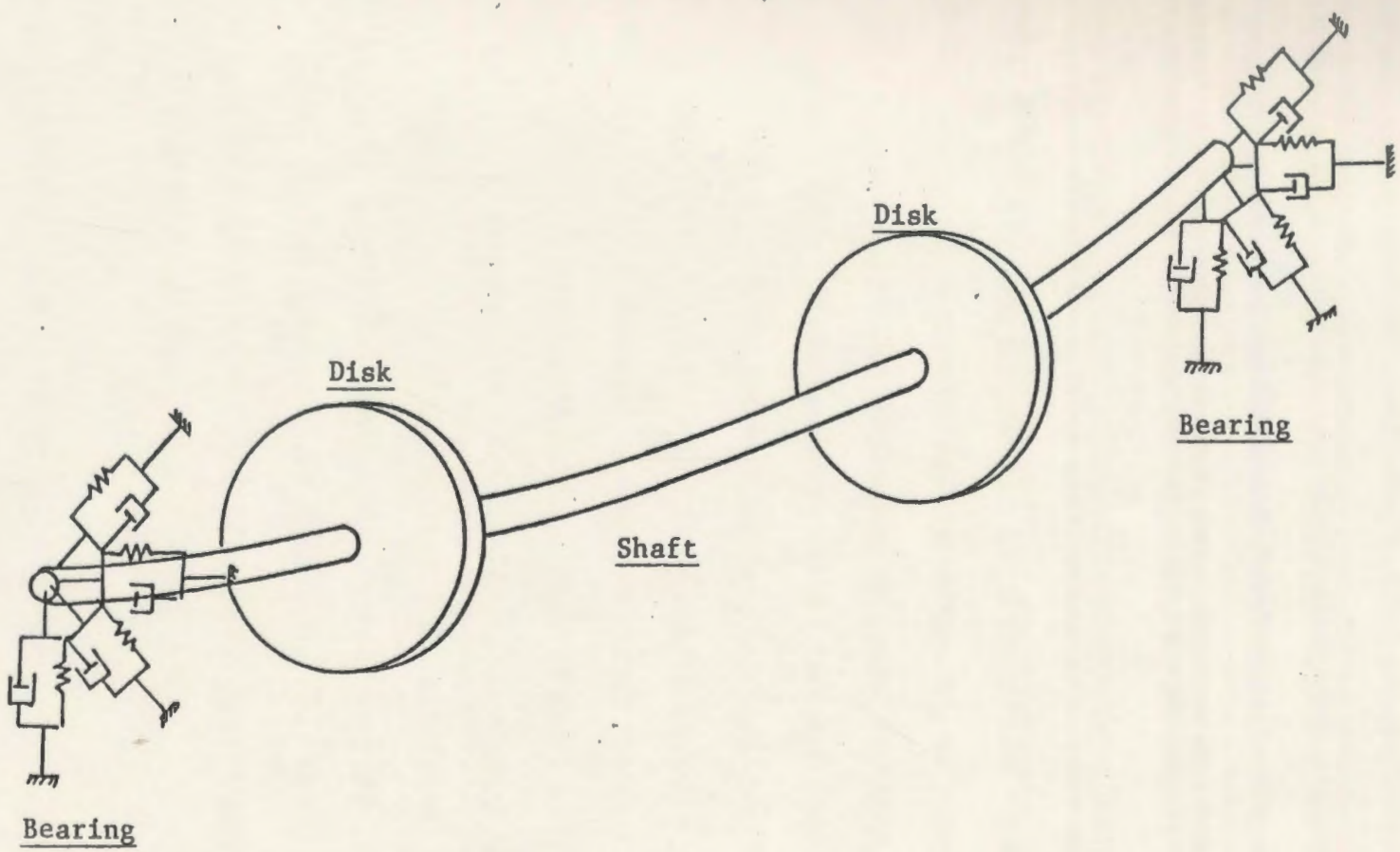

Fig. 1.1 Rotor Supported on Fluid-Film Bearings

Unfortunately, there are unbalance forces present in these systems due to the manufacturing tolerances in various components. The normal machining tolerance for a turbo-machinery is of the order 0.049 μm. These forces are then reduced using dynamic balancing.

Balancing of rotors and rotating systems is an important industrial application of vibration theory. Since any rotating part is a potential source of vibratory force, it is usually necessary to balance rotors designed to run at speeds above 60 rpm. The necessity of balancing every rotor can easily produce a bottleneck in a production line, and therefore production balancing must be done efficiently, if it is to be tolerated from a cost point of view.

In production balancing, the rotor is run in hard bearings, and the unbalance response is reduced by the addition or removal of small correction weights, till a desired response level is reached. The type of balancing technique used, is dependent on the type of rotor. The rotors are generally classified into two categories: (a) a rigid rotor, and (b) a flexible rotor.

1.2 Rigid and Flexible Rotors

Slow speed rotors, operating well below their first critical speed, are categorized as rigid rotors and require only static balancing; for example, crankshaft-drives,

critical speeds, are categorized as flexible rotors which include large compressors and turbine rotors. In such rotors, the existence of forced steady-state response due to the unbalance, can cause deflections of the shaft in the vicinity of the critical speeds (when rotor natural frequencies are equal to the operating speed), which can not be controlled without dynamic balancing. Therefore, in order to balance rotors efficiently, analytical rotor dynamic techniques are necessary.

1.3 Various Considerations in Rotor Dynamics

Since a rotor system is a assembly of several components, a good design of rotor-bearing system requires that all its components be designed with utmost care and precision, and assembled to operate efficiently. The present investigation, which involves dynamic balancing of rotors supported on fluid-film bearings, is a step in this direction.

Any rotor dynamics analysis should involve the following steps:

1. A mathematical modelling of various components of the system, and formulation of dynamic equations of motion.
2. Dynamic response calculations.
3. Control of the vibratory response of the system.

In the following section, a literature survey, on the above

mentioned topics is presented.

1.4 The Literature Survey

There are several methods reported in literature for modelling the rotor-bearing systems. The two commonly used methods are: the transfer matrix method [1-3] and the finite element method [4-6]. Both these methods have been successfully used by Ruhl [5]. He utilized a finite element model of a turbo-rotor system to study the stability and unbalance response. He compared his results with those of Prohl [7] and concluded that the finite element methods are far superior to the transfer matrix method. Ruhl's finite element model included only the elastic bending energy and translational kinetic energy, while the effects of rotary inertia, gyroscopic moments, were not considered. These effects can be quite significant for some configurations as indicated in [8]. Nelson [9] generalized the Ruhl's model by including the effects of rotary inertia, gyroscopic moments and axial loads. The results are given in [9]. They indicate that the model is reliably accurate.

The accuracy of the results, in the case of finite element analysis, is increased by taking smaller sized elements. This approach requires more computer time and storage but yields significantly greater accuracy for a given rotor discretization scheme. Recently, Rouch and Kao [10]

proposed a static condensation technique in rotor dynamics area, in which significant improvement in computer time and core size can be attained while maintaining the basic accuracy and flexibility of the system. This technique yields reasonably accurate results. A dynamic matrix reduction technique, used in structural dynamics area [11] but not yet applied to rotor dynamics area, enables automatic selection of the retained degree of freedom in the condensation scheme. This gives sufficiently accurate results because it ensures that the lower vibrational modes are retained. In this scheme, the diagonal coefficients of mass and stiffness matrices, which can be denoted by [K] and [M] respectively, are scanned, and the degree of freedom i for which K_{ii}/M_{ii} is the smallest, is retained for the condensed system.

1.4.1 Fluid Film Bearing

The influence of the bearing properties [12] has a significant effect on the response of the rotor, and therefore requires careful attention while modelling a rotor-bearing system. This is because of the thin film which separates the moving surface and supports the rotor load. It acts as a spring and provides large damping due to the squeezed film effects. The stiffness and the damping coefficients greatly alter the critical speed and out of balance response of a rotor. The isotropic bearing model

used by many researchers for response calculations, is a vast oversimplification. In fact, an accurate modelling of hydrodynamic bearings should involve both the direct and cross-coupled effects of stiffness and damping respectively.

For such cases even for simple rotors supported on fluid-film bearings, the determination of the critical speeds and the unbalance response, are much more involved. This is because of the asymmetry in the cross-coupled fluid-film stiffness and damping coefficients, which in turn, are dependent on rotor speeds (see Appendix D for the details).

1.4.2 Rotor Response Calculations

There are various techniques reported in literature for determining the unbalance response of rotor-bearing systems. For example Rao [12], Rao, Bhat, and Sankar [13], used a Jeffcott rotor model with identical bearings at the two ends to obtain expressions for the unbalance response of rotors, and the effects of bearing stiffness and damping parameters on the response were studied. Adrayfio and Frohrib [14] analyzed asymmetrically mounted rotor on dissimilar bearings using energy techniques. Rao [15] used transfer matrices to study the rotor response while Nelson and McVaugh [9] used finite element techniques. Lund [16] used Prohl-Myklestad method to calculate the response of rotors. But their investigations did not include the cross-coupled stiffness and damping effects present in fluid film

bearings. Subbiah, Bhat, and Sankar [17] developed equations of motion for a simple rotor supported on dissimilar fluid-film bearings, and solved these equations directly to study the effect of bearing dissimilarity on the rotor response.

A method [17] for calculating the response of a general flexible rotor supported on fluid film bearings is available, which can be said to be the modified modal method. Because of the non-symmetric nature of the problem, the conventional normal mode analysis is not possible. It is therefore necessary to use the biorthogonality relation between the modal vectors of the original system and that of the transposed system, to uncouple the equation of motion. The system response obtained is due to the sum of the response of the individual modes.

Modal analysis has been used in several investigations to study the response of rotors, supported on hydrodynamic bearings. Gunter, Choy and Allaine [18] used the planar modes of undamped rotor systems by ignoring the gyroscopic efects and effects of cross-coupled bearing stiffnesses, to study the critical speeds and the unbalance response of turbo-rotors. Berthier, Ferraris and Lalanne [19] employed the modes of the rotor at rest, for studying the behavior of complex rotors. Lund [3] employed a biorthogional modal analysis to study the behavior of a flexible rotor and Saito and Azuma [20] used this method for

an undamped rotor system. Bhat [21] employed the above modal analysis to study the behavior of a simple rotor without damping. Bhat, Subbiah and Sankar [22] studied a single disk rotor with a shaft of uniform circular cross-section suported on dissimilar hydrodynamic bearings using a lumped mass analysis but did not consider the gyroscopic effects.

1.4.3 Flexible Rotor Balancing

Flexible rotor balancing, is significantly more complex than rigid-rotor balancing. In the latter case, the rotor never changes shape, whereas a flexible rotor continually changes its configuration, as more critical speeds are encountered. Also, because a flexible rotor changes its mode shape with speed, it is apparent that a condition of best balance at one specific speed may not represent the best balance condition over a range of speeds. The rotors, if balanced, for the first three critical speeds, are also balanced for higher speeds for all practical purposes.

In balancing flexible rotors, it is a common practice to balance by the component method [1], whereby every component is individually balanced on mandrels, and assembly balanced with the addition of each component on to the shaft. Before balancing the rotor for critical speed, the rotor is run at half its lowest critical speed, until the temperature in all its components is stabilized and the

unbalance results are repeatable. This is because, as the speed of rotation approaches the lowest natural frequency of transverse vibration for the system, the bending effect, due to the unbalanced rotating inertial forces, increases dramatically. After the stabilization stage, the rotor is then run in a suitable hard bearing balancing machine to a safe speed approaching the first critical and the unbalance response is recorded at particular points along the length of the rotor, for a series of desired speeds. The results constitute the data for the uncorrected rotor, and it is these vibrational amplitudes which should be reduced to a minimum, by inserting small masses or removing masses in the balancing planes, depending on the balancing process being utilized.

The balancing process for flexible rotors involves determining the balance mass magnitudes, the angular location in the planes of rotation, and the axial locations of the plane of rotation, in which the balance masses are applied.

The various techniques which have been developd can be broadly grouped into essentially two different but not contradictory schools of thought. These methods are: the modal method [1], and the influence coefficient method [23].

1.3.4.1 The Modal Balancing Method

The balancing problem has been approached in two different ways, by those who consider the rotor as a series

of point masses, and those who treat the rotor as a continious elastic body. The treatment of the rotor as a continuum has led to the modal concept pioneered by Bishop and Parkinson [24]. In this method, the rotor response is expressed as a power series function of the system undamped eigenvalues. Bishop shows that the general unbalance distribution may be expressed in terms of modal unbalance eccentricities. The rotor amplitude near a critical speed is thus primarily affected by the particular modal unbalance distribution while the higher order modes have little influence on the lower critical speed response. They then postulate that it should be balanced mode by mode by placing proper weights at the antinodes.

In its simple form, modal balancing relies on the critical speeds being well separated from each other, and the response lightly damped, so that at any critical speed, one modal component of reponse is dominant. Since the effect of support asymmetry usually causes fairly small separations of critical speeds, two being formed where only one existed for the axi-symmetric system. However, due to the complexities involved in obtaining the normal modes, this method has not been found to be too practical [1].

1.3.4.2 The Influence Coefficient Method

In the influence coefficient method [1], the unbalance response in the measuring planes are corrected by

placing suitable weights in the balancing planes. At first, the unbalance reponse in the measuring planes, is found by running the rotor at a given speed without any correction weights in the balancing planes. A correction weight is applied in one of the balancing planes and its net vectorial response in all the measuring planes, is evaluated. This process is repeated by applying this correction weight in other balancing planes. In this way, the influence coefficients matrix is established. The required correction weight vector is obtained by multiplying the inverse of the influence coefficient matrix with the unbalance response vector.

If the number of balancing planes available are less than the number of measuring planes then one should use the least-square balancing method [25]. In this method, the response in the measuring planes, are minimized by suitable evaluation of the weights in the balancing planes. An excellent discussion about both of these methods are given in [26-28].

1.5 The Objectives of the Investigation

Based on the literature survey, the following are the objectives of the present investigation:

1. The finite element modelling of the multi-rotor system supported by fluid-film bearings which have direct and

cross-coupled stiffness and damping respectively.

2. Dynamic response calculation of the rotor due to the unbalance forces, using a dynamic reduction technique, and modal analysis.
3. The balancing of the multi-rotor system using least-square method.
4. The study of the balancing process by varying the location and the number of the balancing planes.

In this thesis, the finite element formulation of the system dynamics is carried out first. The mathematical model includes effects of translational as well as rotational inertia, and gyroscopic moments, using the consistent matrix approach. The formulation of the problem is presented in a fixed frame of reference. The bearings utilized in the model, are non-isotropic involving coupled linear stiffness and damping coefficients. A dynamic reduction procedure is utilized whereby the size of the system matrices are reduced. The response is then determined using the biorthogonal modal method for unsymmetrical damping and stiffness matrices. The balancing is carried out using the least-square method. The system is balanced exactly at the critical speed whereas in actual practice, the balance runs are carried out at several speeds around the critical.

In Chapter 2, the dynamic equations of motion of the system have been formulated using the finite element

analysis. Then, a dynamic reduction technique has been used to reduce the system matrices The response is determined using biorthogonal modal analysis. The mathematical expression for the influence coefficient matrix is derived, and the least-square method is discussed.

In Chapter 3, the computer programme for the dynamic analysis is tested by calculating the natural frequencies of a hinged-hinged beam and comparing these with the exact solution. The number of retained coordinates in the matrix reduction process is established by comparing the natural frequencies and the response of the original system with those of the reduced system. The advantage of balancing at the criticals over balancing at various speeds around the criticals, is discussed. The effect of the variation of the number and the location of the balancing planes is analyzed.

Finally, the conclusions and recommendations for future work are given in Chapter 4.

CHAPTER 2

THE ROTOR BEARING SYSTEM AND ITS MATHEMATICAL MODEL

2.1 Introduction

Design and balancing of rotor system depends on its dynamic characteristics. The smooth operation of a rotor is directly related to the dynamic flexural response, influenced by the mass unbalance. The objective of the present work is to calculate the response of the system due to the mass unbalance, and to correct its flexural response.

A step in achieving this objective is to formulate an accurate mathematical model, of rotors supported on fluid-film bearings.

2.2 System Configuration and Coordinates

In modelling a rotor bearing system, important consideration must be given to the set of reference axes utilized to describe its motion. A typical rotor-bearing system is illustrated in Fig. 2.1. This motion studied can be in a rotating or a fixed frame of reference. The rotating frame is particularly useful, when analyzing systems with isotropic bearings. In this case the motion in two normal planes can be treated separately. The fixed frame provides the generality of handling problems with non-symmetric bearing stiffness, and damping effects. The only

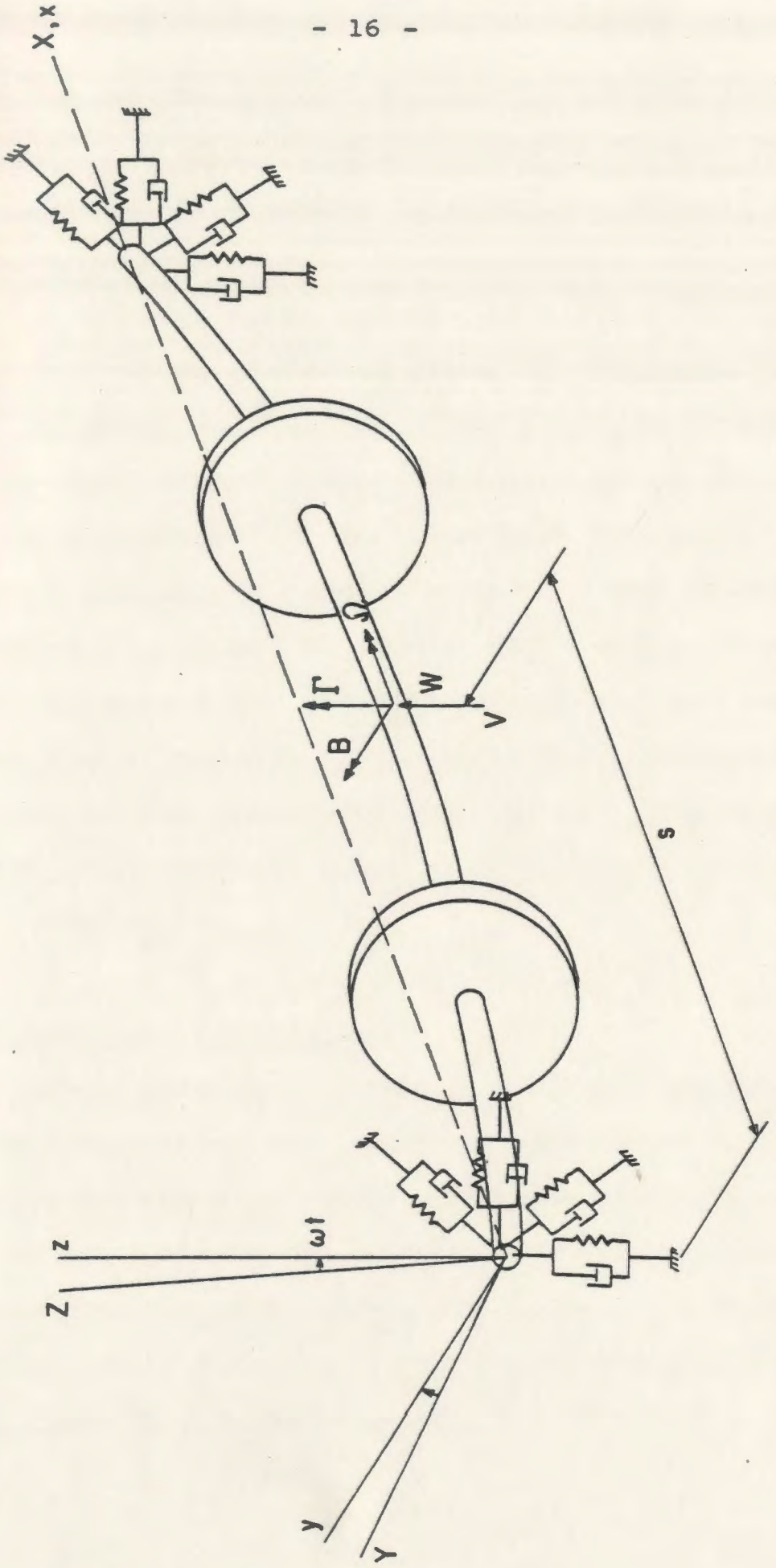

Fig. 2.1 System Configuration and Coordinates.

disadvantage of the fixed frame finite element formulation is that the order of the system matrices is large. This disadvantage can be overcome by using the dynamic matrix reduction technique.

A typical cross section of a rotor in its deformed state as defined in the fixed frame of reference system (XYZ:Ⅲ), is shown in Fig. 2.1. The triad is fixed with the x axis coinciding with X. The cross-section of the element, located at a distance (s) from the left end point, translates and rotates during the general motion of the element. The translations V(s,t) and W(s,t) in the Y and Z directions respectively locate the elastic centerline, and small angle rotations B(s,t) and Γ(s,t) respectively, represents the orientation of the cross-sectional plane. The cross-section also spins at a constant speed ω about the X axis defined by (x,y,z: T) triad.

2.3 Mathematical Formulation

This section is divided into four subsections. In the first subsection, the component equations of a rotor-bearing system are formulated using the finite element method, which includes the effects of translational, and rotational inertia, and gyroscopic moments using the consistent matrix approach. The second subsection deals with a dynamic matrix reduction technique. The third subsection

presents a modified modal analysis method to determine the system. Finally, in the fourth subsection, the mass unbalance response is reduced, using the least-square balancing technique.

2.3.1 Component Equations of a Rotor Bearing System

The rotor bearing system is comprised of a set of interconnecting components, consisting of uniform rotor segments with rigid disks, and fluid film bearings.

The shaft portion of the rotor is modelled as beam elements, by specifying spatial shape functions, and then treating the rotor element as a integration of a infinite set of differential disks. A typical rotor element is shown in Fig. 2.2. The cross-sectional displacements within the element are defined relative to a fixed frame of reference , by translations V(s,t) and W(s,t) and rotation B(s,t) and Γ(s,t). The finite rotor element coordinates are indicated by eight degree of freedom (q_1^e, q_2^e,...., q_8^e), four at each end, with two for translation, and two for rotation.

The rigid disks representing the impellers, coupling, flywheels, are convieniently described by a single plane, with only four degrees of freedom, two for translation and two for rotation.

The equation of motion for the elements are derived, by writing the expressions for kinetic and potential energy, of the components. The kinetic energy consists

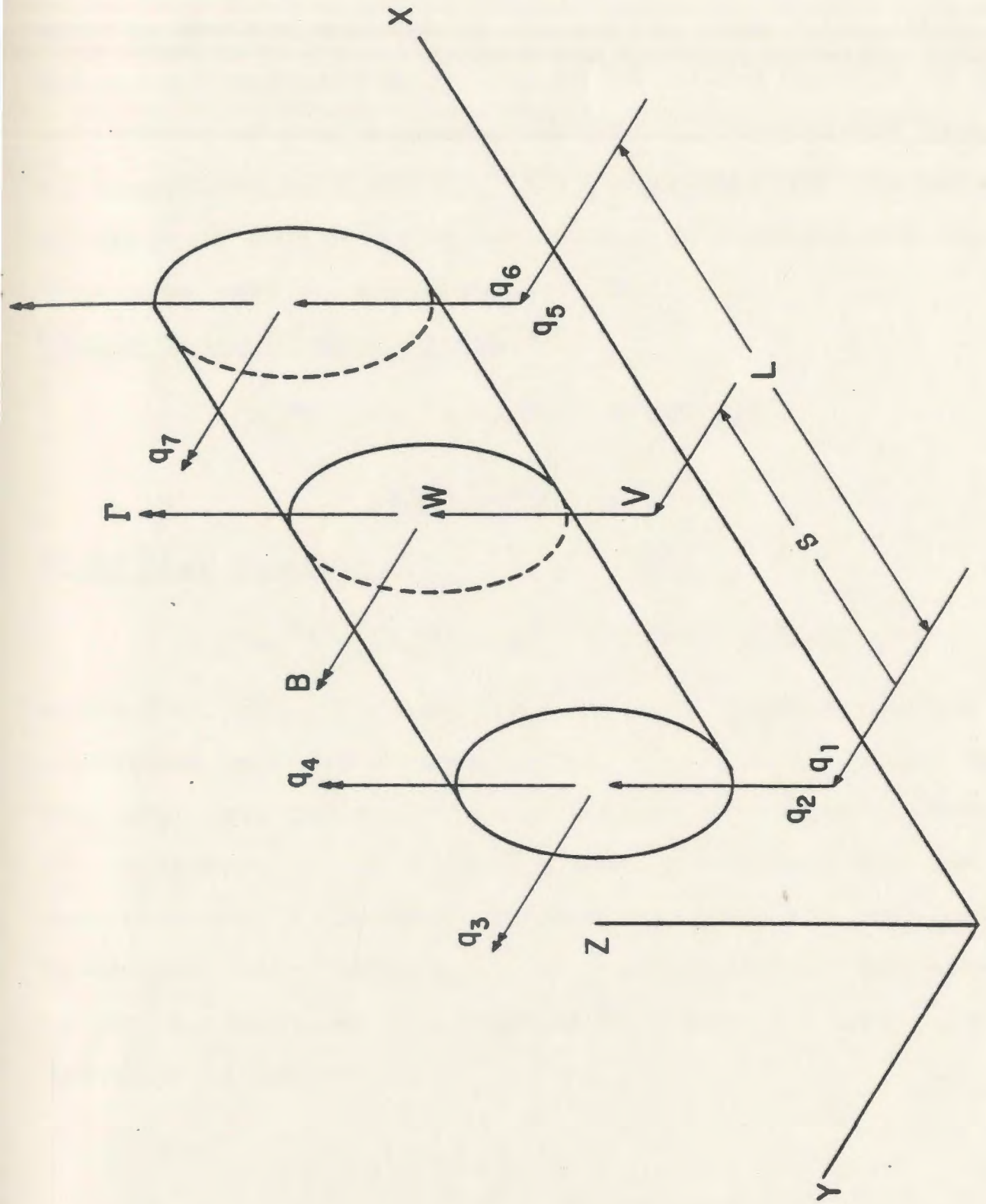

Fig. 2.2 Typical finite rotor element and coordinates.

of both translational and rotational modes. The rotation terms also include gyroscopic effects associated with the spinning of the shaft. The potential energy consists of the elastic bending effects of the shaft. The formulation is based on Timoshenko beam theory [30]. The details of the derivation of the component equation of motion are provided in Appendices A, B and C. The expressions for the matrix equation of motion using Lagrange's formulation for the rotors as well as the disks are [9]:

Finite Rotor Element Equations

$$([M_T^e] + [M_R^e])\ \{\ddot{q}^e\} - \omega[G^e]\ \{\dot{q}^e\} + [K_B^e]\ \{q^e\} = \{Q^e\} \tag{2.2}$$

Rigid Disk Equation

$$([M_T^d] + [M_R^d])\ \{\ddot{q}^d\} - \omega\ [G^d]\ \{\dot{q}^d\} = \{Q^d\} \tag{2.3}$$

where [M], [G], [K] represent the mass gyroscopic, and stiffness matrices respectively. The vector {Q} and {q} are the unbalance force and the displacement vector respectively. The subscripts d, e, refer to disk and element and the subscripts B, T, R refer to bending, translational, and rotational modes respectively. The details of the element matrix formulation is presented in Appendix A and elemental matrices in Appendix B.

Since an accurate representation of a bearing, which supports the rotor is just as critical to the system model as the rotor itself, the bearing properties are modelled using experimental results carried out by Lund [29].

Bearing Equation

The dynamic equation of motion of the bearings, in the fixed frame coordinates as shown in Fig. 2.3, can be written as [9]

$$[C^b]\ \{\dot{q}^b\} + [K^b]\ \{q^b\} = \{Q^b\} \tag{2.4}$$

in fixed frame coordinates, where

$$\{q^b\} = \begin{Bmatrix} V \\ W \end{Bmatrix}, \tag{2.4a}$$

$$[K^b] = \begin{bmatrix} K_{VV}{}^b & K_{VW}{}^b \\ K_{WV}{}^b & K_{WW}{}^b \end{bmatrix}, \tag{2.4b}$$

$$[C^b] = \begin{bmatrix} C_{VV}{}^b & C_{VW}{}^b \\ C_{WV}{}^b & C_{WW}{}^b \end{bmatrix}. \tag{2.4c}$$

In Eqn. (2.4), $\{Q^b\}$ represents the external force vector applied on the bearings. The elements of the stiffness and damping coefficient matrix are considered to be nonlinear. These matrices contain cross-coupling terms representing a non-isotropic bearing with the principle coupled axes oriented at (45°, -45°) to the normal z-axis.

The bearing coefficient curves for a plain cylindrical bearing as analytically obtained by Lund [29]

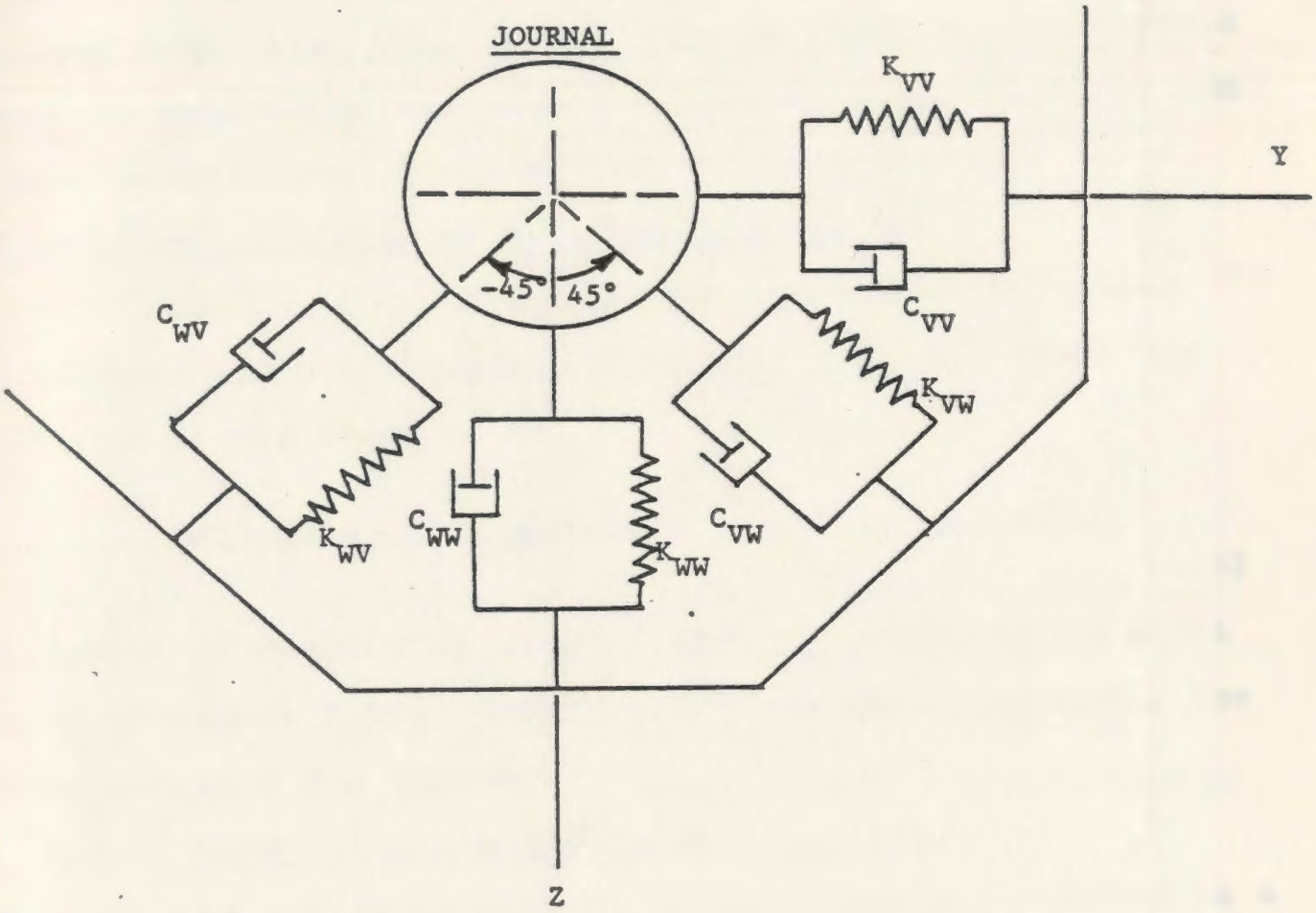

Fig. 2.3 Journal Bearing Stiffness and Damping Coefficients

are given in Appendix D. The curves represent the normal and cross-coupled bearing coefficients for different speed dependent Sommerfeld numbers.

The stiffness and the damping coefficients are obtained from Figs. D-1, to D-2. To do this, the Sommerfeld number is calculated and then the correspondng stiffness and damping coefficients are obtained by interpolation.

The Equation of Motion of the Complete System

The equation of motion for the assembled damped system consisting of components equations (2.2), (2.3) and (2.4), is of the form

$$[M]\{\ddot{q}\} - \omega[G]\{\dot{q}\} + [C]\{\dot{q}\} + [K]\{q\} = \{Q\} \quad \ldots\ldots (2.5)$$

The number of degrees of freedom in Eqn. (2.5) can be quite large, therefore before carrying out the modal analysis, the system matrices are reduced.

2.3.2 Dynamic Matrix Reduction Technique

The reduction process is most simply described as a transformation, relating condensed degree of freedom in terms of retained ones. The computation of the transformation matrix, can proceed by a number of approaches. The most straight forward approach is to minimize the potential energy of the deformed structure, ignoring inertial effects and forces on the condensed degree of freedom, thereby, retaining the lower modes for controlling the vibrations through the

critical speeds. This is done by defining a transformation matrix [T], and writing the relation [11]

$$\{q\}_{nx1} = \begin{Bmatrix} \{q_m\} \\ \{q_s\} \end{Bmatrix}_{nx1} = [T]_{nxm}\ \{q_m\}_{mx1}, \qquad (2.6)$$

where,

$$[T] = \begin{bmatrix} [I] \\ [K_{ss}]^{-1}\ [K_{ms}]^T \end{bmatrix} \qquad (2.6a)$$

The submatrices $[K_{ss}]$ and $[K_{ms}]$ are obtained by partitioning the stiffness matrix [K] in Eqn. (2.5) which can be written as

$$[K]_{nxn} = \left[\begin{array}{c|c} [K_{mm}] & [K_{ms}] \\ \hline [K_{ms}]^T & [K_{ss}] \end{array}\right] \qquad (2.7)$$

In Eqn. (2.6) 'm' refers to the number of master degrees of freedom, and 's' to the slaves. The master degree of freedom are retained, whereas the slaves are removed. Using this transformation matrix, the condensed matrix equation can be written as

$$[M_m]_{mxm}\{\ddot{q}_m(t)\} - \Omega[G_m]_{mxm}\{\dot{q}_m(t)\}_{mx1} + [C_m]_{mxm}$$
$$\{\dot{q}_m(t)\}_{mx1} + [K_m]_{mxm}\{q_m(t)\}_{mx1} = \{Q_m(t)\}_{mx1} \qquad \ldots. (2.8)$$

where the condensed matrices are also symmetrical and given by

$$[M_m]_{mxm} = [T]^T\ [M]_{nxn}\ [T], \qquad (2.8a)$$

$$[K_m]_{mxm} = [T]^T[K]_{nxn}[T], \tag{2.8b}$$

$$[G_m]_{mxm} = [T]^T[G]_{nxn}[T], \tag{2.8c}$$

$$[C_m]_{mxm} = [T]^T[C]_{nxn}[T], \tag{2.8d}$$

$$\text{and} \qquad \{Q_m(t)\}_{mx1} = [T]^T\{Q\}_{nx1}. \tag{2.8e}$$

The disadvantage of using the condensed set of matrices is that the eigenvalues of the condensed system as represented by Eqn. (2.8) are higher than that of the original system because of the imposed constraints. The selection of master and slave degree of freedom is automated so as to ensure that the lower modes are retained, as the masters. The diagonal coefficients of [K] and [M] are scanned, and the degree of freedom i for which K_{ii}/M_{ii} is the smallest, is selected as the first order, and the rows and columns of the system matrices are rearranged accordingly. This is repeated, till the system matrices are arranged in a ascending manner, based on the K_{ii}/M_{ii} ratio of the diagonal elements.

2.3.3 Modal Response Analysis

The modal analysis [22] of the condensed system can then be carried out, after rearranging Eqn. (2.8), into a system of first order differential equation of the form

$$\bar{[M]}\ \dot{\{x(t)\}} + \bar{[K]}\ \{x(t)\} = \bar{\{F\}}, \tag{2.9}$$

where,

$$\bar{[M]} = \begin{bmatrix} [0] & [M_m] \\ [M_m] & (-\Omega[G_m] + [C_m]) \end{bmatrix} \qquad (2.9a)$$

$$\bar{[K]} = \begin{bmatrix} -[M_m] & [0] \\ [0] & [K_m] \end{bmatrix} \qquad (2.9b)$$

$$\bar{\{F\}} = \begin{Bmatrix} \{0\} \\ \{Q_m\} \end{Bmatrix} \qquad (2.9c)$$

$$\dot{\{X(t)\}} = \begin{Bmatrix} \ddot{\{q_m(t)\}} \\ \dot{\{q_m(t)\}} \end{Bmatrix}, \text{ and } \{X(t)\} = \begin{Bmatrix} \dot{\{q_m(t)\}} \\ \{q_m(t)\} \end{Bmatrix} \qquad (2.9d)$$

The damped natural frequencies of the system are then obtained, by finding the eigenvalues of the dynamical matrix [D] which is given by

$$[D] = \bar{[M]}^{-1} \bar{[K]} \qquad (2.9e)$$

The solution of Eqn. (2.9) is assumed in the form,

$$\{X(t)\} = [\phi] \{\eta(t)\} \qquad (2.10)$$

where $[\phi]$ contains the eigenvectors of the reduced system represented by Eqn. (2.9). Introducing Eqn. (2.10) into Eqn. (2.9) and premultiplying the result by $[\phi^*]^T$, which is the transpose of the eigenvectors of the transposed system leads to the following:

$$[\phi^*]^T \bar{[M]} [\phi] \dot{\{\eta(t)\}} + [\phi^*]^T \bar{[K]} [\phi] \{\eta(t)\} = [\phi^*]^T \bar{\{F\}} \qquad \ldots\ (2.11)$$

representing the dynamics of the system in the normal coordinates. Because of non-symmetric nature of the stiffness and damping matrices, a conventional normal mode analysis is not possible, where $[\phi]^T$ is used instead of $[\phi^*]^T$. Eqn. (2.11) can be rewritten as

$$[\mu^*]\ \{\dot{\eta}(t)\} + [\kappa^*]\ \{\eta(t)\} = \{\sigma\} \qquad (2.12)$$

where $[\mu^*]$ and $[\kappa^*]$ are diagonal matrices respectively. The steady state solution for Eqn. (2.12) can be written as [22]

$$\eta_i(t) = N_i \exp(j\omega t) + \bar{N}_i \exp(-j\omega t) \qquad (2.13)$$

and

$$\sigma_i(t) = E_i \exp(j\omega t) + \bar{E}_i \exp(-j\omega t) \quad i=1,2,\ldots,2m \qquad \ldots. (2.14)$$

Substitution of Eqn. (2.13) and (2.14) into Eqn. (2.12) leads to

$$(\kappa_i + j\omega\mu_i)\ N_i \exp(j\omega t) + (\kappa_i - j\omega\mu_i)\ \bar{N}_i \exp(-j\omega t)$$

$$= E_i \exp(j\omega t) + \bar{E}_i \exp(-j\omega t) \qquad (2.15)$$

Equating coefficients of forward and backward whirl, one can write,

$$N_i = \frac{E_i}{(\kappa_i + j\omega\mu_i)} \text{ and } \bar{N}_i = \frac{\bar{E}_i}{(\kappa_i - i\omega\mu_i)} \qquad (2.16)$$

where E_i and $\bar{E}_i$ represent the forces due to mass unbalance in

the normal coordinates.

Eqn. (2.12) can be solved on a mode by mode basis and Eqn. (2.10) can be used to obtain {X}. The nodal displacements, which represent the elements of the vector $\{q_m\}$, are obtained using Eqn. (2.9d) by taking the real part of the lower submatrix of the vector {X}. The displacement vector {q} is obtained using Eqn. (2.6).

2.3.4 The elliptical Response Orbital

The dynamic response of the system is studied by calculating the major diameter of the elliptical orbit [1]. Combining Eqns. (2.10) and (2.13), one can write,

$$X_i(t)=\phi_{i,j_1} N_{j_1} \exp(j\omega_{j_1} t)+\phi_{i,j_1} \bar{N}_{j_i} \exp(-j\omega_{j_1} t) \qquad \begin{matrix} i = 1,2,\ldots,2n \\ j_1= 1,2\ldots,2n \end{matrix} \qquad (2.17)$$

Eqn. (2.17) can be written as

$$X_i(t) = N_i^* \exp(j\omega_{j_1} t) + \bar{N}_i^* \exp(-j\omega_{j_1} t) \qquad (2.18)$$

where,

$$N_i^* = \phi_{i,j_1} N_{j_1} \text{ and } \bar{N}_i^* = \phi_{i,j_1} \bar{N}_{j_1} \qquad (2.18a)$$

In the displacement vector {X}, the arrangement of the nodal degree of freedom are such that the two translational motions are followed by two rotational motions. For example if i represents the motion along the first translational

direction, then i+1 would represent the motion in the next translational direction. The combined motion in the ith and i+1th direction, would be planar motion. Expressing Eqn. (2.18) for the i+1th direction, the corresponding equation can be written as

$$X_{i+1} = N^*_{i+1}\exp(j\omega_{j_1} t) + \bar{N}^*_{i+1} \exp(-j\omega_{j_1} t) \qquad (2.19)$$

Eqn. (2.18a) and (2.19) can be written in simplified form as

$$X_i = (N^*_i + \bar{N}^*_i)\cos \omega_{j_1} t + j(N^*_i - \bar{N}^*_i)\sin \omega_{j_1} t \qquad (2.20a)$$

$$X_{i+1} = (N^*_{i+1} + \bar{N}^*_{i+1})\cos \omega_{j_1} t + j(N^*_{i+1} - \bar{N}^*_{i+1})\sin \omega_{j_1} t \qquad (2.20b)$$

taking the real part of the coefficients of Eqn. (2.20), one can write

$$\bar{W}_1 = v_1 \cos \omega_{j_1} t + v_2 \sin \omega_{j_1} t \text{ , and}$$

$$\bar{W}_2 = w_1 \cos \omega_{j_1} t + w_2 \sin \omega_{j_1} t \qquad (2.21)$$

where the coefficients v_1, v_2, w_1 and w_2 are defined by the real and imaginary functions

$$v_1 = \text{Real } (N^*_i + \bar{N}^*_i) \qquad (2.21a)$$

$$v_2 = \text{Imag } (-N^*_i + \bar{N}^*_i) \qquad (2.21b)$$

$$w_1 = \text{Real } (N^*_{i+1} + \bar{N}^*_{i+1}) \qquad (2.21c)$$

$$w_2 = \text{Imag}\ (-N^{*}_{i+1} + \bar{N}_{i+1}) \qquad (2.21d)$$

The radius vector of the elliptical orbit can be expressed as

$$r = \sqrt{\bar{W}_1^{\,2} + \bar{W}_2^{\,2}} \qquad (2.22)$$

The radius vector r is maximum or minimum, when

$$\frac{d}{d(\omega_{j_1} t)} (r) = 0 \qquad (2.23)$$

Combining Eqns. (2.21), (2.22), and (2.23), an expression for the major or minor diameter of the ellipitical orbit shown in Fig. 2.4, can be writen as

$$R_1, R_2 = \left[\frac{1}{2}\{v_1^{\,2}+v_2^{\,2}+w_1^{\,2}+w_2^{\,2} \pm (v_1^{\,2}+v_2^{\,2}-w_1^{\,2}-w_2^{\,2})^2 + 4(v_1 w_1 + w_2 v_2)^2\}^{1/2}\right]^{1/2} \qquad (2.24)$$

The (+) sign is used for the major diameter R_1, and (-) sign for the minor diameter R_2. The angle made by the major axis with respect to the real axis is given by [32, 33]

$$\delta = \omega_{j_1} t + \alpha^{+}$$

where

$$\tan 2\omega_{j_1} t = \frac{2(v_1 v_2 + w_1 w_2)}{v_1^{\,2} - v_2^{\,2} + v_1^{\,2} - v_2^{\,2}}$$

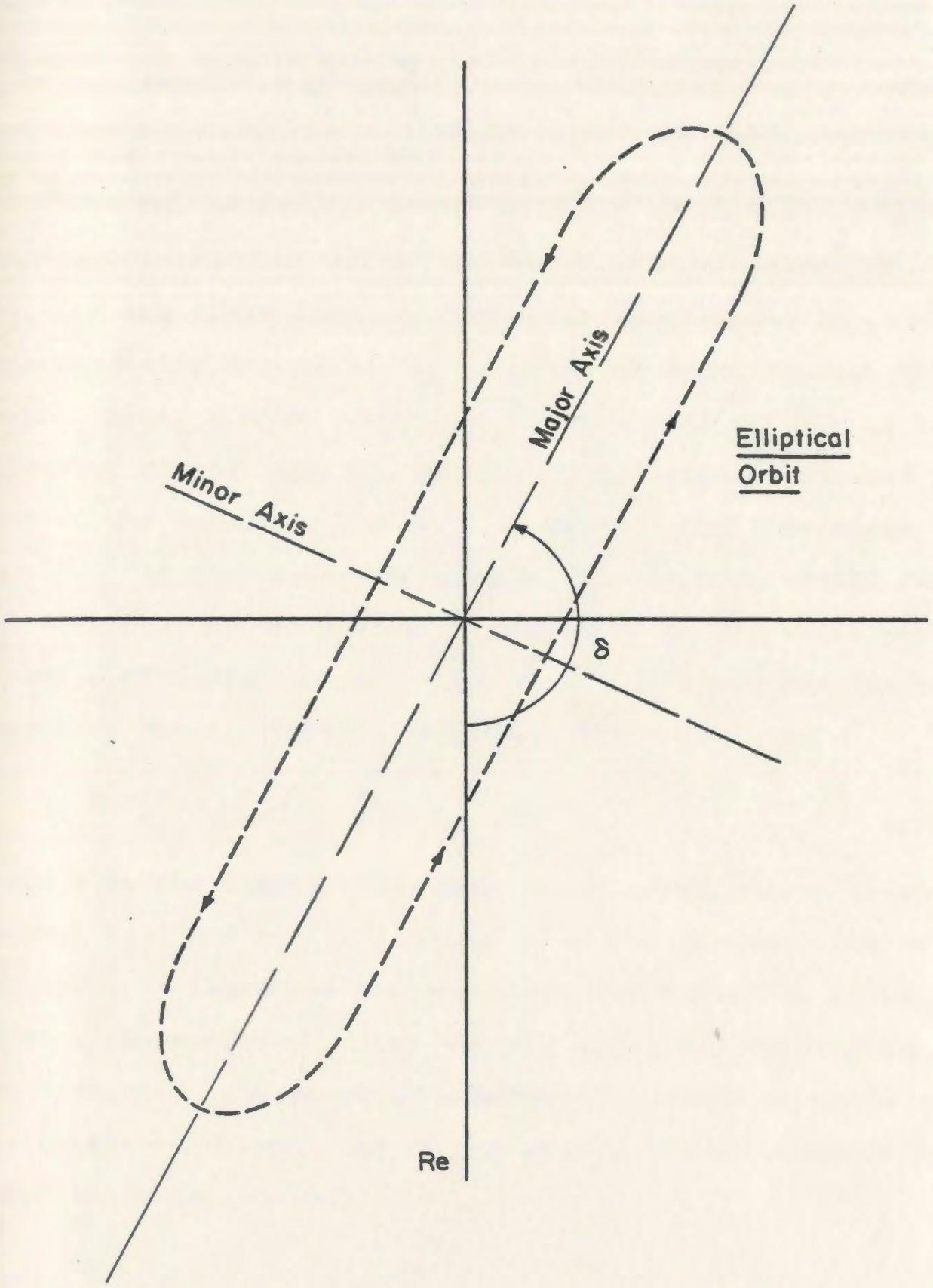

Fig. 2.4 Elliptical response orbital relationship.

and

$$\tan 2\alpha^{+} = \frac{v_1 - w_2}{w_1 + v_2} \tag{2.25}$$

2.3.5 Least Square Balancing

The magnitude of the elements of the vector thus obtained, is reduced using the least square method [27, 33, 34]. As the first step, the first critical speed is experimentally determined by running the rotor through this speed. Next, a known trial weight is placed in each of the balancing planes, and the resulting vibration calculated at each of the measuring planes. By subtracting from these results, the corresponding results for the uncorrected rotor, and dividing the difference by the value of the trial weight, a series of influence coefficients are obtained one for each measuring plane. This is mathematically writen as

$$\alpha_{ij} = \frac{R_{ij} - R_{io}}{T_j} \tag{2.26}$$

where α is the complex influence coefficient; T the trial weight; R_{ij} and R_{io} the elements of the response vector {R} and i, j represent the measuring and balancing plane numbers respectively. Once all the influence coefficients are evaluated, the correction weights required to minimize the unbalance vibrational of the rotor, can be computed by using the relation [25]

$$\{R\}_{qx1} = [A]_{qxp} \{U\}_{px1} \qquad (2.27)$$

where [A] is the influence matrix coefficient whose elements are α_{ij}, {U} is a complex vector defining the correction weights angle and the subscripts q and p represent the available number of measuring and balancing planes respectively.

In exact point method [28], the number of balancing planes are equal to the number of measuring planes i.e. p=q. The least-square method although based on the same principles, permits the condition where the number of measuring planes can exceed the number of balancing planes. This allows an increase in the input data (more measuring planes than balancing planes), whereby the consequence of a single error in the data tend to decrease. The analytical procedure for the least-square method is given in [23, 33, 34].

In general case, where the number of measuring planes exceed the number of balancing planes, the unbalance is reduced by minimizing the square of the residual amplitudes. Expressing the sums of the squares of the residual amplitudes as S one can write,

$$S = \sum_{i=1}^{q} |R_i|^2 = \sum_{i=1}^{q} \underline{R}_i, \bar{\underline{R}}_i. \quad i=1,2,\ldots,n \qquad (2.28)$$

where $\bar{\underline{R}}_i$ is the complex conjugate of $\underline{R}_1$

S is minimized by

$$\frac{\partial S}{\partial \bar{U}_j} = 0 \quad (j = 1, \ldots. p) \qquad (2.29)$$

where $\bar{U}_j$ is a complex conjugate of the elements of the vector {U} and the differentiation is partial.

Substitution of Eqn. (2.28) into Eqn. (2.29) and making use of the relation

$$\{R\} = \{R_o\} + [A]\{U\} \qquad (2.30)$$

where {R} represents the residual response after the correction weight has been applied and $\{R_o\}$ the initial unbalance response.

$$\frac{\partial S}{\partial \bar{U}_j} = \sum_{i=1}^{n} R_i \cdot \frac{\partial \bar{R}_i}{\partial \bar{U}_j} = \sum_{i=1}^{n} R_i \cdot \bar{\alpha}_{ij} = 0 \quad (i=1,\ldots p)$$

.... (2.31)

or by inserting Eqn. (2.30)

$$\sum_{i=1}^{n} \bar{\alpha}_{ij}\left(R_{io} + \sum_{k=1}^{P} \alpha_{ik} \cdot U_k\right) = 0 \quad (j=i, \ldots p)$$

.... (2.32)

which can be written in matrix form as

$$\bar{[A]}^T [A] \{U\} = -\bar{[A]}^T \{R_o\} \qquad (2.33)$$

where $\bar{[A]}^T$ is a conjugate transpose of [A]. This equation can be solved directly to give [33]

$$\{U\} = -[[\bar{A}]^T [A]]^{-1} \cdot [\bar{A}]^T \cdot \{R_o\} \qquad (2.34)$$

The final equation yields that particular combination of correction weights which minimizes the residual vibration of the rotor in the least-square sense.

2.3.5.1 Formulation of the trial weight rotor addition

The trial weight is identified in a balancing plane by its magnitude m, eccentricity ρ and phase angle θ relative to the uniformly rotating reference axis y, z as shown in Fig. 2.5. The addition of the trial weight to the forcing function is as follows:

$$F_y = (m\rho\omega^2) \sin(\omega t + \theta), \text{ and} \qquad (2.35)$$

$$F_z = (m\rho\omega^2) \cos(\omega t + \theta). \qquad (2.36)$$

Expanding Eqns. (2.35) and (2.36), one obtains

$$F_y = (m\rho\omega^2 \sin\theta) \cos\omega t + (-m\rho\omega^2 \cos\theta) \sin\omega t \qquad ....(2.37)$$

$$F_z = (m\rho\omega^2 \cos\theta) \cos\omega t + (m\rho\omega^2 \sin\theta) \sin\omega t \qquad ....(2.38)$$

Rewriting these equations in vector from

$$\{Q^s\} = \{Q_c{}^s\} \cos\omega t + \{Q_s{}^s\} \sin\omega t \qquad (2.39)$$

Eqn. (2.39) is same as the unbalance forcing function represented by Eqn. (A.14) (given in Appendix A). Eqn. (2.39) can be transformed into modal form as

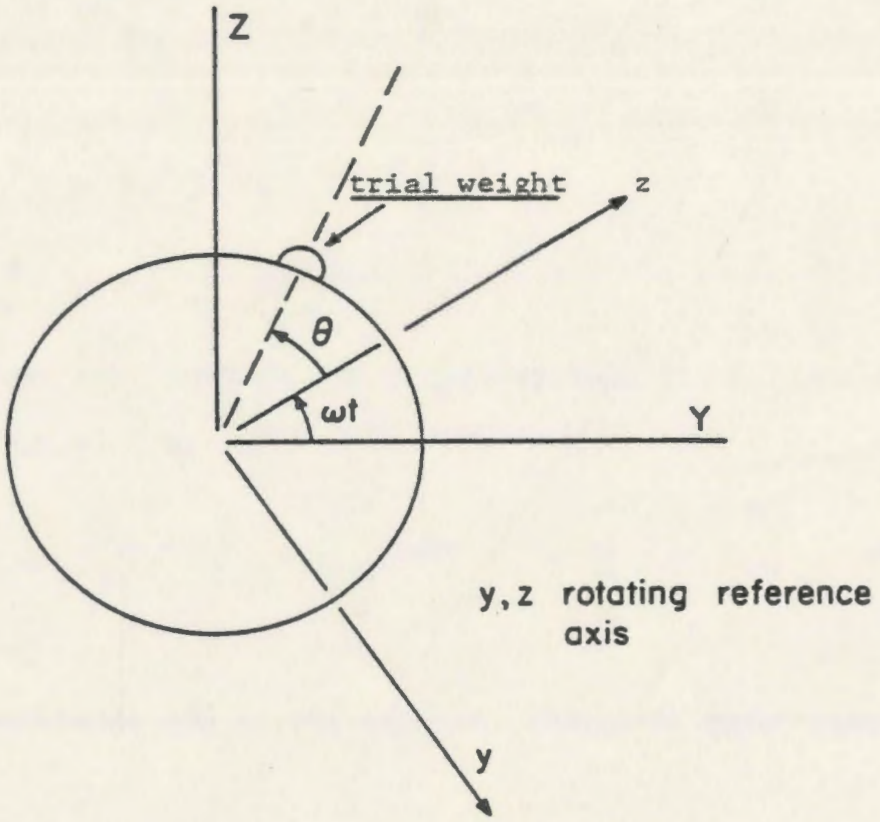

Fig. 2.5 Trial weight addition.

$$\{F\} = [\phi^*]^T \{Q_c^s\} \cos \omega t + [\phi^*]^T \{Q_s^s\} \sin \omega t \quad \ldots\ldots (2.40)$$

Eqn. (2.40) can be written in the form

$$\{F\} = \{Q_c^*\} \cos \omega t + \{Q_s^*\} \sin \omega t \quad (2.41)$$

where

$$\{Q_c^*\} = [\phi^*]^T \{Q_c^s\},$$

$$\{Q_s^*\} = [\phi^*]^T \{Q_s^s\}.$$

Expressing sine and cosine in exponential form, one can rewrite Eqn. (2.41) as

$$\{F\} = \left(\frac{Q_s^*}{2i} + \frac{Q_c^*}{2}\right) e^{i\omega t} + \left(\frac{-Q_s^*}{2i} + \frac{Q_c^*}{2}\right) e^{-i\omega t} \quad \ldots\ldots (2.42)$$

This can be written in terms of the forward and backward whirl as

$$\{F\} = E\, e^{i\omega t} + \bar{E}\, e^{-i\omega t} \quad (2.43)$$

where,

$$E = \left(\frac{Q_s^*}{2i} + \frac{Q_c^*}{2}\right), \text{ and } \bar{E} = \left(-\frac{Q_s^*}{2i} + \frac{Q_c^s}{2}\right) \quad (2.44)$$

2.3.5.2 Balance Planes with Variable Location

To provide further flexibility in rotor balancing, the effect of varying the location of the balancing planes within an element, is incorporated in the system. For a

typical uniform element shown in Fig. 2.6 the variable balance plane is located a distance (a) along the axis of the element, the end planes of the element are shown as b_1 and b_2 respectively. The displacement shape functions are given by

$$\psi_1 = 1 - 3(\frac{s}{\ell})^2 + 2(\frac{s}{\ell})^3, \qquad (2.45a)$$

$$\psi_2 = s[1 - 2(\frac{s}{\ell}) + (\frac{s}{\ell})^2], \qquad (2.45b)$$

$$\psi_3 = 3(\frac{s}{\ell})^2 - 2(\frac{s}{\ell})^3, \qquad (2.45c)$$

$$\psi_4 = \ell[-(\frac{s}{\ell})^2 + (\frac{s}{\ell})^3], \qquad (2.45d)$$

The addition of the trial weight in a plane is given by Eqn. (2.37) and (2.38).

$$F_y = (m\rho\omega^2 \sin\theta)\cos\omega t + (-m\rho\omega^2 \cos\theta) \sin\omega t \quad .... (2.46a)$$

$$F_z = (m\rho\omega^2 \cos\theta) \cos\omega t + (m\rho\omega^2 \sin\theta) \sin\omega t \quad .... (2.46b)$$

Referring to Fig. 2.6 the forces at a joint of a given element, due to a trial weight located at a distance (a) can be obtained by combining Eqns. (2.37), (2.28) and (2.42). The expressions for these forces can be written as

$$F_i = \int_0^{\ell} (m\rho\omega^2 \sin\theta)\, \delta(s-a)\, \psi_i \cos\omega t + (m\rho\omega^2 \cos\theta)\, \delta(s-a)\, \psi_i \sin\omega t \, ds \qquad (2.47)$$

$$i=1,2,3,4$$

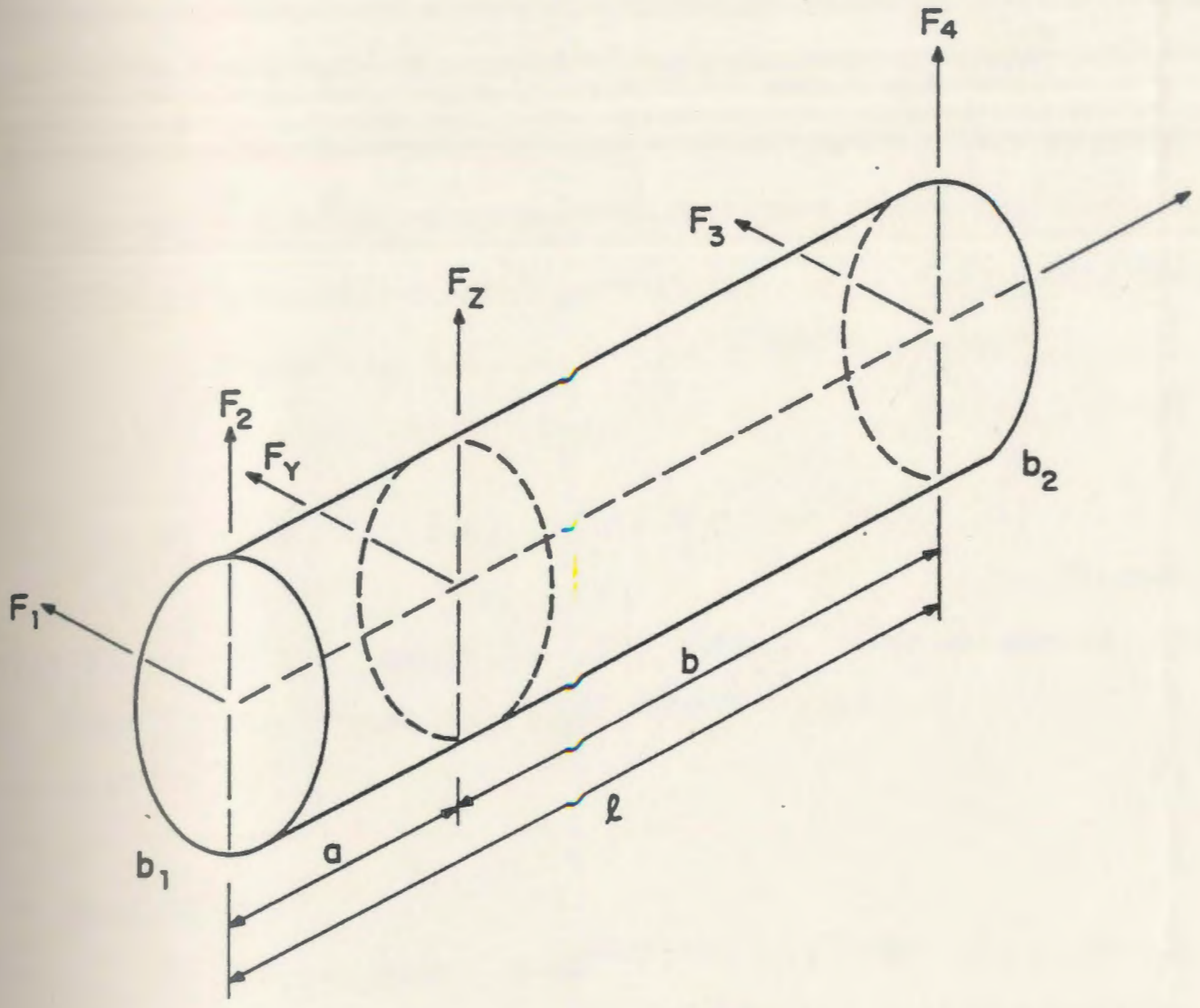

Fig. 2.6 Variable balance plane.

After integrating Eqn. (2.44) for i=1,2,...4, one can write

$$F_1 = m\rho\omega^2 \psi_1 (\sin\theta \cos\omega t + \cos\theta \sin\omega t) \quad .... (2.48a)$$

$$F_2 = m\rho\omega^2 \psi_2 (\cos\theta \cos\omega t - \sin\theta \sin\omega t) \quad .... (2.48b)$$

$$F_3 = m\rho\omega^2 \psi_3 (\sin\theta \cos\omega t + \cos\theta \sin\omega t) \quad .... (2.48c)$$

$$F_4 = mp\omega^2 \psi_4 (\cos\theta \cos\omega t - \sin\theta \sin\omega t) \quad .... (2.48d)$$

These forces at the joints of the elements are assembled into the global force vector for the dynamic response calculations.

2.4 Conclusions

In this chapter, a mathematical model based on the finite element analysis, of a rotor-bearing system has been formulated. In order to reduce the size of the system matrices, a dynamic matrix reduction technique has been used. For controlling the vibration levels, two methods are discussed which are, the exact point speed method, and the least square method. The expressions for the joint forces, due to the variable location of the trial weight in an

element, are obtained.

In the next chapter, the balancing of the rotors, is illustrated by numerical examples.

CHAPTER 3

ANALYSIS OF A ROTOR BEARING SYSTEM

3.1 Introduction

In Chapter 2, the rotor-bearing system was mathematically modelled. The equation of motion was formulated as a matrix differential equation, using the finite element method. A steady state solution for modal analysis was presented to calculate the system unbalance response. The equations for calculation of the correction weights using least-square analysis were then derived.

In this chapter, the analytical concepts developed earlier, are illustrated by numerical examples. The system was modeled on a VAX 11/780 digital computer with a package developed by the author in FORTRAN language which is given in Appendix E.

3.2 Analysis of the Rotor as a Hinged-Hinged Beam

In order to verify the formulation and assembly of the system matrices, the rotor was analyzed as beam with hinged-hinged end conditions. The beam was first discretized using 6 elements of equal length to determine its natural frequencies as illustrated in Fig. 3.1. The system frequencies were compared with those using the flexural beam theory [4]. The agreement in the calculated natural frequencies was very good. These calculations were repeated

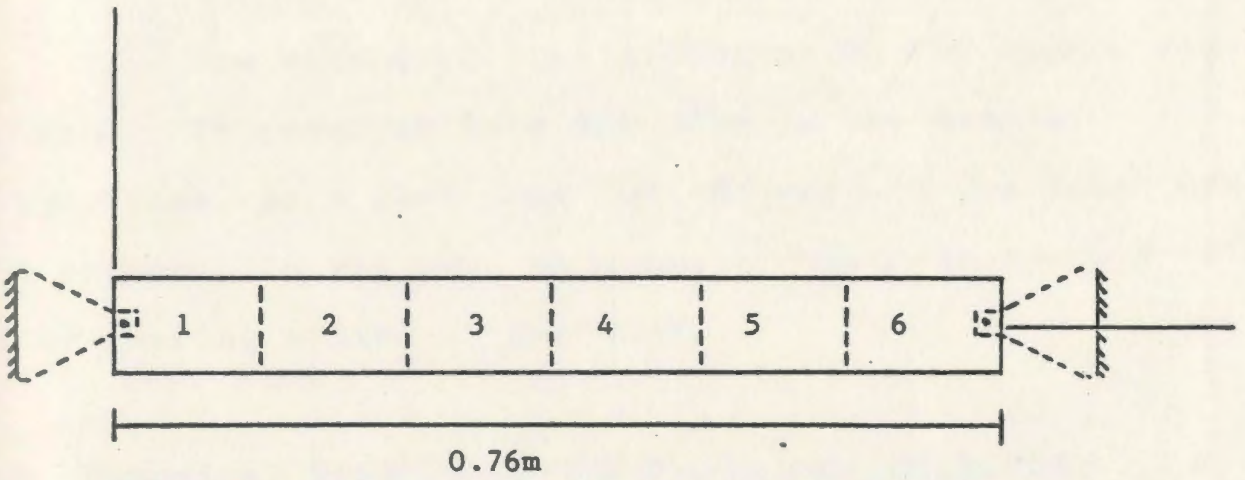

Fig. 3.1 Rotor Shaft Analyzed for Hinged-Hinged End Condition
(6 uniform diameter sections 50 x 127mm)

by increasing the number of elements. It was found that, as the element number was increased, the natural frequencies decreased slightly and that 6 elements gave sufficiently accurate results. Therefore, only 6 elements were used for the further dynamic analysis of the rotor-bearing system. The validity of the theoretical model is checked in Appendix F.

The effect of disk additions on the system was also studied. It resulted in a decrease in the natural frequencies, as a result of the increase in the total mass of the system. In the next section, a numerical example of a rotor-bearing system is discussed.

3.3 Numerical Example of the Rotor Bearing System

To demonstrate the application of the finite element model, a typical rotor-bearing system with six elements, as illustrated in Fig. 3.2 was considered. The details of the rotor are provided in Table 3.1. It consists of a shaft, with a uniform diameter of 0.050 m, and an overall length of 0.76 m. The rotor is symmetrical and most of the mass concentrated in the two disks. A density of 7806 kg/m^3, and elastic modulus of 2.078×10^{11} N/m^2 was used to model the rotor shaft. The two disks, with a mass of 20.45 kg each, polar moment of inertia of 0.0020 $kg\text{-}m^2$ and diametrial inertia of 0.0010 $kg\text{-}m^2$, were located 0.254 m from the ends. The rotors were supported on plain cylindrical

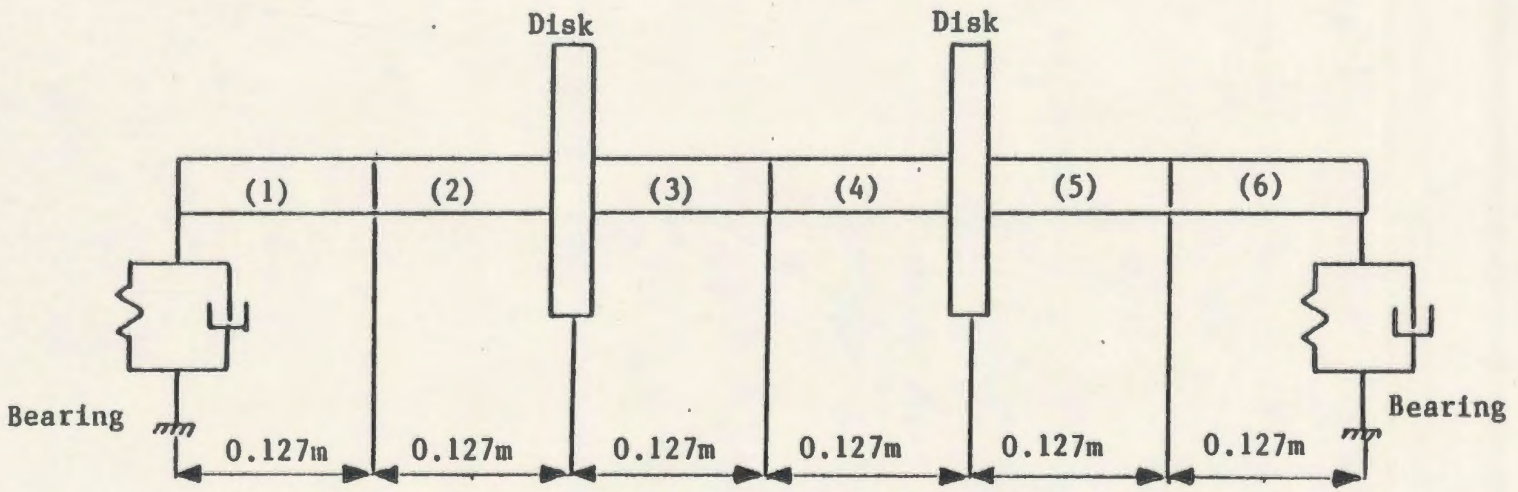

Fig. 3.2 Multi-Mass Rotor Supported on Fluid-Film Bearings

Table 3.1 Rotor Detail

Shaft Diameter	0.05 m
Total Length of Shaft	0.76 m
Modulus of Elasticity of Shaft	2.07×10^{11} Pa.
Shaft Density	7.68×10^{4} kg/m^3
Disk Weight	20.45 kg.
Type of Bearing	Plain Cylindrical
Bearing L/D Ratio	1
Viscosity of Oil	69×10^{-4}N sec/m^2
Disk Eccentricity	6.35×10^{-4}m (In-plane 45°)

fluid-film bearings witha L/D ratio of 1 and a bearing clearance of 0.000635 m. The unbalance condition was represented by the two disks with a in-line, in-phase mass centre eccentricity of 0.000635 m. This configuration was similar to impellers keyed to the shaft with the same key.

3.4 Results and Discussions

3.4.1 The Dynamic Matrix Reduction Technique

In the dynamic reduction technique, the original system matrices were reduced to smaller sizes by using a transformation matrix defined by using Eqn. (2.6a). In this reduction process, care was taken that the properties of the original system, such as the natural frequencies, did not alter significantly. The greater is the degree of reduction, the more will be the deviation of such properties.

For the present system, the number of degree of freedom were 28. This had to be reduced as much as possible. Trial runs on the computer for the calculation of the natural frequencies, using Eqn. (2.9e), were made by varying the degrees of freedom between 12 to 25. Some of the results obtained, are shown in Table 3.2. In this table, the first five natural frequencies were computed by varying the number of master degree of freedom. As the number of master degrees were increased, the natural frequencies decreased. However, this rate of decrease in the frequency value with respect to

Table 3.2 Comparison of the Damped Natural Frequencies of Original and the Reduced Systems

Frequency No.	Original System CPM	Retained Degree of Freedom											
		12 CPM	Percent Deviation %	13 CPM	Percent Deviation %	14 CPM	Percent Deviation %	15 CPM	Percent Deviation %	16 CPM	Percent Deviation %	25 CPM	Percent Deviation %
1	1260.417	1288.009	2.5	1282.845	0.4	1282.845	1.2	1260.417	2.1	1256.153	0.03	1256.114	0.0
2	3532.476	3935.456	21.6	3934.310	11.3	3934.310	21.5	3532.476	10.2	3236.352	0.0	3236.323	0.0
3	4976.434	5142.606	3.6	5008.300	2.6	5008.300	0.3	4576.434	3.2	4965.775	0.0	4965.902	0.0
4	94802.36	94901.76	0.3	94900.05	0.0	94900.05	0.3	94802.36	0.1	94780.93	0.2	94564.60	0.0
5	122354.28	135613.95	11.4	135592.75	0.1	135592.75	3.9	122354.28	9.6	122342.5	0.5	121819.65	0.1

the increase in the degree of freedom, becomes very small when the degrees of freedom were 16. Therefore, the reduced system, for further analysis, was chosen to have 16 degrees of freedom, which represents 42 percent reduction in the each of the system matrix sizes.

3.4.2 The Variations of the Natural Frequencies of the System with the Operating Speed

The first three damped natural frequencies of the system are given in Fig. 3.3. The critical speeds are frequencies when the system natural frequencies are equal to the operating speed. The abrupt changes in the frequency map are because of the speed dependent fluid-film bearing coefficients. The rotor, light in weight, has a Sommerfeld number ranging between 1.0 to 10.0, within the operating speed range. The response at the first three critical speeds for the original and reduced system are compared in Table 3.3. The location of the measuring planes are shown in Fig. 3.4. A maximum deviation of 1.05 percent indicates the efectiveness of the matrix reduction technique.

3.4.3 The Effect of Gyroscopic Moment on the Rotor Response

The unbalance damped response values, for the three critical speeds were calculated to study the effect of gyroscopic moments on the rotor-bearing response. The response values obtained are shown in Table 3.3a. As can be seen from this table, the gyroscopic moments have very little effect on the overall response of the system. This can be

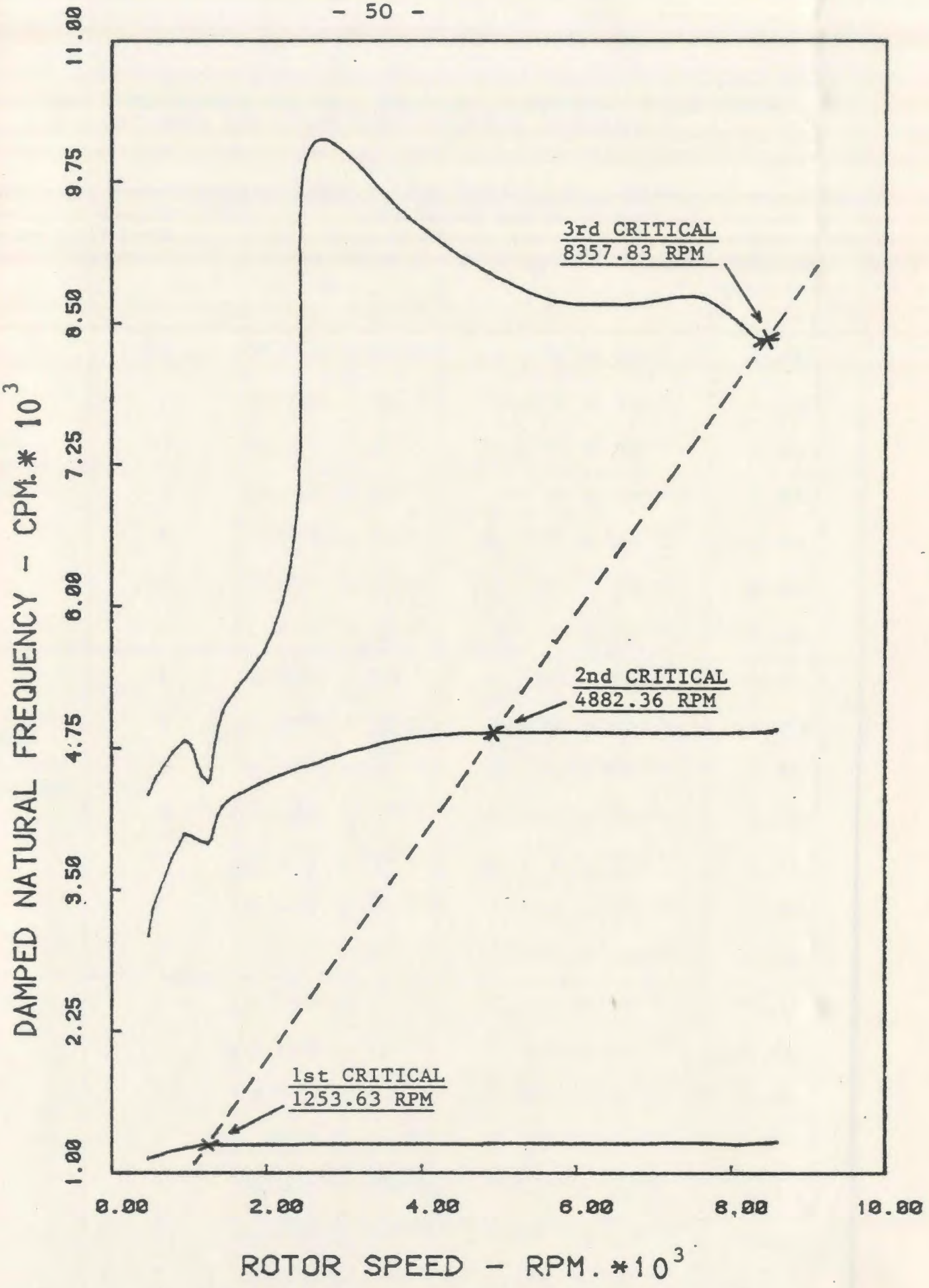

Fig 3.3 Damped Critical Speed Map for Rotor System

Table 3.3 Comparison of the Maximum Response Amplitudes betweem the Full and Reduced Systems

Rotor Speed RPM	Measuring Plane No.	Maximum Rotor Response		
		Full System m	16 Degrees System m	Percent Deviation %
The First Critical (1253.63)	1	7.178×10^{-5}	7.170×10^{-5}	0.48
	2	2.979×10^{-4}	2.964×10^{-4}	0.56
	3	6.184×10^{-4}	6.774×10^{-4}	0.63
	4	7.769×10^{-4}	7.724×10^{-4}	0.63
	5	6.814×10^{-4}	6.774×10^{-4}	0.63
	6	2.979×10^{-4}	2.964×10^{-4}	0.56
	7	7.178×10^{-5}	7.170×10^{-5}	0.48
The Second Critical (4882.36)	1	2.380×10^{-6}	2.370×10^{-6}	0.40
	2	3.655×10^{-5}	3.644×10^{-5}	0.29
	3	6.172×10^{-5}	6.169×10^{-5}	0.05
	4	7.137×10^{-5}	7.089×10^{-5}	0.71
	5	6.172×10^{-5}	6.169×10^{-5}	0.05
	6	3.655×10^{-5}	3.644×10^{-3}	0.29
	7	2.380×10^{-6}	2.370×10^{-6}	0.40
The Third Critical (8357.83)	1	1.554×10^{-6}	1.586×10^{-6}	0.52
	2	3.490×10^{-5}	3.469×10^{-5}	0.61
	3	5.928×10^{-5}	5.877×10^{-5}	0.87
	4	6.847×10^{-5}	6.776×10^{-5}	1.05
	5	5.928×10^{-5}	5.877×10^{-5}	0.87
	6	3.490×10^{-5}	3.469×10^{-5}	0.61
	7	1.594×10^{-6}	1.586×10^{-6}	0.52

m = Measuring plane

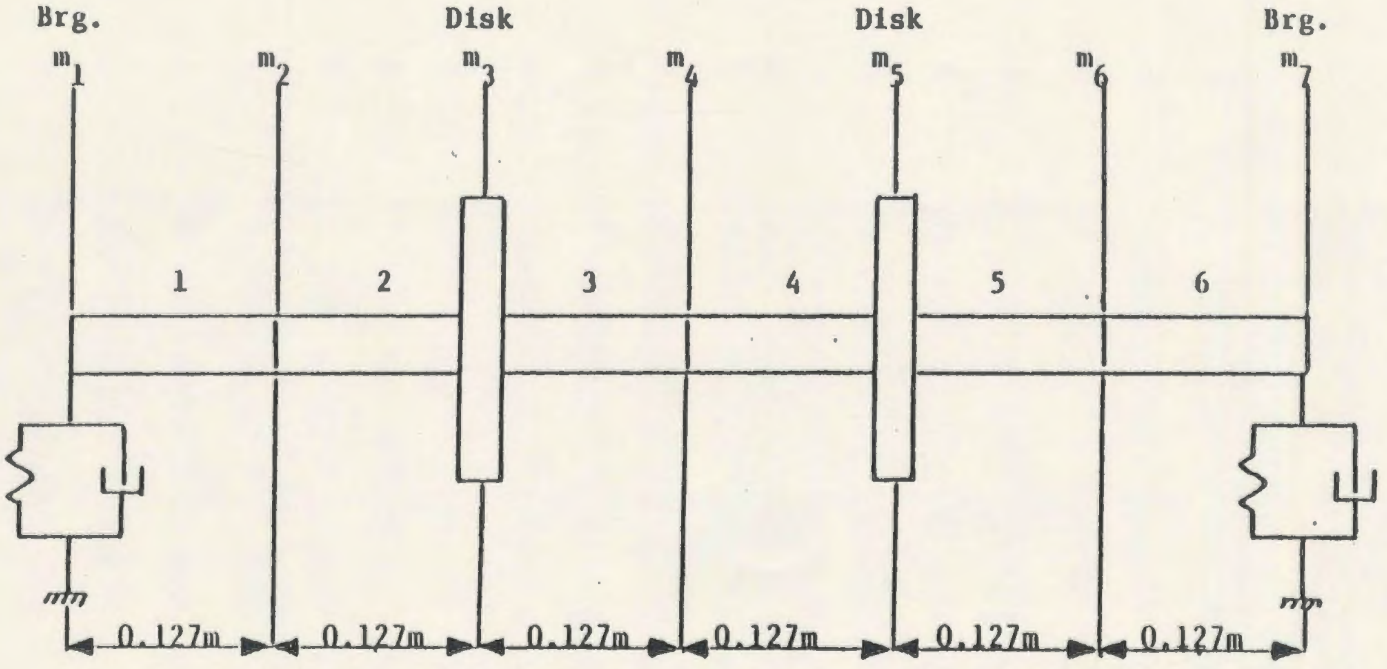

Fig. 3.4 Rotor Measuring Plane locations .

Table 3.3a Comparison of Unbalance Response for Cases with and without Gyroscopic effects

Rotor Speed RPM.	Measuring Plane No.	Maximum Response Amplitude		Percent Deviation %
		With Gyroscopic Effect m	Without Gyroscopic Effect m	
The First Critical (1253.63)	1	7.170×10^{-5}	7.176×10^{-5}	0.09
	2	2.964×10^{-4}	2.966×10^{-4}	0.06
	3	6.774×10^{-4}	6.783×10^{-4}	0.13
	4	7.724×10^{-4}	7.730×10^{-4}	0.08
	5	6.774×10^{-4}	6.783×10^{-4}	0.13
	6	2.964×10^{-4}	2.966×10^{-4}	0.06
	7	7.170×10^{-5}	7.176×10^{-5}	0.09
The Second Critical (4882.36)	1	2.370×10^{-6}	2.374×10^{-6}	0.17
	2	3.644×10^{-5}	3.619×10^{-5}	-0.68
	3	6.169×10^{-5}	6.138×10^{-5}	-0.50
	4	7.089×10^{-5}	7.063×10^{-5}	-0.37
	5	6.169×10^{-5}	6.138×10^{-5}	-0.50
	6	3.644×10^{-5}	3.619×10^{-5}	-0.68
	7	2.370×10^{-6}	2.374×10^{-6}	-0.17
The Third Critical (8357.83)	1	1.586×10^{-6}	1.590×10^{-6}	0.25
	2	3.469×10^{-5}	3.454×10^{-5}	-0.43
	3	5.877×10^{-5}	5.872×10^{-5}	-0.08
	4	6.776×10^{-5}	6.774×10^{-5}	-0.03
	5	5.887×10^{-5}	5.872×10^{-5}	-0.08
	6	3.469×10^{-5}	3.454×10^{-5}	-0.43
	7	1.586×10^{-6}	1.590×10^{-6}	0.25

because of the damping present in the system, which tends to mask the gyroscopic effects of the shaft and the two disks. Although the gyroscopic effects were small for this system, they were included in the overall system analysis.

3.4.4 The Dynamic Response as a Function of Rotor Speed

The unbalance response at the middle of the rotor, for various operating speeds, is shown in Fig. 3.5. The three criticals speeds are clearly indicated by peaks in this curve. The response is very high at the first critical whereas it is almost equal at the second and third critical speeds.

It is obvious from this study that the vibration levels at the criticals must be controlled. The maximum whirl amplitude, at the measuring planes, at various criticals, are shown in Table 3.3. It can be clearly seen that 16 master degrees of freedom are sufficient for the dynamic response study because the deviations are very small. In addition, the deflections are symmetrical along the rotor as shown in Fig. 3.6. This is because the measuring planes (refer to Fig. 3.4) have been located in a symmetrical manner, and the deflection of the corresponding points on either ends, are equal. for example, the measuring plane number 2, and 6 are equidistant from the ends and their respective response values are equal.

The response orbitals of the disk and the bearing

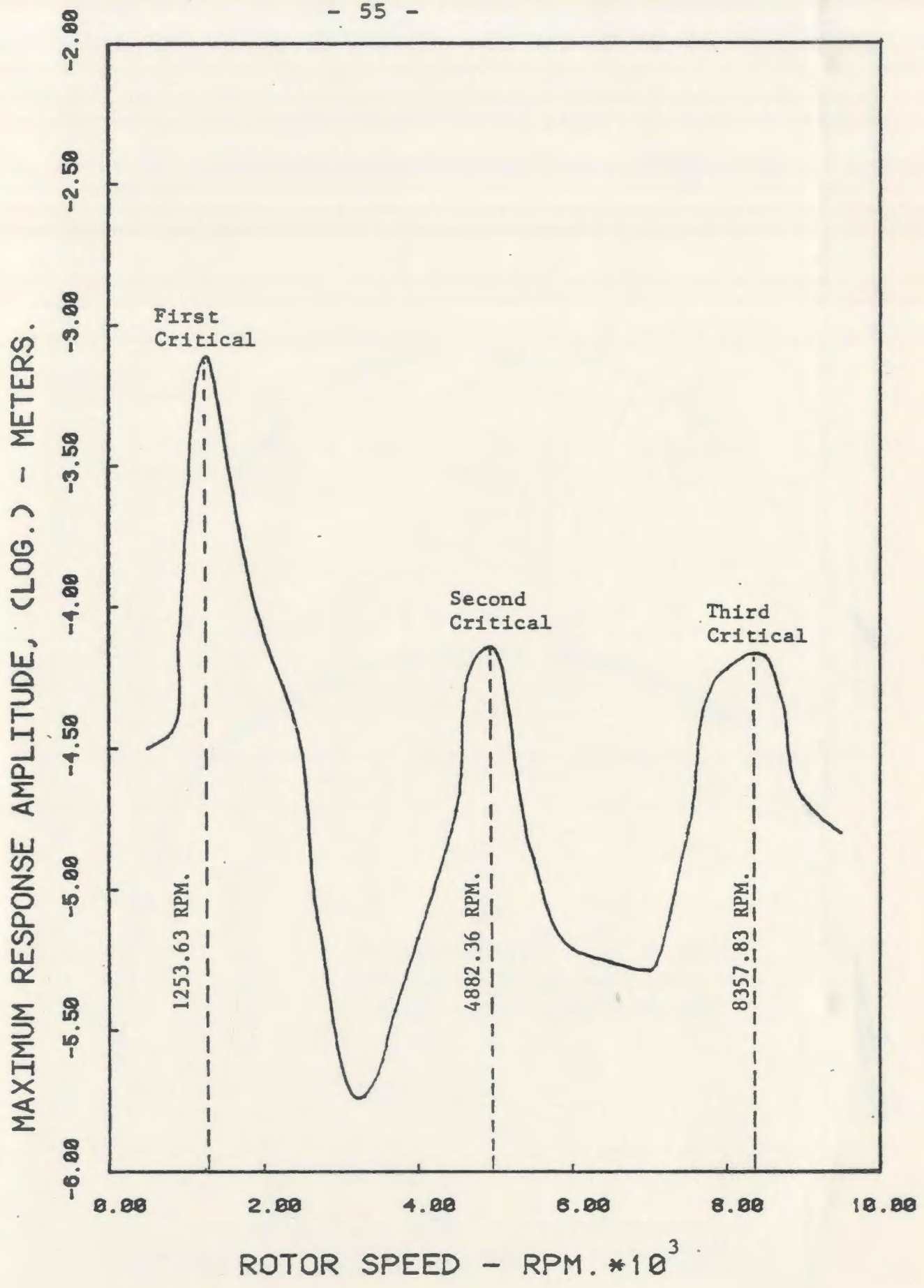

Fig. 3.5 Unbalance Rotor Response at the Middle of the Rotor

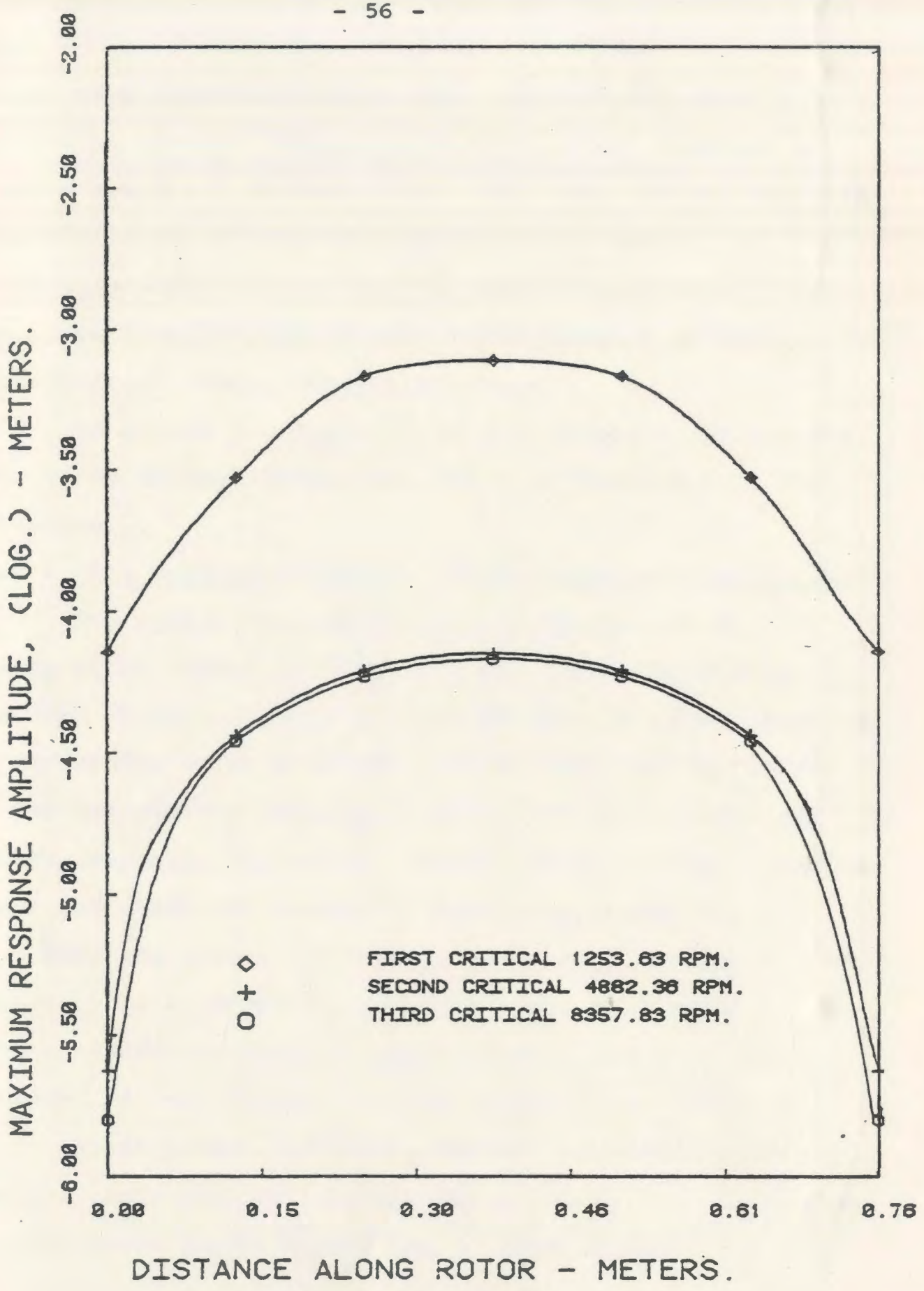

Fig. 3.6 Unbalance Response at the First Three Critical Speeds

locations were calculated using Eqn. (2.24), and were elliptical in nature. The major and the minor diameter of the orbits are shown in Table 3.4. The ratio of the major to the minor diameter at the bearing locations, was approximately equal to one, in the computer printout. They appear to be equal to one in this table because of the rounding off, of their respective values.

In actual practice, these peak response values are reduced using dynamic balancing, which is discussed in the next section.

3.4.5 The Dynamic Balancing of the Rotor-Bearing System

The dynamic balancing can be carried out by selecting equal number of measuring and balancing planes. For rotors, which are symmetrically loaded, it often leads to large correction weights at the centre [28]. On the other hand, one can use the least-square method, where the rotor amplitude response, can be minimized without adding excessive weights, and where the number of measuring planes can be greater than the number of balancing planes. Another advantage of this method is that there can be several measuring planes and even if there is some error in the measurement in one or more than one planes, still the computed values yield very good results. In other words, by increasing the number of the measuring planes, the influence of a measurement error in any one of these planes, is

Table 3.4 Elliptical Response Oribitals at the Bearing and Disk Locations

Rotor Speed RPM	Bearing			Disk		
	Major Diameter μm	Minor Diameter μm	Angle Deg.	Major Diameter μm	Minor Diameter μm	Angle Deg.
1200.0	56.642	56.642	-11.4	480.031	333.274	-63.0
1253.6	71.628	71.628	12.0	763.042	358.445	51.2
3300.0	4.648	4.648	-43.7	67.106	66.573	80.1
4800.0	2.369	2.369	43.4	63.322	61.239	76.8
8100.0	1.585	1.585	2.7	58.826	58.724	63.3
8355.6	1.662	1.662	38.9	61.239	59.512	68.1

diminished. The greater the number of balancing planes, better will be the balancing of the system. Unfortunately, due to the limitations of the accessibility and other constraints, the balancing planes can not be increased beyond certain number, for a given system. However, in these situations, the best one can do is to increase the number of measuring planes and carry out the balancing using the least-square analysis.

The rotor was then balanced at the first critical speed using three fixed balancing planes as shown in Fig. 3.7. In order to present a meaningful comparison of the balance improvement as a result of balancing at the critical speeds, two balancing methods were considered.

Method 1 involves a commercially used balancing technique [28]. In it, the rotor is first balanced at little above half its first critical speed, to stabilize the higher modes, and then balanced at 1190 rpm., a speed close to the first critical without actually balancing the rotor at its critical speed.

Method 2 involves balancing the rotor at its critical speed only. The results for the two methods, are presented in Table 3.5. In method 1 the unbalance response at various measuring planes was calculated using Eqn. (2.9) and is shown in column 3. The response at various speeds after balancing at 760 rpm, is shown in column 4. Similarly,

m = Measuring plane

b = Balancing plane

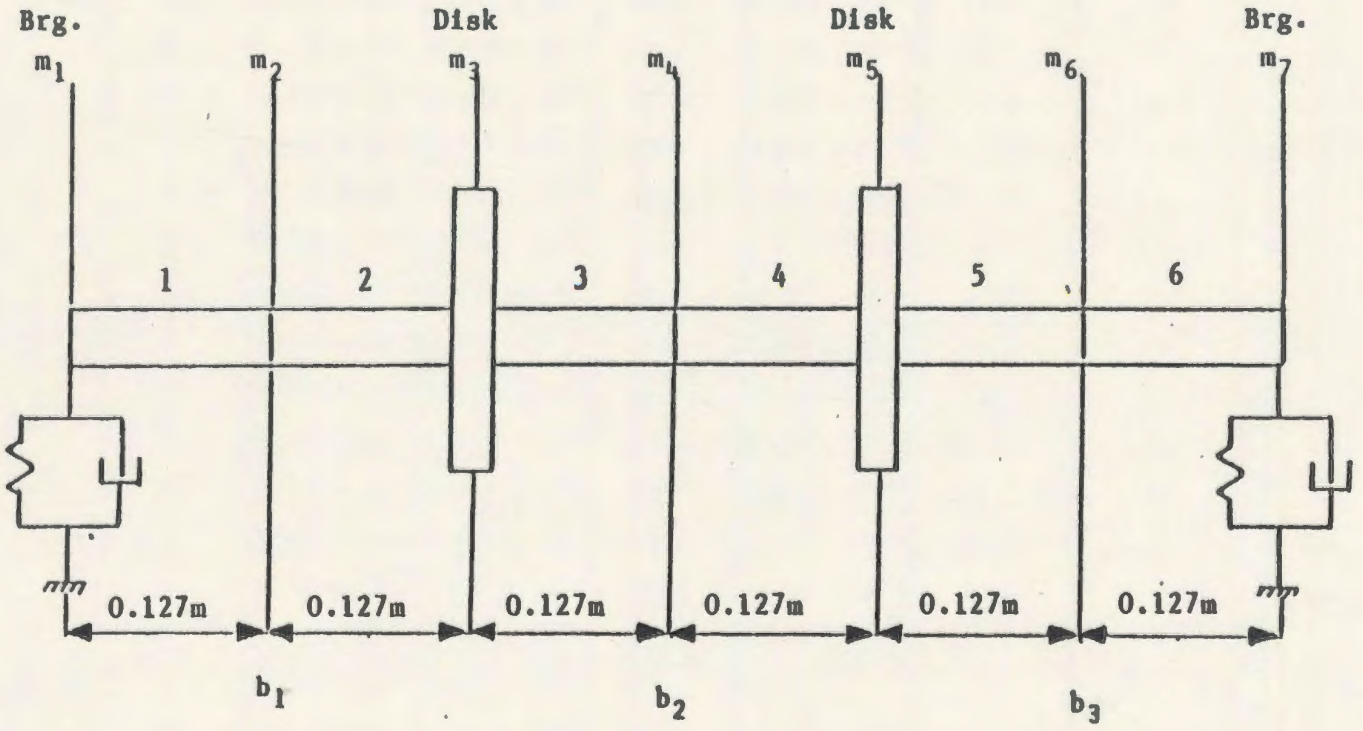

Fig. 3.7 Schematic of the Rotor Bearing System (Shaft-0.05 x0.76m)
(3-plane balance)

Table 3.5 Balance Improvements when Balancing below and at Critical Speeds

Rotor Speed R.P.M. (1)	Measuring Plane No. (2)	Before Balancing m (3)	After 1st Balance Run (760 RPM.) m (4)	% Reduction Due to 1st Balance Run (5)	After 2nd Balance Run (1190 RPM.) m (6)	% Reduction Due to 2nd Balance Run (7)	Critical Speed Balance (1253.60 RPM.) m (8)	% Reduction (9)
760.00	1	6.014×10^{-6}	6.89×10^{-8}	98.8	6.883×10^{-8}	0.4	-	-
	2	1.947×10^{-5}	8.965×10^{-8}	99.5	8.257×10^{-8}	5.7	-	-
	3	3.075×10^{-5}	1.102×10^{-7}	99.6	1.092×10^{-7}	0.8	-	-
	4	3.479×10^{-5}	1.904×10^{-7}	99.4	1.831×10^{-7}	3.8	-	-
	5	3.075×10^{-5}	1.102×10^{-7}	99.6	1.092×10^{-7}	0.8	-	-
	6	1.947×10^{-5}	8.965×10^{-8}	99.5	8.257×10^{-8}	5.7	-	-
	7	6.014×10^{-6}	6.891×10^{-8}	98.8	6.883×10^{-8}	0.4	-	-
1190.00	1	5.671×10^{-5}	1.851×10^{-7}	99.6	1.010×10^{-7}	45.4	-	-
	2	2.938×10^{-4}	1.147×10^{-6}	99.5	3.190×10^{-7}	72.2	-	-
	3	4.803×10^{-4}	1.853×10^{-6}	99.3	4.208×10^{-7}	77.2	-	-
	4	5.463×10^{-4}	1.620×10^{-6}	99.7	8.026×10^{-7}	50.4	-	-
	5	4.803×10^{-4}	1.853×10^{-6}	99.3	4.208×10^{-7}	77.2	-	-
	6	2.938×10^{-4}	1.147×10^{-6}	99.5	3.190×10^{-7}	72.2	-	-
	7	5.671×10^{-5}	1.851×10^{-7}	99.6	1.010×10^{-7}	45.4	-	-
1253.60	1	7.170×10^{-5}	3.672×10^{-7}	99.4	1.774×10^{-7}	51.7	1.708×10^{-7}	99.7
	2	2.964×10^{-4}	1.682×10^{-6}	99.4	1.006×10^{-6}	40.1	1.003×10^{-6}	99.6
	3	6.774×10^{-4}	2.839×10^{-6}	99.5	1.753×10^{-6}	38.2	1.750×10^{-6}	99.7
	4	7.724×10^{-4}	3.373×10^{-6}	99.5	1.330×10^{-6}	60.5	1.328×10^{-6}	99.8
	5	6.774×10^{-4}	2.839×10^{-6}	99.5	1.753×10^{-6}	38.2	1.750×10^{-6}	99.7
	6	2.964×10^{-4}	1.682×10^{-6}	99.4	1.006×10^{-6}	40.1	1.003×10^{-6}	99.6
	7	7.170×10^{-5}	3.672×10^{-7}	99.4	1.774×10^{-7}	51.7	1.708×10^{-7}	99.7

the response at various speeds after balancing at 1190 rpm, is shown in column 6. The percentage improvements, due to the first and the second balancing are shown in columns 5 and 7 respectively. Referring to this table it can be easily seen that the major reduction in the response is carried out by the first balancing at 760 rpm. The second balancing is more effective at higher speeds such as 1190 or 1253 rpm (percentage reduction in response is higher).

In method 2, the balancing is done only at the critical speed and the results after this balancing, are shown in column 8. The percentage reduction due to this balancing is the percent difference of the results given in columns 3 and 8 respectively.

The results, obtained either by method 1 or 2 are quite good, but method 2 yields better results. The balance results, along the length of the rotor, are shown in Fig. 3.8. As stated earlier, the deflections are symmetrical. The curve obtained using method 2, shows a slight dip at the middle of the rotor. This is due to the presence of the balancing plane at this location.

After balancing the rotor for the first critical speed, method 2 was selected for further balancing. The rotor response at the second and third critical speeds were obtained and the corresponding correction weights were calculated. The system unbalance and balance response values

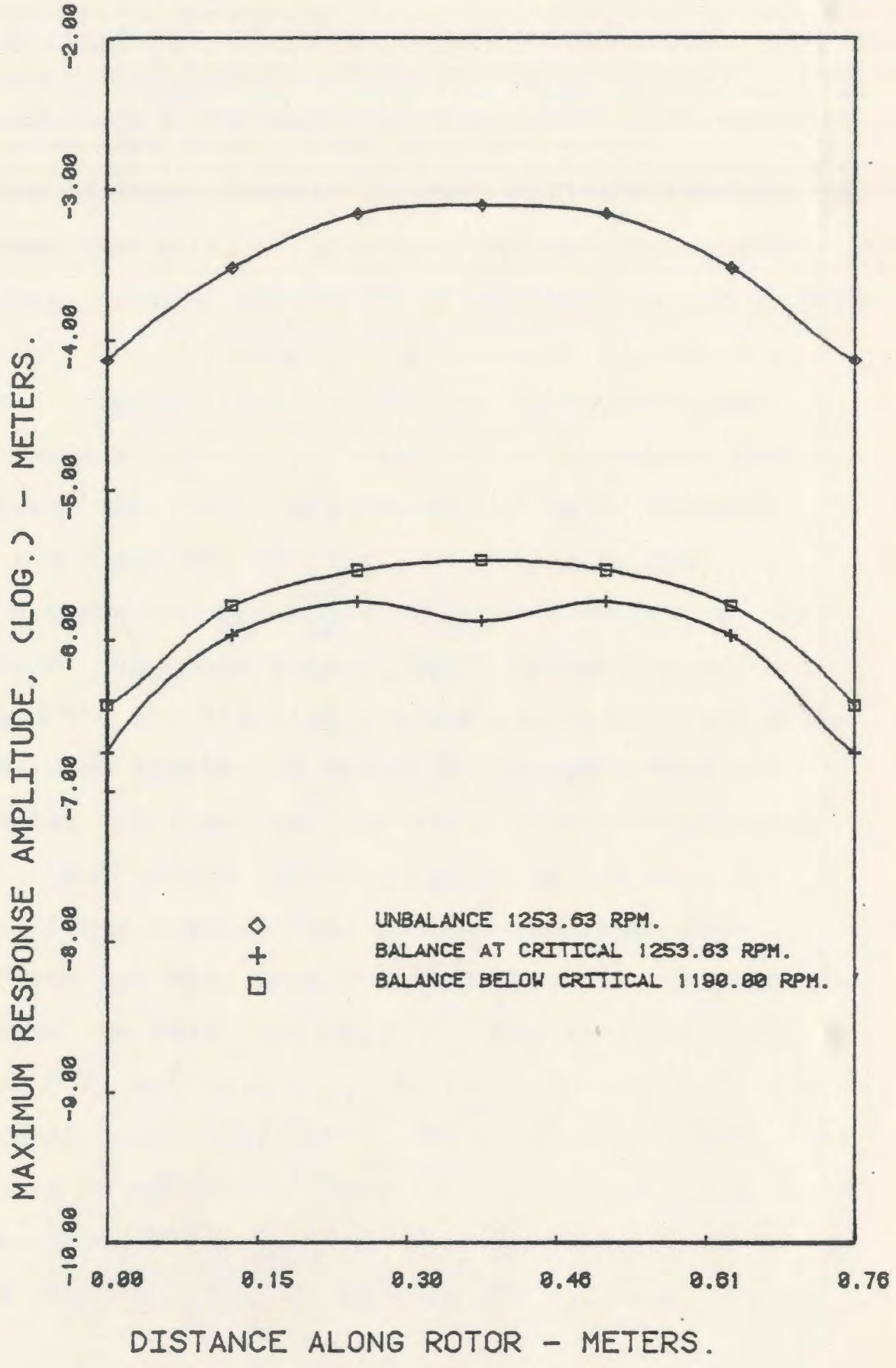

Fig. 3.8 Balance Improvements when Balancing at and below Critical Speeds

at the three criticals are given in Table 3.6a. The magnitude of the correction weights and their phase angles at these criticals, are given in Table 3.6b.

The maximum reduction in the unbalance response is attained under the first balance run. The effect of the second critical balance results in an increase in the overall balance condition. The increase is probably because the balance plane locations are ineffective in reducing the response. Similar results are reported by Tessarzik [28].

Next, the rotor response at the third critical speed with the first set of correction weights, was calculated and the corresponding correction weights at this critical speed, were determined. The response values, with the first and the third set of correction weights, are shown in column 8. The results in column 9, indicate that the response, after the first and the third critical balancing, decreases at most of the location except at and near the bearings. This is possibly due to the balancing planes locations which are away from the bearings. The dynamic response along the length of the rotor due to these balancing are shown in Fig. 3.9 to 3.11. Referring to Fig. 3.9, there is quite significant reduction in the unbalance response due to the correction weights. The deflection curve along the rotor, is symmetrical even after the balancing, in all of these three figures. This is because the balancing planes

Table 3.6a Balance Improvements when Balancing at Critical Speeds

Rotor Speed RPM. (1)	Measuring Plane No. (2)	Before Balancing m (3)	After 1st Balance Run m (4)	% Reduction Due to 1st Balance Run (5)	After 2nd Balance Run m (6)	% Reduction Due 1st & 2nd Balance Run (7)	After 3rd Balance m (8)	% Reduction 1st and 3rd Balance Run (9)
First Critical (1253.63)	1	7.170×10^{-5}	1.780×10^{-7}	99.7	1.216×10^{-7}	31.3	1.497×10^{-7}	-23.1
	2	2.964×10^{-4}	1.007×10^{-6}	99.6	1.021×10^{-6}	-1.5	4.137×10^{-7}	59.5
	3	6.774×10^{-4}	1.790×10^{-6}	99.7	1.772×10^{-6}	-0.1	6.985×10^{-7}	60.6
	4	7.724×10^{-4}	1.328×10^{-6}	99.8	1.656×10^{-6}	-24.4	1.453×10^{-6}	12.2
	5	6.774×10^{-4}	1.790×10^{-6}	99.7	1.772×10^{-6}	-0.1	6.985×10^{-7}	60.6
	6	2.964×10^{-4}	1.007×10^{-6}	99.6	1.021×10^{-6}	-1.5	4.137×10^{-7}	59.5
	7	7.170×10^{-5}	1.780×10^{-7}	99.7	1.216×10^{-7}	31.3	1.497×10^{-7}	-23.1
Second Critical (4082.36)	1	2.370×10^{-6}	1.381×10^{-6}	41.7	1.520×10^{-6}	-10.0	1.382×10^{-6}	0.0
	2	3.644×10^{-5}	1.123×10^{-6}	96.9	2.128×10^{-6}	-89.3	1.123×10^{-6}	0.0
	3	6.169×10^{-5}	1.603×10^{-7}	99.7	1.247×10^{-6}	-67.7	1.602×10^{-7}	0.1
	4	7.089×10^{-5}	1.289×10^{-5}	81.8	1.152×10^{-6}	91.0	1.288×10^{-5}	0.1
	5	6.169×10^{-5}	1.603×10^{-7}	99.7	1.247×10^{-6}	-67.7	1.602×10^{-7}	0.1
	6	3.644×10^{-5}	1.123×10^{-6}	96.9	2.128×10^{-6}	-89.3	1.123×10^{-6}	0.0
	7	2.370×10^{-6}	1.381×10^{-6}	41.7	1.520×10^{-6}	-10.0	1.382×10^{-6}	0.0
Third Critical (8357.83)	1	1.586×10^{-6}	2.758×10^{-6}	173.8	1.234×10^{-6}	44.7	4.074×10^{-6}	-47.6
	2	3.469×10^{-5}	4.231×10^{-6}	87.8	3.243×10^{-5}	-666.5	1.594×10^{-5}	-273.0
	3	5.877×10^{-5}	7.061×10^{-8}	99.9	5.664×10^{-5}	--	2.664×10^{-6}	62.2
	4	6.776×10^{-5}	3.764×10^{-5}	44.4	6.733×10^{-5}	-78.0	3.835×10^{-6}	8.9
	5	5.887×10^{-5}	7.061×10^{-8}	99.9	5.644×10^{-5}	--	2.664×10^{-6}	61.2
	6	3.469×10^{-5}	4.231×10^{-6}	87.8	3.243×10^{-5}	-666.5	1.594×10^{-5}	-273.0
	7	1.586×10^{-6}	2.758×10^{-6}	173.8	1.234×10^{-6}	44.7	4.074×10^{-6}	-47.6

Table 3.6b Corresponding Balance Weights Magnitude and Angles when Balancing Rotor at the first three Critical Speeds

Balance Plane No.	Calculated Correction Weights					
	1253.63 RPM		4882.36 RPM		8357.83 RPM	
	Weight g	Angle Deg.	Weight g	Angle Deg.	Weight g	Angle Deg.
1	7.13	-36.5	30.2	-39.6	6.1	-37.5
2	51.5	-46.2	46.3	-48.9	2.3	-43.1
3	7.13	-36.5	30.2	-39.6	6.1	-37.5

have been symmetrically located along the length of the rotor. However, the percentage decrease in the rotor response, after the balancing, at the second and the third critical, is much less than that at the first critical. For example, at a distance of 0.15 m along the rotor, the difference in the unbalance and balance response in Fig. 3,9, is much more than a similar difference in Fig. 3.10 and 3.11.

Referring to Table 3.6b, the angular location of the correction weights is approximately opposite to the disk mass centre eccentricity, which is 45°.

It must be added here that the overall saving of CPU time and memory storage for a balancing run using the condensation technique were 38 and 42 percent respectively.

3.4.6 The effect of the Location of the Balancing Planes on the Rotor Response

In the previous section, three balancing planes were used; one located at the middle and two others symmetrically located away from the first one. Since the rotor disks are symmetrically located on the rotor shaft, it appears logical to place these two balancing planes also symmetrically. Therefore, in order to study the effect of the location of these planes on the response of the system, the location of the two outer planes, and the locations of the third plane, have been chosen as variables for the parametric study.

The effect of balancing plane loction, for reducing

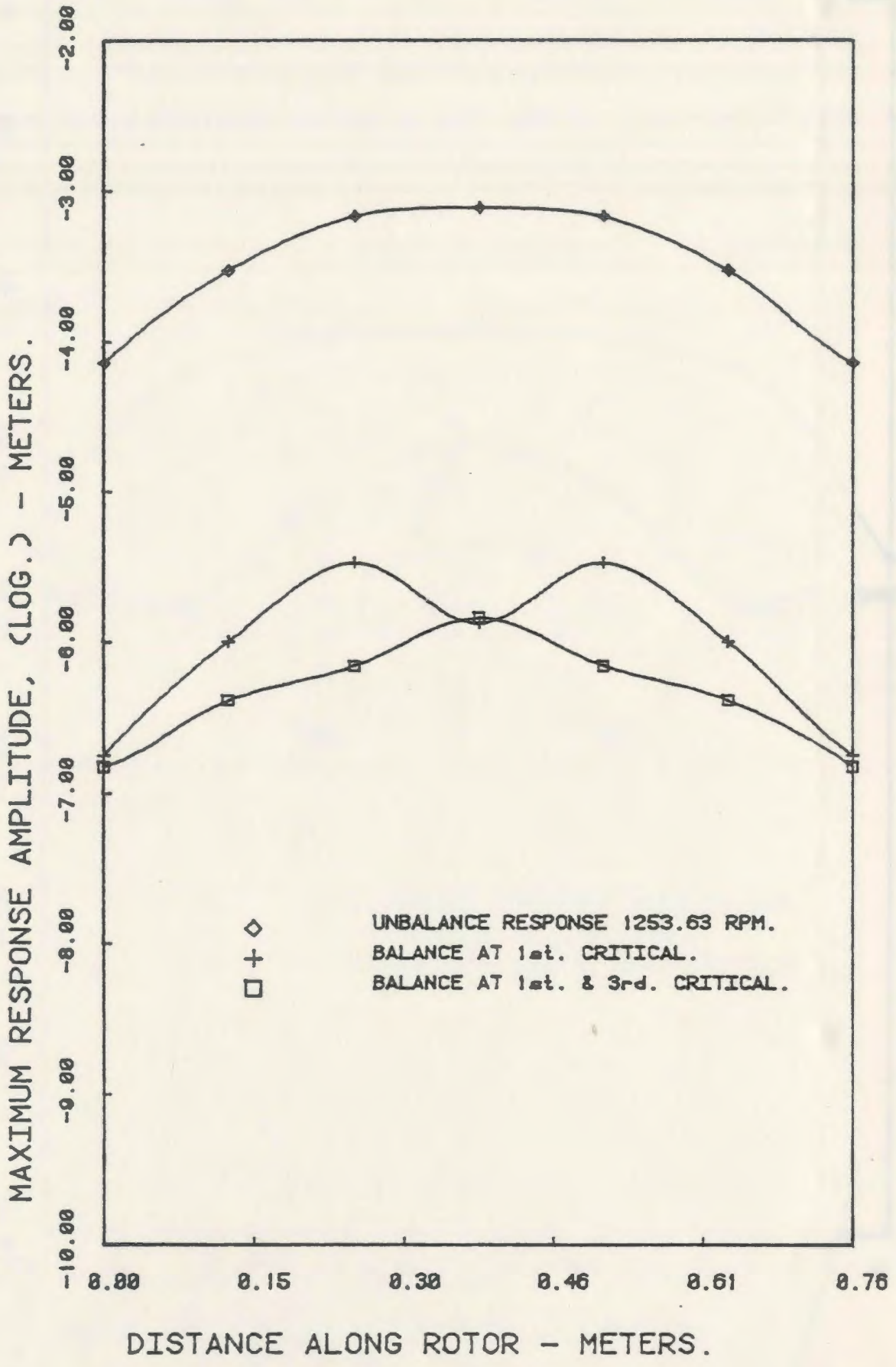

Fig. 3.9 Damped Rotor Response
at First Critical Speed

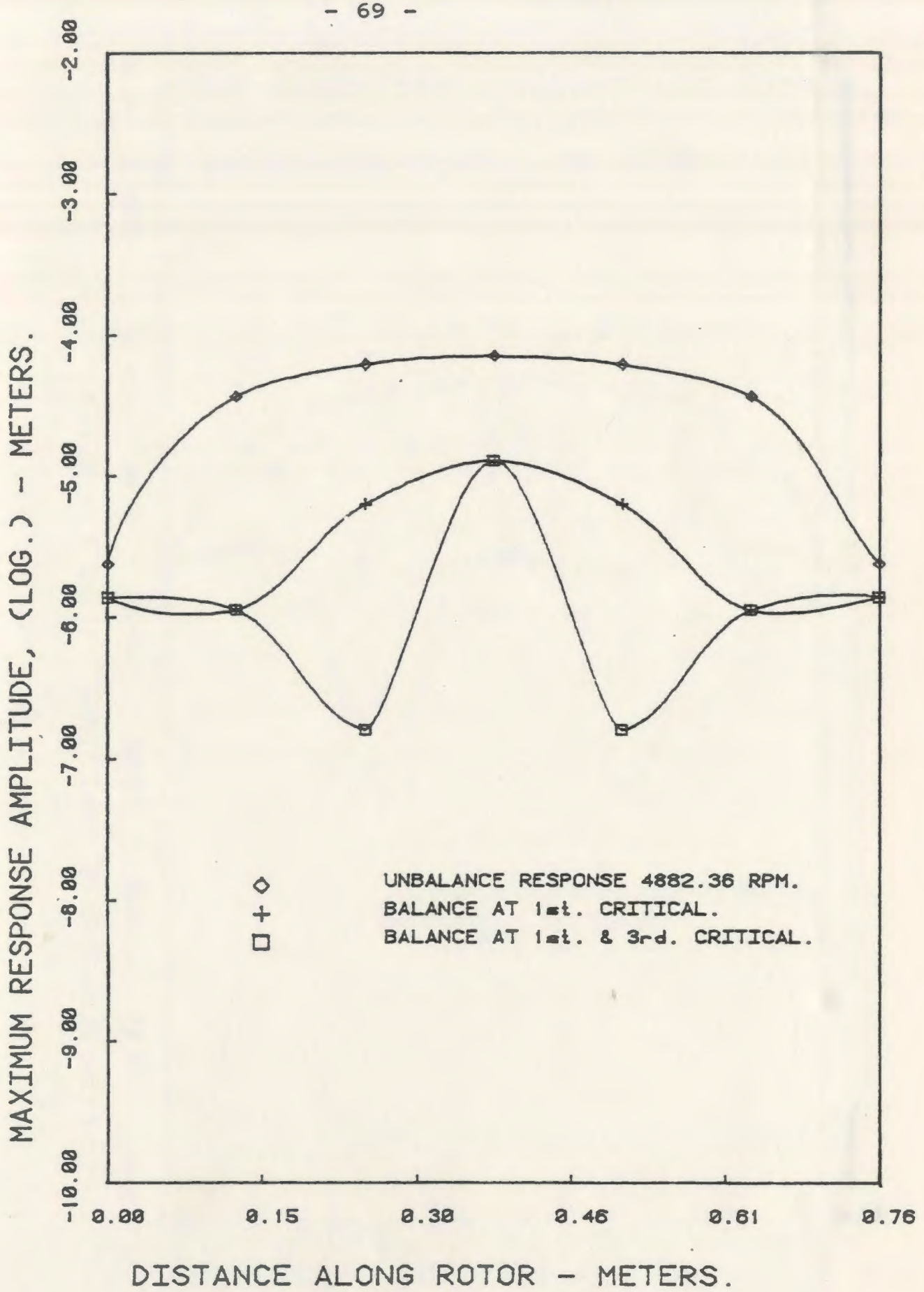

Fig. 3.10 Damped Rotor Response
at Second Critical Speed

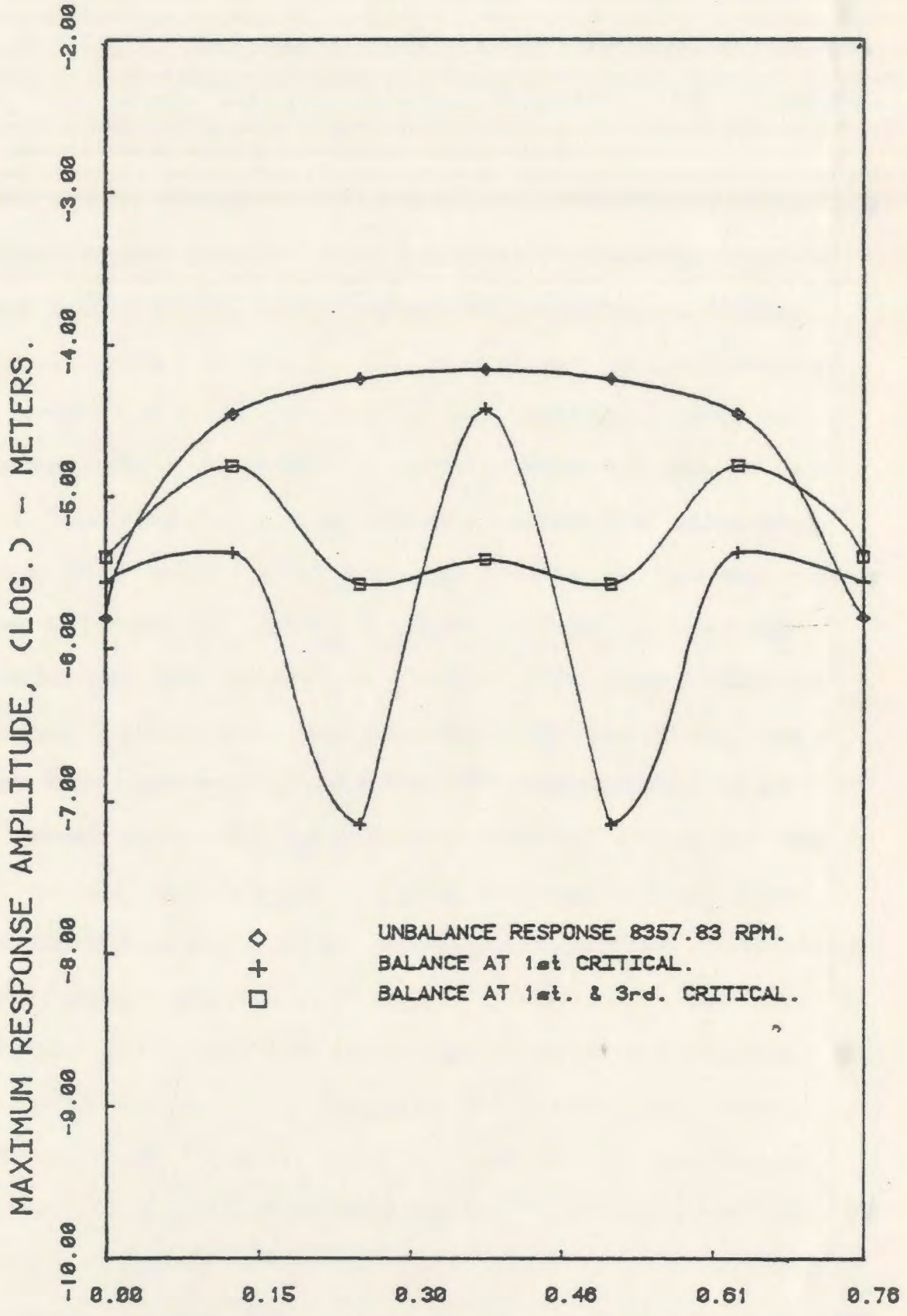

Fig. 3.11 Damped Rotor Response
at Third Critical Speed

the system response, is studied using three balancing planes, as shown in Fig. 3.12, here a_1 and a_2 represent the location of the two outer and inner planes, respectively.

At first, a_1 was varied with a_2 fixed corresponding to the middle of the rotor. The resulting response values are shown in Table 3.7a, and correction weights in Table 3.7b. It is evident from Table 3.7a that as the balancing planes are moved towards the disks, the residual response value decrease. This is because of the flexibility in the rotor shaft, the greater the spacing between the unbalance forces at the disk and the correcting forces in the balancing planes, less will be the effectiveness of the correcting forces in reducing the response. Table 3.7b shows that as these measuring planes are moved in towards the disk, the magnitude of the correction weights in these planes also increases. When these two planes are located close to the disks, most of the correction weights are needed in these variable balancing planes; the weight in the fixed balancing plane is negligibly small.

Table 3.8a and 3.8b show the effect of varying the center balancing plane while keeping the other two fixed. It can be seen in these tables, that as the center balancing plane is moved, both the response as well as the magnitude of the correction weights, increase. In addition the maximum deflection curve, along the length of the rotor, is no longer

m = measuring plane

b = balancing plane

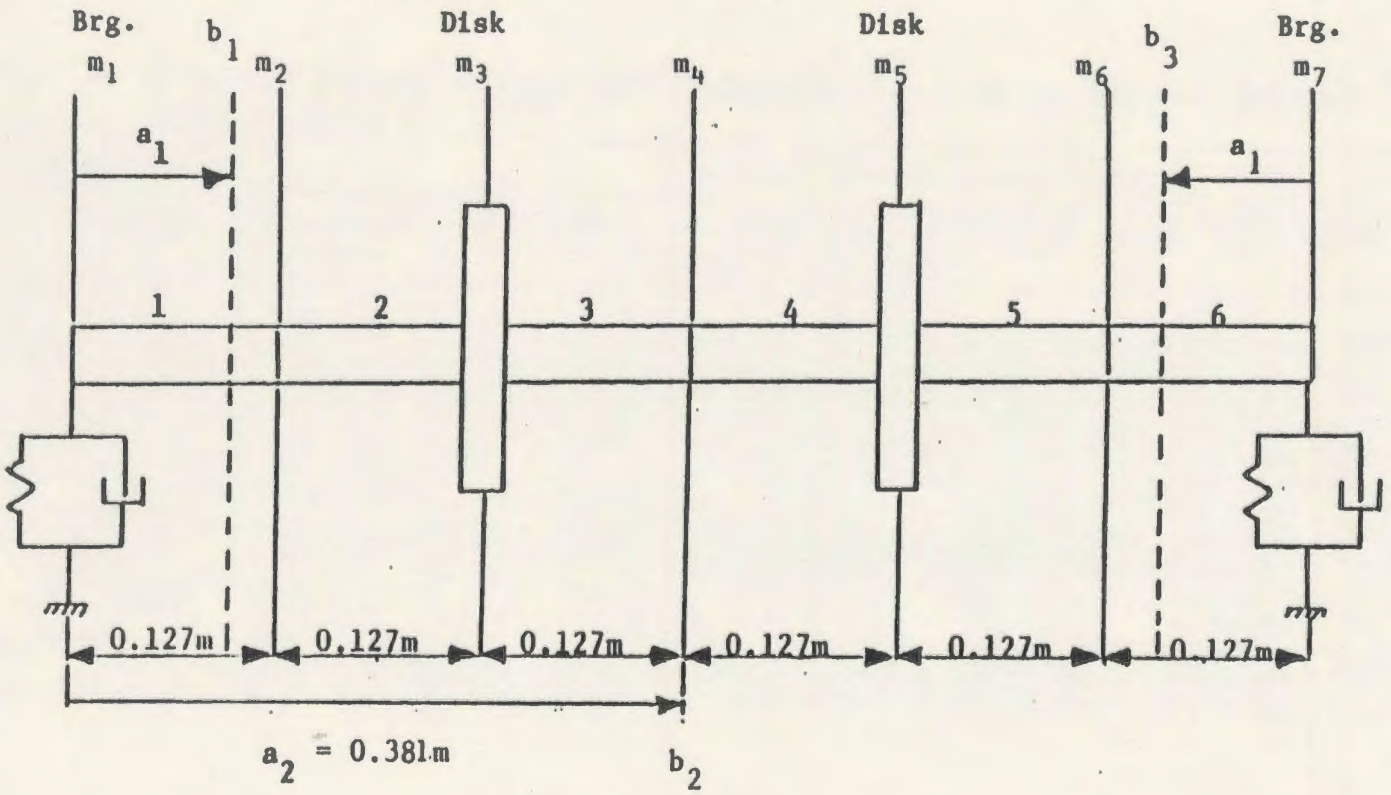

Fig. 3.12 Schematic of a Rotor Bearing System Relative Balance Plane Locations

Table 3.7a Effect of Varying the two Outer Balancing Planes on the Balanced Response for the first Critical Speed

Measuring Plane No.	Distance Along Rotor m	Maximum Response Amplitude - m						
		Unbalanced Response	a_1 = 0.025	a_1 = 0.063	a_1 = 0.127	a_1 = 0.190	a_1 = 0.228	a_1 = 0.292
1	0.0	7.170×10^{-5}	1.394×10^{-6}	1.157×10^{-6}	1.774×10^{-7}	1.736×10^{-9}	1.637×10^{-9}	1.752×10^{-9}
2	0.127	2.964×10^{-4}	9.131×10^{-6}	9.184×10^{-6}	1.006×10^{-6}	9.839×10^{-9}	9.512×10^{-9}	9.888×10^{-9}
3	0.254	6.774×10^{-4}	1.561×10^{-6}	1.547×10^{-5}	1.753×10^{-6}	1.614×10^{-8}	1.564×10^{-8}	1.625×10^{-8}
4	0.381	7.724×10^{-4}	1.889×10^{-5}	1.700×10^{-5}	1.3301×10^{-6}	1.843×10^{-8}	1.785×10^{-8}	1.849×10^{-8}
5	0.508	6.774×10^{-4}	1.561×10^{-5}	1.547×10^{-5}	1.753×10^{-6}	1.614×10^{-8}	1.564×10^{-8}	1.625×10^{-8}
6	0.635	2.964×10^{-4}	9.131×10^{-6}	9.184×10^{-6}	1.006×10^{-6}	9.839×10^{-9}	9.512×10^{-9}	9.888×10^{-9}
7	0.762	7.170×10^{-5}	1.394×10^{-6}	1.157×10^{-6}	1.774×10^{-7}	1.736×10^{-9}	1.637×10^{-9}	1.752×10^{-9}

Table 3.7b Corresponding Balance Weight magnitudes and angles due to the effect of varying the location of the two Outer Balancing Planes

Balancing Plane No.	Calculated Correction Weights											
	$a_1 = 0.025$		$a_1 = 0.063$		$a_1 = 0.127$		$a_1 = 0.190$		$a_1 = 0.228$		$a_1 = 0.292$	
	Weight g	Angle Deg.	Weight g	Angle Deg.	Weight g	Angle Deg.	Weight g	Angle Deg.	Weight g	Angle Deg.	Weight g	Angle Deg.
1	0.54	48.4	13.0	36.2	13.23	37.5	19.35	-44	38.0	-45.0	38.75	44.9
2	66.74	44.3	45.8	50.6	53.8	46.8	0.04	-86	0.001	-37.0	.001	-37.0
3	0.54	48.4	13.0	36.2	13.23	37.5	19.35	-44	38.0	-45.0	38.75	44.9

Table 3.8a Effect of Varying the Middle Balancing Plane on the Balanced Response for the First Critical Speed

Measuring Plane No.	Distance Along Rotor m	Maximum Response Amplitude - m			
		Unbalanced Response	$a_1 = 0.127$ $a_2 = 0.381$	$a_1 = 0.127$ $a_2 = 0.444$	$a_1 = 0.127$ $a_2 = 0.469$
1	0.0	7.170×10^{-5}	1.708×10^{-7}	5.735×10^{-6}	8.023×10^{-6}
2	0.127	2.964×10^{-4}	1.003×10^{-6}	7.665×10^{-6}	1.043×10^{-6}
3	0.254	6.774×10^{-4}	1.750×10^{-6}	1.506×10^{-6}	2.228×10^{-6}
4	0.381	7.724×10^{-4}	1.328×10^{-6}	8.486×10^{-6}	1.101×10^{-6}
5	0.508	6.774×10^{-4}	1.750×10^{-6}	7.848×10^{-6}	1.0127×10^{-6}
6	0.635	2.964×10^{-4}	1.003×10^{-6}	6.538×10^{-6}	8.600×10^{-6}
7	0.762	7.170×10^{-5}	1.708×10^{-7}	5.59×10^{-6}	7.658×10^{-6}

Table 3.8b Corresponding Balance Weight Magnitudes and angles due to the effect of varying the location of the Middle Balancing Plane

Balance Plane No.	Calculated Correction Weight					
	$a_1 = 0.127$ $a_2 = 0.381$		$a_1 = 0.127$ $a_2 = 0.444$		$a_1 = 0.127$ $a_2 = 0.469$	
	Weight	Angle Deg.	Weight	Angle Deg.	Weight	Angle Deg.
1	13.23	-37.5	21.23	-31.86	24.99	-30.76
2	53.8	-46.8	80.11	-46.3	62.0	-46.41
3	13.23	-37.5	21.23	-34.84	24.99	-17.31

symmetrical. The best balance condition, using the locations of the measuring planes (a_1, a_2) as the variable parameters, is achieved when a_1 = 0.228 m and a_2 = 0.381 m. Fig. 3.13 shows the unbalance response along the rotor; the balance response with a_1 = 0.127 m, a_2 = 0.381 m; and the best balance response after the parametric variation, with a_1 = 0.228 m, and a_2 = 0.381 m. It clearly shows that significant benefits can be realized by this parametric variation study.

3.4.7 The Effect of the Number of Balancing Planes on the Rotor Response

In carrying out balancing using the least-square method, an important consideration is the ratio of the number of measuring planes to the balancing plane. In the previous section this ratio used was 7 to 3. The effect of the variation of this ratio on the response, has been studied in this section. The number of the balancing planes have been varied between 3 and 7 while keeping the number of the measuring planes equal to 7. The various plane configurations are shown in Fig. 3.14. The rotor response, as a result of these variations, are shown in Table 3.9a and the corresponding correction weights in Table 3.9b.

Fig. 3.14 shows that when the total number of balancing planes are 5, or 7, there is a balancing plane on the either side of a disk at equal distance, besides a plane at the middle; but there are balancing planes on both sides of the disk at equal distance. The results in Table 3.9a

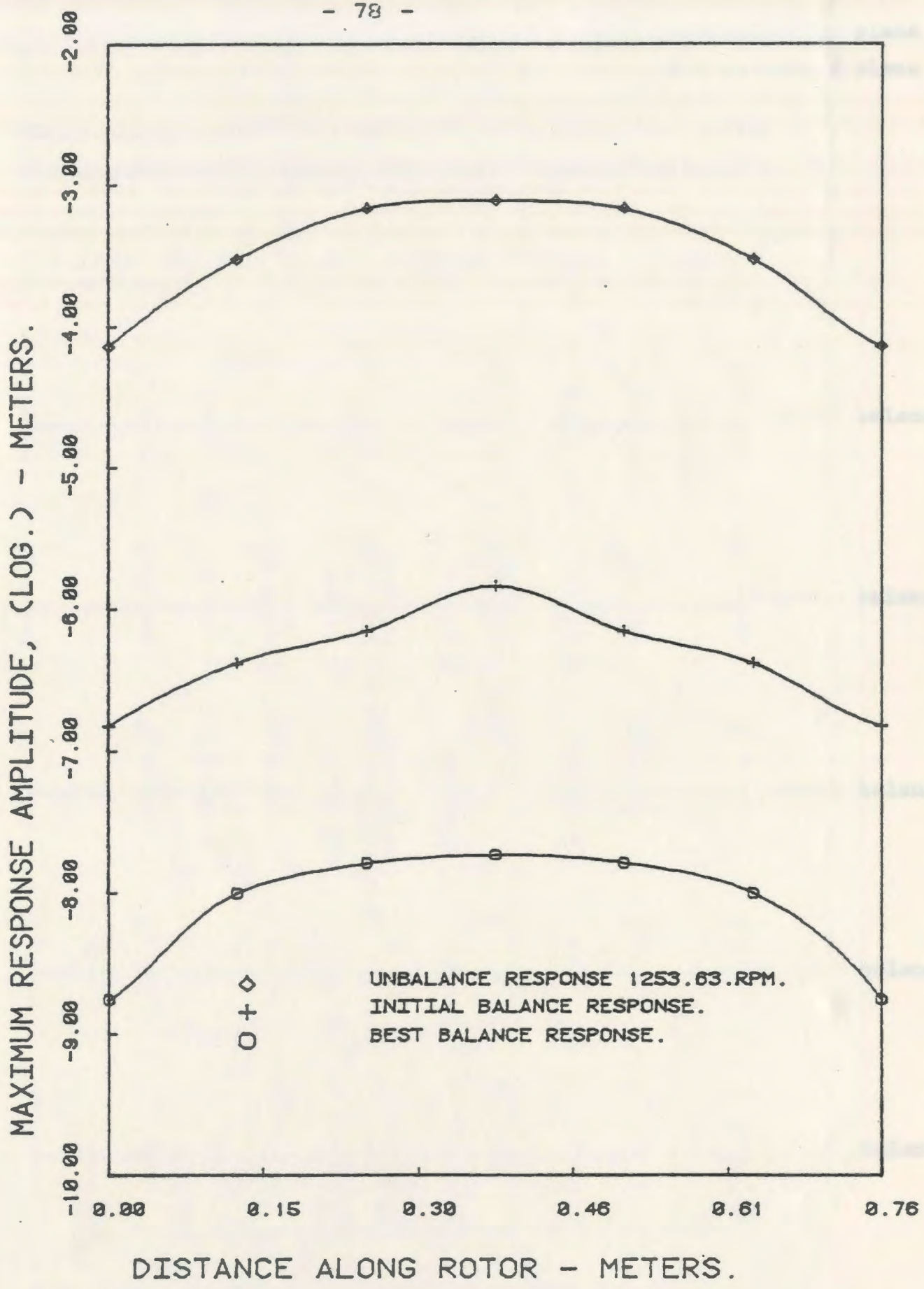

Fig. 3.13 Balance Improvements when Balancing at First Critical by varying the two Outer Planes

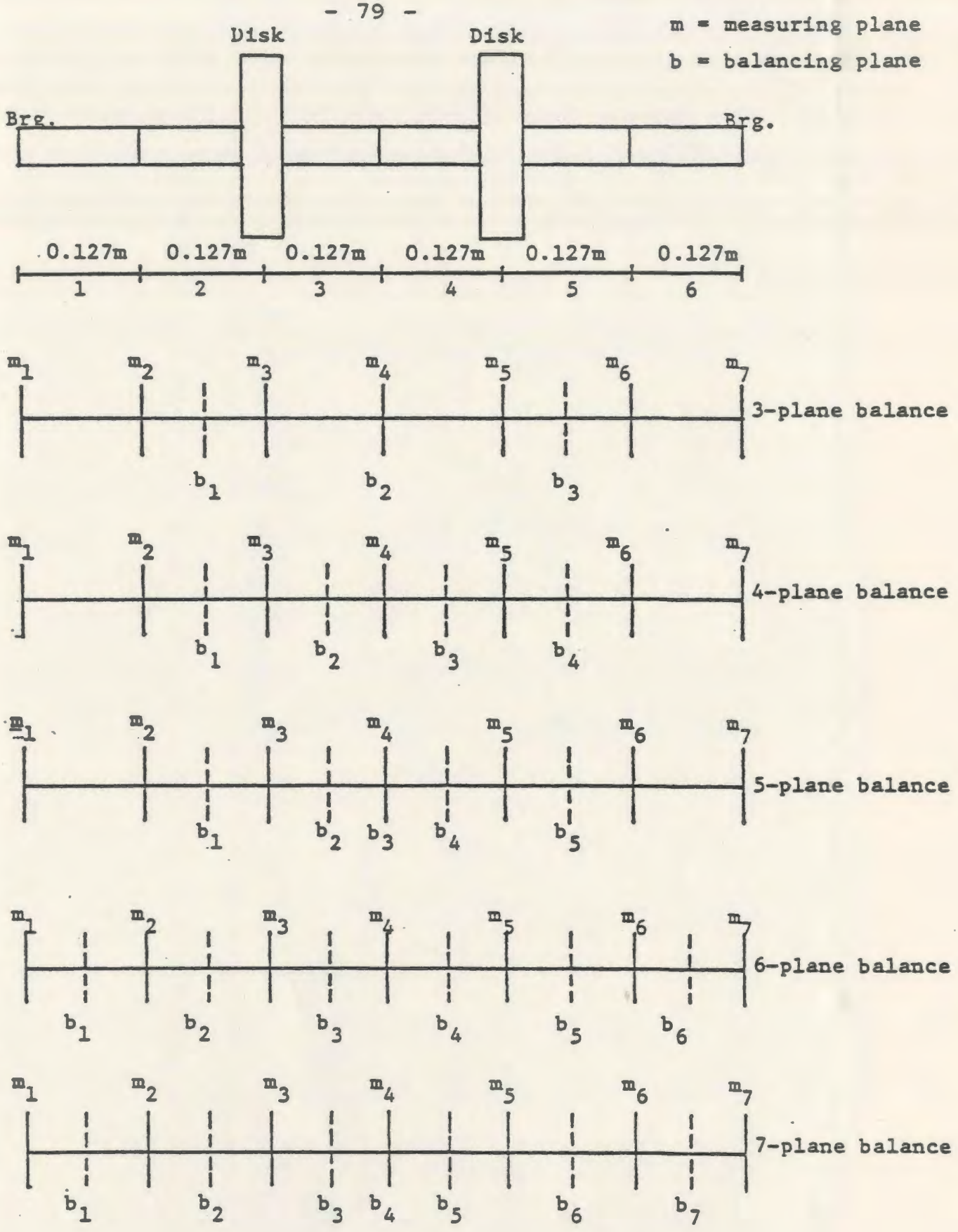

Fig. 3.14 Schematic of the Balancing and Measuring Plane Rotor locations

Table 3.9a Balanced Response Amplitude with Different Number of Balancing Planes

Measuring Plane No.	Distance Along Rotor	Maximum Response Amplitude - m					
		Unbalanced Response	3	4	5	6	7
1	0.0	7.170×10^{-5}	1.736×10^{-9}	1.639×10^{-8}	1.637×10^{-9}	2.103×10^{-8}	2.102×10^{-9}
2	0.127	2.964×10^{-4}	9.839×10^{-9}	9.484×10^{-8}	5.476×10^{-9}	1.282×10^{-7}	1.389×10^{-8}
3	0.254	6.774×10^{-4}	1.614×10^{-8}	1.557×10^{-7}	1.556×10^{-8}	2.118×10^{-7}	2.111×10^{-8}
4	0.381	7.724×10^{-4}	1.843×10^{-8}	1.786×10^{-7}	1.785×10^{-8}	2.395×10^{-7}	2.395×10^{-8}
5	0.508	6.774×10^{-4}	1.614×10^{-8}	1.557×10^{-7}	1.556×10^{-8}	2.112×10^{-7}	2.111×10^{-8}
6	0.635	2.564×10^{-2}	9.837×10^{-9}	9.484×10^{-8}	9.476×10^{-9}	1.282×10^{-7}	1.389×10^{-8}
7	0.762	7.170×10^{-5}	1.736×10^{-9}	1.637×10^{-8}	1.637×10^{-9}	2.103×10^{-8}	2.102×10^{-9}

Table 3.9b Corresponding Balance Weight magnitudes and angles due to the number of Balancing Planes

Balancing Plane No.	Calculated Correction Weights									
	Number of Balancing Planes									
	3		4		5		6		7	
	Weight g	Angle Deg.	Weight g	Angle Deg.	Weight g	Angle Deg.	Weight g	Angle Deg.	Weight g	Angle Deg.
1	19.35	-44.0	19.35	-46.2	19.35	-37.2	0.002	-75.3	0.002	-73.6
2	00.4	-86.0	19.35	-43.4	19.35	-38.4	19.35	-39.6	19.35	-38.4
3	19.35	-44.0	19.35	-43.4	0.009	-43.0	19.35	-45.0	19.35	-43.2
4	--	--	19.35	-46.2	19.35	-38.4	19.35	-45.0	0.006	-16.0
5	--	--	--	--	19.35	-37.2	19.35	-39.6	19.35	-43.2
6	--	--	--	--	--	--	0.02	-75.3	19.35	-38.4
7	--	--	--	--	--	--	--	--	0.002	-73.6

show that the odd number of balancing planes yield better results than the even number of these planes. Among the odd number of planes, the best results are obtained when the balancing planes are equal to 5. The results shown in Table 3.9b indicate that for odd number of balancing planes, the correction weight in the middle balancing plane, is very small. This indicates that the forces generated due to the correction weights located near the disks, are mainly responsible for the balance condition. It was also reported by Tessarzik [28] that increasing the number of balancing planes does not necessarily lead to better balance results.

3.5 Conclusions

The finite element approach provides a convenient and accurate means of balancing a multi-rotor system, supported on fluid-film bearings. The use of matrix reduction technique in calculation of the reduced set of system matrices, enabled subsequent saving in computational memory storage of 42 percent, and that of computational time for a balancing run of almost 38 percent. Besides, in the reduction process, the retained degrees were the translational degree of freedom, therefore one could work with the reduced system only. There was no necessity of recovering all the degree of freedom where the rotational degrees were also included. The modal analysis gives an

effective means of determining the unbalance force response, and the relevant mode information. The use of least-square method, for the case investigated, provided good results, whereby balancing at the first critical speed was sufficient to bring the rotor amplitude down over the other critical speeds also. Further, by varying the number and location of balancing planes, better balance conditions were achieved. The results revealed that when using least-square method, the odd number of balancing planes yield better results than even number of balancing planes.

CHAPTER 4

CONCLUSIONS AND RECOMMENDATIONS

4.1 A Brief Discussion of Modelling and Results

The objective of this investigation has been to calculate the dynamic response of the rotor-bearing systems, and then to reduce these response values using balancing techniques.

A mathematical model using finite element analysis, where the translational and rotational inertia and the gyroscopic moment effects have been considered, has been formulated. The rotor shaft has been supported by fluid-film bearings having asymmetrical stiffness and damping properties. In order to reduce the size of the system matrices, a dynamic matrix reduction technique has been used. The dynamic response values have been obtained using a modified modal analysis method where the orthogonality relationship of the modes of the original, and that of the adjoint system have been used. The balancing has been carried out by the least-square method which is generally used in situations where the number of measuring planes are greater than the balancing planes. The analytically derived relationships are illustrated by suitable numerical examples.

Based on this investigation the following conclusions can be drawn:

(1) A comprehensive mathematical model of the rotor system is developed which utilizes finite element method in conjunction with modal analysis, and the least-square balancing technique.

(2) The dynamic matrix reduction technique is effective in reducing the original system accurately to provide computational savings in both time and space on the digital computer.

(3) The analytical model enables balancing at critical speed which is more efficient than balancing below critical speeds normally done when balancing rotors on test stands.

(4) The parametric variation study, where the number of measuring planes and their locations are used as design variables, leads to significant improvements in the balance condition.

(5) The odd number of balancing planes yield better results then even number of balancing planes.

(6) The increase in number of balancing planes for a given number of measuring planes, does not necessarily lead to improved results.

(7) The effect of gyroscopic moments, on the dynamic response of rotors supported on fluid-film bearings, is insignificant.

4.2 Industrial Applications of this Investigation

The technique adopted in this investigation is fairly general. The technique can be used for rotors of pumps, compressor, turbines, fans, etc., without any change in the methodology. The rotor system to be analyzed can include:

(i) multi-rotor systems

(ii) multi-bearing supports

(iii) variable shaft diameters

(iv) distributed mass centre eccentricity of elements, and out of plane disk unbalance.

4.3 Limitations of the Investigation

The approach used in the present investigation in optimally balancing a rotor bearing system, has the following limitations:

(1) The rotor system has been assumed to exhibit a linear behaviour.

(2) The shear deformation, torsional effects, and material damping have been assumed to be neglible.

(3) The analysis makes the assumption that the bearing pedestal and housing are infinitely stiff in comparision with the oil film.

4.5 Recommendations for Future Work

The basic purpose of this investigation was to balance the flexural response of a rotor bearing system due

to mass unbalance. This work can be extended into several areas which are listed below:

(1) The rotor can be further generalized to include the effects of shear deformation, torsional effects, axial loads, material damping and shaft hysteresis.

(2) The system can be made to include stiffness of the foundation.

(3) The rotor can be analyzed to include thermal effects on the bearing housing and pedestal deformations.

(4) Schemes of optimization using multi-plane balancing can be included.

(5) The influence of casing stiffness in turbomachinery vibration can be studied.

(6) The response of the system due to seismic excitation can be analyzed.

(7) The dynamic response of the system under the random excitation can be studied.

(8) The influence of bearing stiffness and damping coefficients on the unbalance response and balancing of rotor disks.

REFERENCES

1. Rao, J. S., "Rotor Dynamics", Wiley Eastern, New Delhi, India 1983, Chapters 2, 4, 5, 6, 7, 8, 12 and 13.

2. Lund, J. W., and Orcutt, F. K., "Calculations and Experiments on the Unbalance Response of a Flexible Rotor", ASME, Journal of Engineering for Industry, Vol. 89, Nov. 1966, pp. 785-796.

3. Lund, J. W., "Modal Response of a Flexible Rotor in Fluid Film Bearings", ASME, Journal of Engineering for Industry, Vol. 96, No. 2, 1974, pp. 525-533.

4. Hurty, W. C., Rubinstein, M. F., "Dynamic of Structures" Prentice Hall, Englewood Cliffs, New Jersey, 1964, pp. 210-15.

5. Ruhl, R., "Dynamic of Distributed Parameter Rotor Systems: Transfer Matrix and Finite Element Techniques", Ph.D Thesis, Cornell University, 1970.

6. Archer, J. S., "Consistent Matrix Formulations for Structural Analysis Using Finite-Element Techniques", American Institute of Aeronautics Journal, Vol. 3, 1965, pp. 1910-1918.

7. Prohl, M. A., "A General Method of Calculating Critical Speed of Flexible Rotors", Journal of Applied Mech., Vol. 12, No. 3, Trans. ASME, Vol. 67, Sept 1945, pp. A-142.

8. Eshleman, R. L., "Critical Speeds and Response of Flexible Rotor Systems", Flexible Rotor-Bearing System Dynamics, ASME, Vol. 1, 1972.

9. Nelson, H. D. and McVaugh, J. N., "The Dynamics of Rotor Bearing System Using Finite Elements", Journal of Engineering for Industry, Vol. 98, 1976, pp. 593-602.

10. Rouch, K. E., and Kao, J. S., "Dynamic Reduction in Rotor Dynamics by the Finite Element Method", Journal of Engineering for Industry, Vol. 102, 1980, pp. 360-368.

11. Cook, R. D., "Concepts and Applications of Finite Element Analysis", 2nd ed., John Wiley and Sons, New York, pp. 313, 1981.

12. Rao, J. S., "Conditions for Backward Synchronous Whirl of a Flexible Rotor in Hydrodynamic Bearings", Mechanism and Machine Theory Journal, Vol. 17, No. 2, 1982, pp. 143-152.

13. Rao, J. S., Bhat, R. B. and Sankar, T. S., "Effect of Damping on the Synchronous Whirl of a Rotor in Hydrodynamic Bearings", Trans. CSME, Vol. 6, No. 3, 1981.

14. Ardayfio, D. and Frohrib, D. A., "Vibration of an Asymmetrically Mounted Rotor with Gyroscopic Effects", Trans. ASME, Journal of Engineering for Industry, Feb. 1976, pp. 327.

15. Rao, J. S., "Out of Balance Response of Turbo-Alternator Rotors", Computer Program, Bharat Heavy Electricals Ltd., Hyderabad, India, 1980.

16. Lund, J. W., "Rotor Bearings Dynamics Design Technology, Part V: Computer Program Manual for Rotor Response and Stability", Mechanical Technology Inc., Latham, N.Y., AFAPL-Tr-65-45, 1965.

17. Subbiah, R., Bhat, R. B., and Sankar, T. S., "Unbalance Response of a Single Mass Rotor Mounted on Dissimilar Hydro-Dynamic Bearings", Presented at 53rd. Shock and Vibration held at Danvers, MA., 1982.

18. Gunter, E. J., Choy, K. C., and Allaire, P. E., "Modal Analysis of Turborotors Using Planar Modes Theory", Journal of Franklin Institute, Vol. 305, No. 4, April 1978.

19. Berthier, P., Ferraris, G. and Lalanne, M., "Prediction of Critical Speed, Unbalance and Nonsynchronous Forced Response of Rotors", present at 53rd Shock and Vibration Symposium held at Danvers, MA., 1982.

20. Saito, S. and Azuma, T., "Balancing of Flexible Rotors by the Complex Modal Method", Paper No. 81-DET-46, ASME Design Engineering Conference, Hartford, 1981.

21. Bhat, R. B., "Unbalance Response of a Single Mass Rotor on Fluid Film Bearings Using Modal Analysis", Proceedings of the 1st International Modal Analysis Conference held at Orlando, 1982, pp. 648.

22. Bhat, R. B., Subbiah, R., Sankar, T. S., "Dynamic Behaviour of a Simple Rotor with Dissimilar Hydro-Dynamice Bearings by Modal Analysis", Paper No. 83-Det-75, ASME.

23. Gunter, E. T., Barrett, L. E., and Allaire, P. E., "Balancing of Multimass Flexible Rotors", Proceedings of the Fifth Turbomachinery Symposium, 1978.

24. Bishop, R. E. D., and A. G. Parkinson, "Vibrations and Balancing of Flexible Shafts", Applied Mechanics Review, Vol. 20, No. 5, May 1968, p. 439.

25. Goodman, T. P., "A Least Square Method for Computing Balance Corrections", Journal of Engineering for Industry, Trans. ASME, Series B, Vol. 86, No. 3, Aug. 1964, pp. 273-279.

26. Tessarzik, J. M., Badgley, R. H., and Anderson, W. J., "Flexible Rotor Balancing by the Exact Point-Speed Influence Coefficient Method", Journal of Engineering for Industry, TRANS. ASME, Feb. 1972, p. 148.

27. Rieger, N. F., "Computer Program for Balancing of Flexible Rotors", Technical Report MTI 6TTR68, prepared by Mechanical Technology Incorporated, Latham, N.Y., for the NASA-Lewis Research Centre, Sept. 1967.

28. Tessarzik, J. M., Badgley, R. H., "Experimental Evaluation of the Exact Point-Speed and Least Square Procedures for Flexible Rotor Balancing by the Influence Coefficient Method", Journal of Engineering for Industry, May 1974, pp. 633-643.

29. Lund, J. W., "Rotor Bearings Dynamic Design Technology", Part III: Design Handbood for fluid film bearings, Mechanical Technology Inc., AFAPL-TR-65-45, 1965.

30. Timoshenko, S., "Vibration Problems in Engineering", 3rd. ed., in collaboration with D. H. Young, D. Van Nostrand Company, Inc., Princeton, N.J., 1955.

31. Pilkey, W. D., and Chang, P. Y., "Modern Formulas for Statics and Dynamics", McGraw Hill Book Co., 1978.

32. Bigret, R., "Vibrations des Machines Tournantes et des Structures", Tome I to IV, Technique et documentution, Paris, 1980.

33. Lund, J. W., Tonnesen, J., "Analysis and Experiments on Multi-Plane Balancing of a Flexible Rotor", Journal of Engineering for Industry, Feb. 1972, pp. 233-241.

APPENDIX-A

COMPONENT EQUATIONS OF A ROTOR BEARING SYSTEM

A.1 Finite Rotor Element Model

In order to obtain the expressions for the elemental mass, gyroscopic, damping, and stiffness matrices, Lagrange's equation of motion is used.

A typical finite rotor element is shown in Fig. A.1 It should be noted that the time dependent cross-section displacements (V, W, B, Γ) are also functions of position (s) along the axis of the element. The rotations (B, Γ) are related to the translations (V, W) by the equations

$$B = -\frac{\partial W}{\partial s},$$

$$\Gamma = \frac{\partial V}{\partial s} . \qquad (A.1)$$

The coordinates (q_1^e, q_2^e, ... q_8^e) are the time dependent end point displacements (translations and rotations) of the finite rotor element. Thus a joint can undergo both translational and rotational displacements. Correspondingly, there are not only inertial forces to consider but also bending moments. The translation of a typical point internal to the elment is chosen to obey the relation [9]

$$\begin{Bmatrix} V(s,t) \\ W(s,t) \end{Bmatrix} = [\psi(s)] \{q^e(t)\} \qquad (A.2)$$

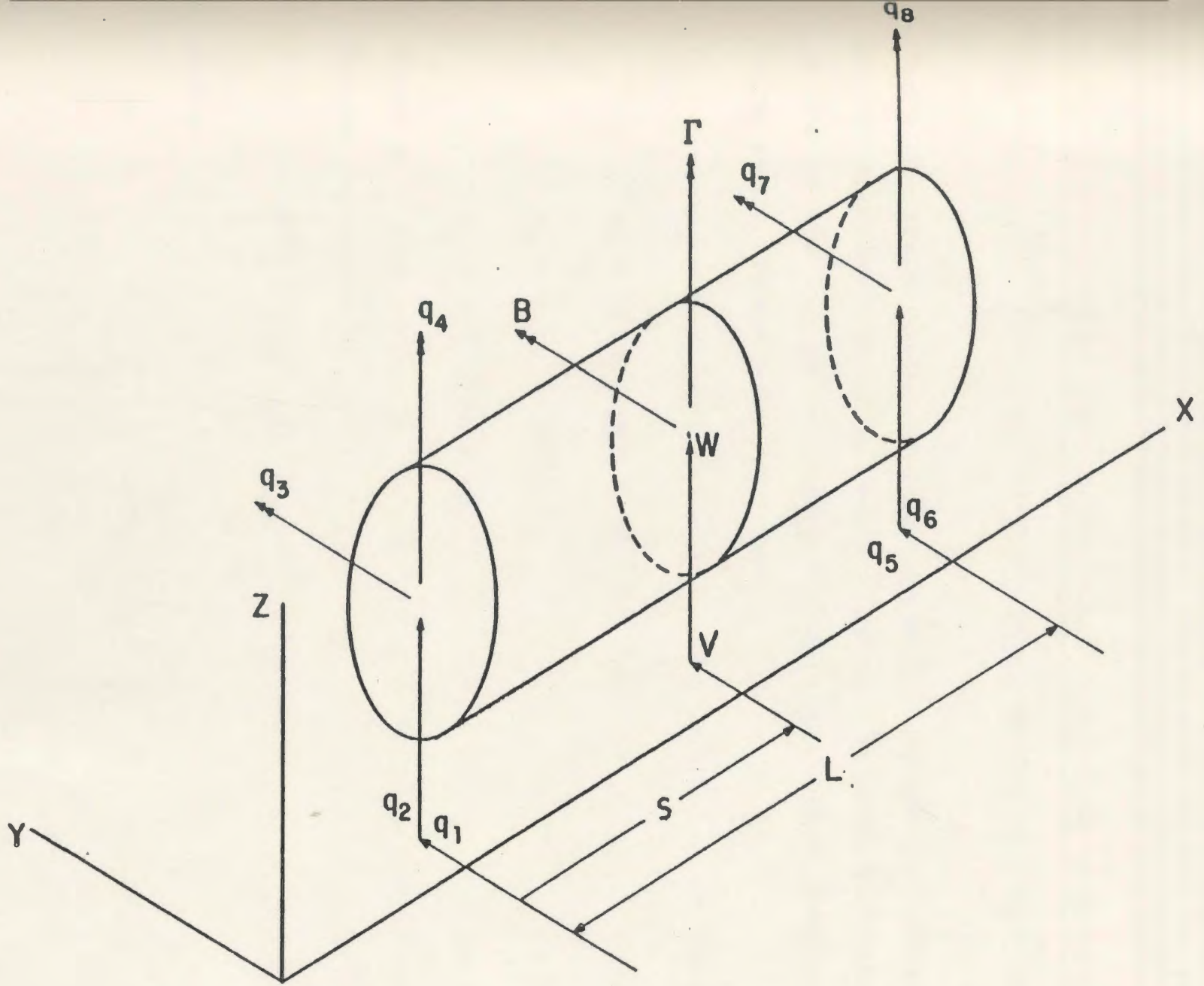

Fig. A.1 Typical finite rotor element and coordinates.

where $[\psi(s)]$ represents the spatial constraint matrix, s is the local position coordinate, and $\{q^e(t)\}$ is the joint displacement vector. The spatial constraint matrix is given by

$$[\psi] = \begin{bmatrix} \psi_1 & 0 & 0 & \psi_2 & \psi_3 & 0 & 0 & \psi_4 \\ 0 & \psi_1 & -\psi_2 & 0 & 0 & \psi_3 & \psi_4 & 0 \end{bmatrix} \tag{A.2a}$$

where the shape functions comprising the matrix are given by static displacement modes associated with a unit displacement of one of the end point coordinate with all other constraints to be zero. These functions are

$$\psi_1 = 1 - 3\left(\frac{s}{\ell}\right)^2 + 2\left(\frac{s}{\ell}\right)^3 \tag{A.3a}$$

$$\psi_2 = s\left[1 - 2\left(\frac{s}{\ell}\right) + \left(\frac{s}{\ell}\right)^2\right] \tag{A.3b}$$

$$\psi_3 = 3\left(\frac{s}{\ell}\right)^2 - 2\left(\frac{s}{\ell}\right)^3 \tag{A.3c}$$

$$\psi_4 = \ell\left[-\left(\frac{s}{\ell}\right)^2 + \left(\frac{s}{\ell}\right)^3\right] \tag{A.3d}$$

where ℓ is the length of an element. Similarly the rotation can be expressed as

$$\begin{Bmatrix} B \\ \Gamma \end{Bmatrix} = [\Phi]\ \{q^e\} \tag{A.4}$$

where

$$[\Phi] = \begin{Bmatrix} [\Phi_B] \\ [\Phi_\Gamma] \end{Bmatrix} = \begin{bmatrix} 0 & -\psi_1' & \psi_2' & 0 & 0 & -\psi_3' & \psi_4' & 0 \\ \psi_1' & 0 & 0 & \psi_2' & \psi_3' & 0 & 0 & \psi_4' \end{bmatrix} \tag{A.4a}$$

The matrix $[\phi]$ represents a matrix of rotation shape function.

For a differential disk located at (s) the elastic bending and kinetic energy expressions are respectively

$$d\,\bar{P}_B^{\,e} = \frac{1}{2}\begin{Bmatrix} V'' \\ W'' \end{Bmatrix}^T \begin{bmatrix} EI & 0 \\ 0 & EI \end{bmatrix} \begin{Bmatrix} V'' \\ W'' \end{Bmatrix}$$

$$d\,\bar{T}^e = \frac{1}{2}\begin{Bmatrix} \dot{V} \\ \dot{W} \end{Bmatrix}^T \begin{bmatrix} u & 0 \\ 0 & u \end{bmatrix} ds + \frac{1}{2}\,\dot{\phi}^2\,\bar{I}_p ds$$

$$+ \frac{1}{2}\begin{Bmatrix} \dot{B} \\ \dot{\Gamma} \end{Bmatrix}^T \begin{bmatrix} I_D & 0 \\ 0 & I_D \end{bmatrix} \begin{Bmatrix} \dot{B} \\ \dot{\Gamma} \end{Bmatrix} ds - \dot{\phi}\,\dot{\Gamma}\,B\,\bar{I}_p\,ds \qquad \ldots\ (A.5)$$

where

E = modulas of elasticity

I_D = diametrial moment of inertia

$\bar{I}_p$ = element diametrial inertia

$\dot{\phi}$ = spin speed

m = element mass per . unit length

Rewriting Eqn. (A.5) using spatial shape functions, one obtains

$$d\,\bar{P}_B^{\,e} = \frac{1}{2} EI \{q^e\}^T [\phi'']^T [\phi''] \{q^e\}\, ds$$

$$d\,\bar{T}^e = \frac{1}{2} \mu \{\dot{q}^e\}^T [\phi]^T [\phi] \{\dot{q}^e\}\, ds$$

$$+ \frac{1}{2} \dot{\phi}^2 \bar{I}p\, ds + \frac{1}{2} \bar{I}_D \{\dot{q}^e\} [\Phi]^T [\Phi] \{\dot{q}^e\}\, ds$$

$$- \dot{\phi}\, \bar{I}_p \{\dot{q}^e\}^T [\Phi_\Gamma]^T [\Phi_B] \{q^e\}\, ds \quad .... \quad (A.6)$$

The energy of the complete system is obtained by integrating Eqn. (A.6) over the length of the element to obtain

$$\bar{P}_B^{\,e} + T^e = \frac{1}{2} \{q^e\}^T [K_B^{\,e}]$$

$$+ \frac{1}{2} \{\dot{q}^e\}^T ([M_T^{\,e}] + [M_R^{\,e}]) \{\dot{q}^e\}$$

$$+ \frac{1}{2} I_p^{\,e} \dot{\phi}^2 + \dot{\phi} \{\dot{q}^e\}^T [N^e] \{q^e\}$$

.... (A.7)

where,

$$[M_T^{\,e}] = \int_0^{\ell} \mu [\Psi]^T [\Psi]\, ds, \qquad (i)$$

$$[M_R^{\,e}] = \int_0^{\ell} \bar{I}_D [\phi]^T [\phi]\, ds, \qquad (ii)$$

$$[N^e] = \int_0^{\ell} \bar{I}_p [\Phi_\Gamma]^T [\Phi_B]\, ds, \qquad (iii)$$

$$[K_B^{\,e}] = \int_0^{\ell} EI [\Psi'']^T [\Psi'']\, ds \qquad (iv)$$

The Lagrangian equation of motion for finite rotor element using Eqn. (A.7) and constant spin speed restriction $\dot{\phi} = \Omega$, is

$$([M_T^e] + [M_R^e])\ \{\ddot{q}^e\} - \Omega\ [G^e]\ \{\dot{q}^e\}$$

$$+ [K_B^e]\ \{q^e\} = \{Q^e\} \qquad \ldots\ (A.9)$$

with

$$[G^e] = ([N^e] - [N^e]^T)$$

where $[M^e]$, $[G^e]$, $[K^e]$ represent the mass, gyroscopic, and stiffness matrices. The vector $\{Q\}$ and $\{q\}$ represent the unbalance forces and the displacement vector respectively. The subscripts d, e refer to disk and element, and the subscripts B, T, R refer to bending, translational and rotational loads respectively. The forcing vector $\{Q^e\}$ representing mass eccentricity is equivalently represented by a force using the consistent matrix approach introduced by Archer [6], is given by

$$\{Q^e\}_{8x1} = \int_0^{\ell} \mu\ \Omega^2\ [\psi]^T \begin{Bmatrix} \eta(s) \\ \zeta(s) \end{Bmatrix} \cos\ \Omega t + \begin{Bmatrix} -\zeta(s) \\ \eta(s) \end{Bmatrix} \sin\ \Omega t\ ds$$

$$= \{Q_c^e\}\ \cos\ \Omega t + \{Q_s^e\}\ \sin\ \Omega t \quad \ldots\ (A.10)$$

For the case of a linear distribution over the element, the shape function expressions are given as

$$\eta(s) = \eta_L \left(1 - \frac{s}{\ell}\right) + \eta_R \left(\frac{s}{\ell}\right)$$

$$\zeta(s) = \zeta_L \left(1 - \frac{s}{\ell}\right) + \zeta_R \left(\frac{s}{\ell}\right) \qquad \ldots\ldots (A.11)$$

with (η_L, ζ_L) and (η_R, ζ_R) denoting the mass centre eccentricity at s=0 and s=ℓ respectively. The elemental matrices thus formulated are presented in Appendix B.

A.2 Rigid Disk Formulation

The kinetic energy of a typical rigid disk with mass centre coincident with the elastic rotor centerline is given by the expression [9]

$$\bar{T}_d = \frac{1}{2}\begin{Bmatrix} \dot{V} \\ \dot{W} \end{Bmatrix}^T \begin{bmatrix} m_d & 0 \\ 0 & m_d \end{bmatrix} \begin{Bmatrix} \dot{V} \\ \dot{W} \end{Bmatrix} + \frac{1}{2}\begin{Bmatrix} \dot{B} \\ \dot{\Gamma} \end{Bmatrix}^T \begin{bmatrix} I_D & 0 \\ 0 & I_D \end{bmatrix} \begin{Bmatrix} \dot{B} \\ \dot{\Gamma} \end{Bmatrix} - \dot{\phi}\,\dot{\Gamma}\, B\, I_p$$

$\ldots\ldots (A.12)$

The Lagrangian equation of motion of the rigid disk using Eqn. (A.12) with constant speed Ω relative to τ is

$$([M_T{}^d] + [M_R{}^d])\,\{\ddot{q}^d\} - \Omega\,[G^d]\,\{\dot{q}^d\} = \{Q^d\}$$

$\ldots\ldots (A.13)$

where $[M^d]$ and $[G^d]$ represent the mass and the gyroscopic matrices and $\{q\}$ represents the time dependent translations and rotations.

The forcing vector $\{Q^d\}$ represents mass unbalance. For a disk centre located at (η_d, ζ_d) relative to T, the unbalance force in $\mathbb{H}$ is

$$\{Q^d\} = m_d\Omega^2 \begin{Bmatrix} \eta_d \\ \zeta_d \\ 0 \\ 0 \end{Bmatrix} \cos \Omega t + m_d\Omega^2 \begin{Bmatrix} -\zeta_d \\ \eta_d \\ 0 \\ 0 \end{Bmatrix} \sin \Omega t \quad \text{(A.14)}$$

$$= \{Q_c{}^d\} \cos \Omega t + \{Q_s{}^d\} \sin \Omega t$$

The elemental matrices thus formulated are presented in Appendix B.

APPENDIX-B

MATRICES OF A ROTOR BEARING SYSTEM

B.1 Finite Shaft Element Matrices

$$[M_T^e]=\frac{\mu\ell}{420}\begin{bmatrix}
156 & & & & & & & \\
0 & 156 & & & & & & \\
0 & -22\ell & 4\ell^2 & & & & & \\
22\ell & 0 & 0 & 4\ell^2 & & \text{Sym} & & \\
54 & 0 & 0 & 13\ell & 156 & & & \\
0 & 54 & -13\ell & 0 & 0 & 156 & & \\
0 & 13\ell & -3\ell^2 & 0 & 0 & 22\ell & 4\ell^2 & \\
-13\ell & 0 & 0 & -3\ell^2 & -22\ell & 0 & 0 & 4\ell^2
\end{bmatrix}$$

$$[M_R^e]=\frac{\mu r^2}{120\ell}\begin{bmatrix}
36 & & & & & & & \\
0 & 36 & & & & & & \\
0 & -3\ell & 4\ell^2 & & & & & \\
3\ell & 0 & 0 & 4\ell^2 & & \text{Sym} & & \\
-36 & 0 & 0 & -3\ell & 36 & & & \\
0 & -36 & 3\ell & 0 & 0 & 36 & & \\
0 & -3\ell & -\ell^2 & 0 & 0 & 3\ell & 4\ell^2 & \\
3\ell & 0 & 0 & -\ell^2 & -3\ell & 0 & 0 & 4\ell^2
\end{bmatrix}$$

$$[G^e]=\frac{2\mu r^2}{120\ell}\begin{bmatrix}
0 & & & & & & & \\
36 & 0 & & & & & & \\
-3\ell & 0 & 0 & & & & & \\
0 & -3\ell & 4\ell^2 & 0 & & \text{Sym} & & \\
0 & 36 & -3\ell & 0 & 0 & & & \\
-36 & 0 & 0 & -3\ell & 36 & 0 & & \\
-3\ell & 0 & 0 & \ell^2 & 3\ell & 0 & 0 & \\
0 & -3\ell & -\ell^2 & 0 & 0 & 3\ell & 4\ell^2 & 0
\end{bmatrix}$$

Finite Shaft Element Matrices

$$[K_B{}^e] = \frac{EI}{\ell^3} \begin{bmatrix} 12 & & & & & & & \\ 0 & 12 & & & & & & \\ 0 & -6\ell & 4\ell^2 & & & & & \\ 6\ell & 0 & 0 & 4\ell^2 & & \text{Sym.} & & \\ -12 & 0 & 0 & -6\ell & 12 & & & \\ 0 & -12 & 6\ell & 0 & 0 & 12 & & \\ 0 & -6\ell & 2\ell^2 & 0 & 0 & 6\ell & 4\ell^2 & \\ 6\ell & 0 & 0 & -6\ell & -6\ell & 0 & 0 & 4\ell^2 \end{bmatrix}$$

B.2 Finite Element Unbalance Force Vector

$$\{Q_c{}^e\}=\mu\Omega^2\begin{Bmatrix} \frac{7}{20}\eta_L\ell+\frac{3}{20}\eta_R\ell \\ \frac{7}{20}\zeta_L\ell+\frac{3}{20}\zeta_R\ell \\ -\frac{1}{20}\zeta_L\ell^2-\frac{1}{30}\zeta_R\ell^2 \\ \frac{1}{20}\eta_L\ell^2+\frac{1}{30}\eta_R\ell^2 \\ \frac{3}{20}\eta_L\ell+\frac{7}{20}\eta_R\ell \\ \frac{3}{20}\zeta_L\ell+\frac{7}{20}\zeta_R\ell \\ \frac{1}{30}\zeta_L\ell^2+\frac{1}{20}\zeta_R\ell^2 \\ -\frac{1}{30}\eta_L\ell^2-\frac{1}{20}\eta_R\ell^2 \end{Bmatrix}$$

$$\{Q_s{}^e\}=\mu\Omega^2\begin{Bmatrix} -\frac{7}{20}\zeta_L\ell-\frac{3}{20}\zeta_R\ell \\ \frac{7}{20}\eta_L\ell+\frac{3}{20}\eta_R\ell \\ -\frac{1}{20}\eta_L\ell^2-\frac{1}{30}\eta_R\ell^2 \\ -\frac{1}{20}\zeta_L\ell^2-\frac{1}{30}\zeta_R\ell^2 \\ -\frac{3}{20}\zeta_L\ell-\frac{7}{20}\zeta_R\ell \\ \frac{3}{20}\eta_L\ell+\frac{7}{20}\eta_R\ell \\ \frac{1}{30}\eta_L\ell^2+\frac{1}{20}\eta_R\ell^2 \\ \frac{1}{30}\zeta_L\ell^2+\frac{1}{20}\zeta_R\ell^2 \end{Bmatrix}$$

B.3 Rigid Disk Matrices

$$[M_T{}^d] = \begin{bmatrix} m_d & 0 & 0 & 0 \\ 0 & m_d & 0 & 0 \\ 0 & 0 & 0 & 0 \\ 0 & 0 & 0 & 0 \end{bmatrix}$$

$$[M_R{}^d] = \begin{bmatrix} 0 & 0 & 0 & 0 \\ 0 & 0 & 0 & 0 \\ 0 & 0 & I_D & 0 \\ 0 & 0 & 0 & I_D \end{bmatrix}$$

$$[G^d] = \begin{bmatrix} 0 & 0 & 0 & 0 \\ 0 & 0 & 0 & 0 \\ 0 & 0 & 0 & I_P \\ 0 & 0 & I_P & 0 \end{bmatrix}$$

* $I_P = 2I_D$

B.4 Rigid Disk Unbalance Force Vector

$$\{Q_c{}^d\} = \begin{Bmatrix} \eta_d \\ \zeta_d \\ 0 \\ 0 \end{Bmatrix} \text{ and } \quad Q_s{}^d = \begin{Bmatrix} -\zeta_d \\ \eta_d \\ 0 \\ 0 \end{Bmatrix}$$

APPENDIX-C

GYROSCOPIC EFFECT FORMULATION

Rotating shafts of turbines, compressors, pumps, etc. carry one or more disk, which with angular momentum can under certain conditions introduce a gyroscopic couple. In a particular mode shape if the disk is located at the nodal point, there will be precession and obvious gyroscopic couple. And in antinodal point, there will be pure translation of disk. This effect is illustrated in Fig. C.1 for a simply supported two disks.

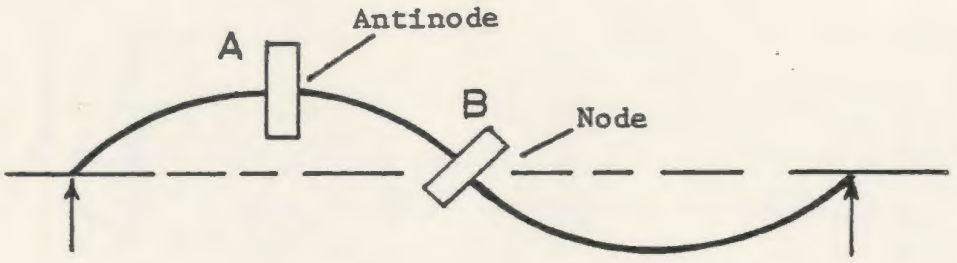

Fig. C.1 Disk at Nodal Points

In the mode shape shown, the disc 'A' will go through a pure translation and disk 'B' would have angular momentum or gyroscopic couple. But for cases where the disk is located in between the nodal points it will be subjected to both translation and angular momentum as rotation. This has considerable influence on the dynamic behaviour of the system.

From practical point of view gyroscopic couple has effect on both critical speed and mode shape of a system. Results of a study [31] showed that the gyroscopic effects tend to alternately raise and lower the effective compliance of the rotor.

In defining the gyroscopic inertia effects the rotation of the cross-section relative to the rotating set of axes, abc:T attached to the cross-section, must be transformed to the fixed set of reference axes XYZ:Ⅲ. This is done using the Euler angle formulation [34] that defines a transformation matrix [9] for the angular rate components of e relative to the coordinates

$$\begin{Bmatrix} \omega_a \\ \omega_b \\ \omega_c \end{Bmatrix} = \begin{bmatrix} -\sin\beta & 1 & 0 \\ \cos\beta \sin\phi & 0 & \cos\phi \\ \cos\beta \cos\phi & 0 & -\sin\phi \end{bmatrix} \begin{Bmatrix} \dot{\Gamma} \\ \dot{\phi} \\ \dot{\beta} \end{Bmatrix} \quad ..(C.1)$$

The kinetic energy of the disk for the translational, and rotational displacements including the gyroscopic effects is given by [9].

$$\bar{T}_d = \frac{1}{2} \begin{Bmatrix} \dot{V} \\ \dot{W} \end{Bmatrix}^T \begin{bmatrix} m_d & 0 \\ 0 & m_d \end{bmatrix} \begin{Bmatrix} \dot{V} \\ \dot{W} \end{Bmatrix}$$

$$+ \frac{1}{2} \begin{Bmatrix} \omega_a \\ \omega_b \\ \omega_c \end{Bmatrix}^T \begin{bmatrix} I_D & 0 & 0 \\ 0 & I_D & 0 \\ 0 & 0 & I_p \end{bmatrix} \begin{Bmatrix} \omega_a \\ \omega_b \\ \omega_c \end{Bmatrix} \quad ...(C.2)$$

The use of Eqn (C.1) in Eq. (C.2) reduces the equation to

$$\bar{T}_d = \frac{1}{2}\begin{Bmatrix}\dot{V}\\ \dot{W}\end{Bmatrix}^T \begin{bmatrix} m_d & 0 \\ 0 & m_d \end{bmatrix} \begin{Bmatrix}\dot{V}\\ \dot{W}\end{Bmatrix} + \frac{1}{2}\begin{Bmatrix}\dot{B}\\ \dot{\Gamma}\end{Bmatrix}^T \begin{bmatrix} I_D & 0 \\ 0 & I_D \end{bmatrix} \begin{Bmatrix}\dot{B}\\ \dot{\Gamma}\end{Bmatrix} - \dot{\phi}\,\dot{\Gamma}\,BI_p \qquad \ldots(C.3)$$

Similarly for a finite element the kinetic energy equation is given by

$$d\bar{T}^e = \frac{1}{2}\begin{Bmatrix}\dot{V}\\ \dot{W}\end{Bmatrix}^T \begin{bmatrix} \mu & 0 \\ 0 & \mu \end{bmatrix} \begin{Bmatrix}\dot{V}\\ \dot{W}\end{Bmatrix} ds + \frac{1}{2}\dot{\phi}^2\,\bar{I}_p ds$$

which can be rewritten as

$$d\bar{T}^e = \frac{1}{2}\begin{Bmatrix}\dot{V}\\ \dot{W}\end{Bmatrix}^T \begin{bmatrix} \mu & 0 \\ 0 & \mu \end{bmatrix} \begin{Bmatrix}\dot{V}\\ \dot{W}\end{Bmatrix} ds + \frac{1}{2}\dot{\phi}^2\,\bar{I}_p\,ds + \frac{1}{2}\begin{Bmatrix}\dot{B}\\ \dot{\Gamma}\end{Bmatrix}^T \begin{bmatrix} I_D & 0 \\ 0 & I_D \end{bmatrix} \begin{Bmatrix}\dot{B}\\ \dot{\Gamma}\end{Bmatrix} - \dot{\phi}\,\dot{\Gamma}\,B\,\bar{I}_p\,ds \qquad \ldots(C.4)$$

APPENDIX-D

BEARING STIFFNESS AND DAMPING COEFFICIENT CURVES

D.1 Plain Cylindrical Bearing Coefficients are given in Figs. D.1 to D.2 [29]. The coefficients are shown as functions of the "Sommerfeld number" (S_1). The Sommerfeld number given by

$$S_1 = \frac{\mu N'}{P} \left(\frac{r}{c}\right)^2 \quad , \; P = \frac{W}{2rL}$$

where:

μ = coefficient of viscosity of oil

N' = speed of rotation of the rotor, in revolutions per second (rps)

r = radius of journal

c = radial clearance of journal bearing

P = load per unit of projected area

W = bearing load

L = length of bearing

At a given operating speed, the Sommerfeld number is calculated first; then using Figs. D.1 to D.2, various bearing parameters are obtained. Fig. D.2 shows a range of sommerfeld numbers where $\alpha K_{VW/W}$ is negative. This can lead to instability in rotors. However instability analysis is not the subject of the present investigation.

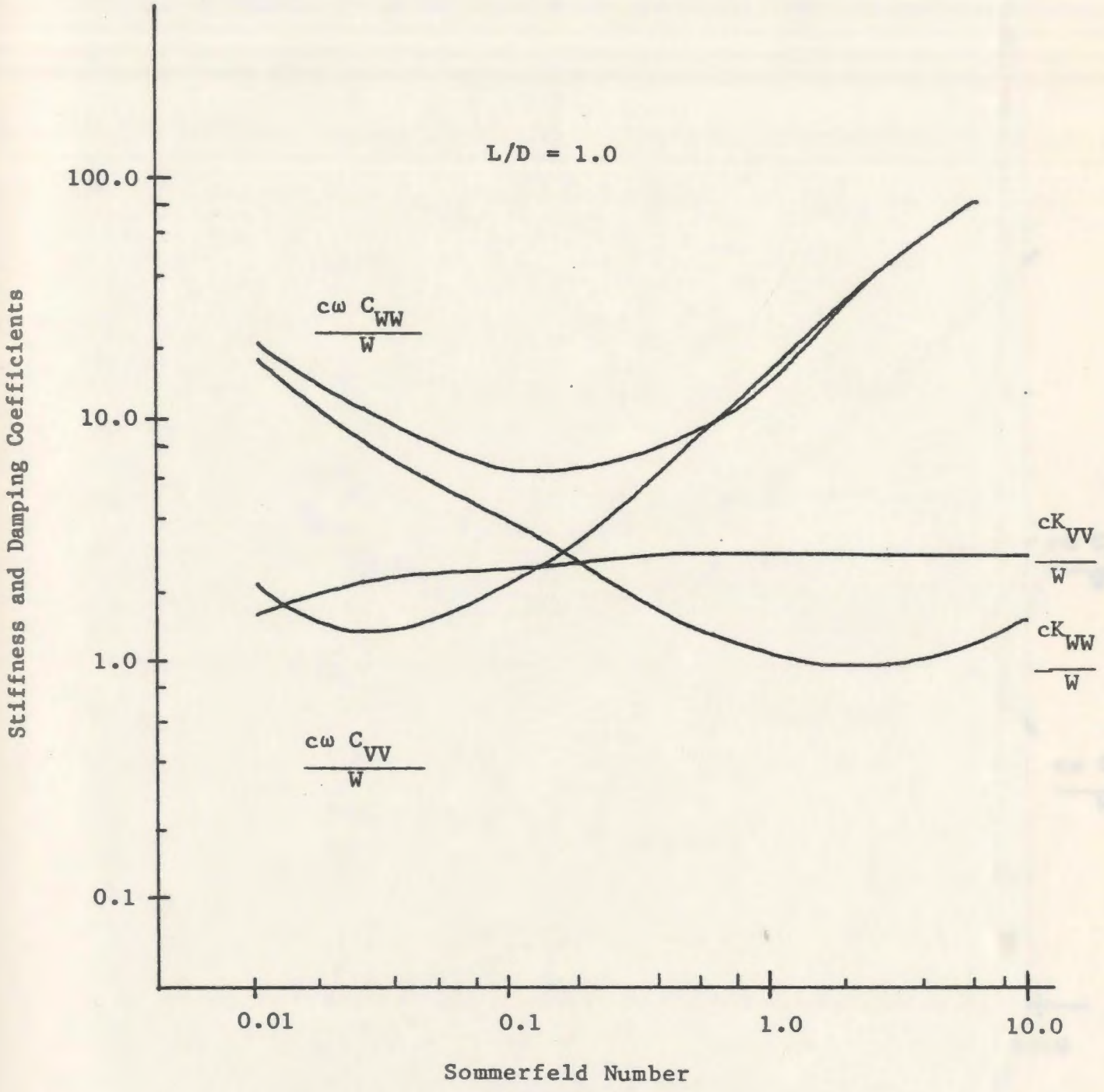

Fig. D.1 Direct Stiffness and Damping Coefficients of a Plain Cylindrical Bearing

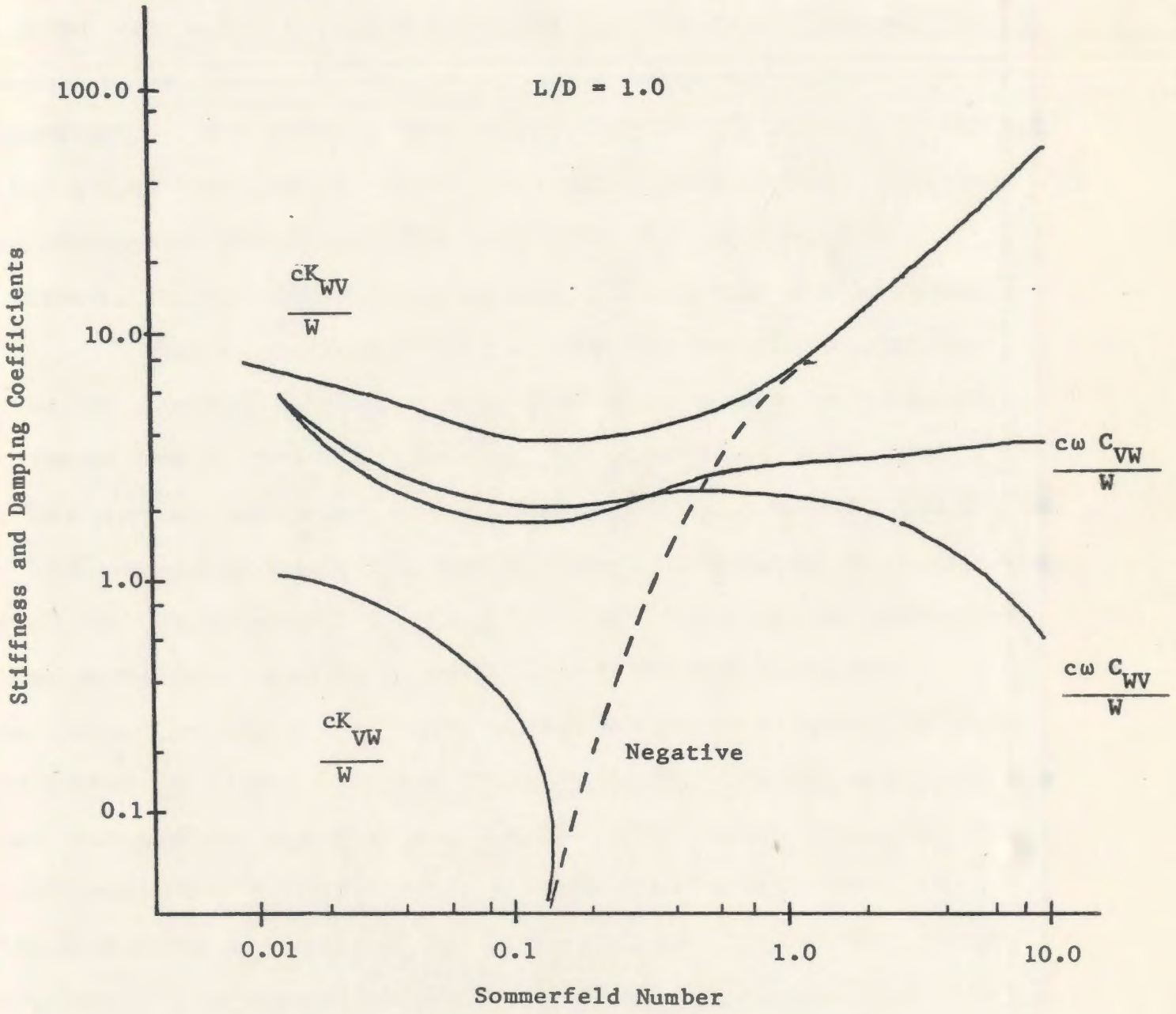

Fig. D.2 Cross Stiffness and Damping Coefficients of a Plain Cylindrical Bearing

APPENDIX-E

COMPUTER MODEL

The computer model for the multi-rotor system consists of four separate programs. All four programs for a balance run must be run sequentially, but for information regarding critical speed, or balance weights they can be run separately. The output from each program is stored in output files which in turn is used as input into the next program. The advantage being interim availability of computer information, and added flexibility in running the program.

The program FINITE ELEMENT is the first program based on the rotor element and disk parameters information. It forms the elemental matrices and assembles them into global system matrices. The program DYNAMIC MATRIX REDUCTION is the second program, it calculates the bearing coefficients based on the Sommerfeld number for the particular operating speed condition and adds them to the system matrices. Similarly the effect of disk eccentricity and trial weights are added into the forcing function. The system matrices are then reduced to the desired degree of freedom, required for modal response calculation. The program MODAL ANALYSIS diagionalizes the system matrices and calculates the modal response. The unbalance response information and the response for the trial weight is input into the fourth program BALANCE WEIGHT. This program then determines the

balance weight magnitudes and their associated angles required to reduce the response. The programs DYNAMIC MATRIX REDUCTION and MODAL ANALYSIS are run again with the balance weight information to calculate the residual response. In the same manner, by changing the rotor speed and using these programs, the rotor can be balanced for higher critical speeds.

The computer programs are developed in FORTRAN language using the VAX 11/780 system, and include the standard IMSL subroutine available with it.

```
        FINITE ELEMENT ROTOR COMPONENT ASSEMBLY

C*******************************
C       THIS PROGRAM FORMS THE GLOBAL MATRICES
C       FOR THE [GM] [GK] GC]
C       [QU1] [QU2]
C       THE MATRICES ARE PRINTED ON DATA.DAT FILE
C       TO BE READ BY RED. PR
C       THE BEARING ARE SET AT NODES 1 AND 7
C       THE DISK ARE SET ON ELEMENT NODES.
C*******************************
        DIMENSION ETM(20,8,8),EBK(20,8,8),EL(20),EH(20),ERMC(20)
        DIMENSION EBKC(20),ETMC(20),GM(80,80),GK(80,80),R(20)
        DIMENSION QC(20,8),QS(20,8),RO(20),RI(20),QU(76),QU2(72)
        DIMENSION QU1(72),XL(20),XR(20),SL(20),SR(20)
        COMPLEX Z(24,24),ALFA(24),XE(24)
        DIMENSION BETA(24),WK(9000)
        DIMENSION GMK(80,80),ERM(20,8,8),XER(80),EG(20,8,8)
        DIMENSION EGC(20),GG(80,80)
        DIMENSION GKK(24,24),GMM(24,24)
C*******************************
        OPEN(UNIT=1,FILE='T.DAT',TYPE='OLD')
        OPEN(UNIT=2,FILE='D.DAT',TYPE='NEW')
        OPEN(UNIT=3,FILE='R.DAT',TYPE='NEW')
        OPEN(UNIT=18,FILE='W.DAT',TYPE='NEW')
C*******************************
        READ (1,*) EM,E
C       INPUT NUMBER OF ELEMENTS
C       INITIALIZE THE ELEMENTAL MATRICES
        READ (1,*) IE
        DO 5 I=1,IE
        DO 5 J=1,8
        DO 5 K=1,8
        ETM(I,J,K)=0.0
        EG(I,J,K)=0.0
        ERM(I,J,K)=0.0
5       EBK(I,J,K)=0.0
        DO 10 I=1,IE
10      READ (1,*) EL(I),R(I)
C       INPUT MASS PER UNIT LENGTH ,MODULAS OF
C       ELASTICITY 'E'
        DO 30 I=1,IE
        U=(3.1415*(R(I)**2)*EM)/386.0
C       CALCULATE THE REQ'D CONSTANTS OF MULTIPLICATION
        ETMC(I)=U*EL(I)/420.0
        ERMC(I)=U*(R(I)**2)/(120.*EL(I))
        EGC(I)=2.0*(ERMC(I))
        EBKC(I)=(E*(R(I)**4)*3.14)/(4.*EL(I)**3)
        P1=ETMC(I)
C*******************************
```

```
C       FORMATION OF THE ELEMENTAL MATRIX
C*******************************
        ETM(I,1,1)=156.0*P1
        ETM(I,2,2)=ETM(I,1,1)
        ETM(I,3,3)=(4.0*EL(I)**2)*P1
        ETM(I,7,7)=ETM(I,3,3)
        ETM(I,8,8)=ETM(I,3,3)
        ETM(I,4,4)=(4.0*EL(I)**2)*P1
        ETM(I,5,5)=ETM(I,1,1)
        ETM(I,6,6)=ETM(I,5,5)
        ETM(I,3,2)=-(22.0*EL(I))*P1
        ETM(I,7,6)=-(ETM(I,3,2))
        ETM(I,4,1)=ETM(I,7,6)
        ETM(I,8,5)=ETM(I,3,2)
        ETM(I,5,1)=54.0*P1
        ETM(I,7,2)=13.0*EL(I)*P1
        ETM(I,6,3)=-(ETM(I,7,2))
        ETM(I,8,1)=-ETM(I,7,2)
        ETM(I,8,4)=-3.0*(EL(I)**2)*P1
        ETM(I,5,4)=ETM(I,7,2)
        ETM(I,6,2)=ETM(I,5,1)
        ETM(I,7,3)=ETM(I,8,4)
C       THE [ETM] MATRIX IS CREATED
C*******************************
C       CREATE THE [EBK] MATRIX
        P4=EBKC(I)
        EBK(I,1,1)=12.0*P4
        EBK(I,2,2)=EBK(I,1,1)
        EBK(I,3,3)=4.0*(EL(I)**2)*P4
        EBK(I,4,4)=EBK(I,3,3)
        EBK(I,5,5)=EBK(I,1,1)
        EBK(I,6,6)=EBK(I,1,1)
        EBK(I,7,7)=EBK(I,3,3)
        EBK(I,8,8)=EBK(I,3,3)
        EBK(I,3,2)=-6.*EL(I)*P4
        EBK(I,4,1)=-(EBK(I,3,2))
        EBK(I,5,4)=EBK(I,3,2)
        EBK(I,6,3)=EBK(I,4,1)
        EBK(I,7,2)=EBK(I,3,2)
        EBK(I,7,6)=EBK(I,4,1)
        EBK(I,8,1)=EBK(I,4,1)
        EBK(I,8,5)=EBK(I,3,2)
        EBK(I,5,1)=-(EBK(I,1,1))
        EBK(I,6,2)=EBK(I,5,1)
        EBK(I,7,3)=EBK(I,3,3)/2.0
        EBK(I,8,4)=EBK(I,7,3)
C       THE [EBK] MATRIX IS CREATED
C*******************************
        P2=ERMC(I)
        ERM(I,1,1)=36.*P2
        ERM(I,2,2)=ERM(I,1,1)
        ERM(I,3,3)=4.*(EL(I)**2)*P2
```

```
        ERM(I,4,4)=ERM(I,3,3)
        ERM(I,6,6)=36.*P2
        ERM(I,5,5)=ERM(I,6,6)
        ERM(I,7,7)=ERM(I,3,3)
        ERM(I,8,8)=ERM(I,7,7)
        ERM(I,3,2)=-(3.*EL(I)*P2)
        ERM(I,4,1)=-(ERM(I,3,2))
        ERM(I,5,4)=ERM(I,3,2)
        ERM(I,6,3)=ERM(I,4,1)
        ERM(I,7,2)=ERM(I,3,2)
        ERM(I,8,1)=ERM(I,4,1)
        ERM(I,7,6)=ERM(I,4,1)
        ERM(I,8,5)=ERM(I,3,2)
        ERM(I,5,1)=-(ERM(I,1,1))
        ERM(I,6,2)=ERM(I,5,1)
        ERM(I,8,4)=-(EL(I)**2)*P2
        ERM(I,7,3)=ERM(I,8,4)
C       CREATE THE [EG] MATRIX
C*******************************
        P3=EGC(I)
        EG(I,2,1)=36.0*P3
        EG(I,5,2)=EG(I,2,1)
        EG(I,6,1)=-(EG(I,2,1))
        EG(I,6,5)=EG(I,2,1)
        EG(I,3,1)=-3.0*P3*EL(I)
        EG(I,4,2)=EG(I,3,1)
        EG(I,5,3)=EG(I,4,2)
        EG(I,6,4)=EG(I,4,2)
        EG(I,7,1)=EG(I,4,2)
        EG(I,7,5)=-(EG(I,4,2))
        EG(I,8,2)=EG(I,3,1)
        EG(I,8,6)=EG(I,7,5)
        EG(I,4,3)=4.0*(EL(I)**2)*P3
        EG(I,7,4)=(EL(I)**2)*P3
        EG(I,8,3)=-(EG(I,7,4))
        EG(I,8,7)=EG(I,4,3)
C       THE [EG] MATRIX IS CREATED
C*******************************
        DO 75 J=1,8
        DO 75 K=1,J
        ERM(I,K,J)=ERM(I,J,K)
        ETM(I,K,J)=ETM(I,J,K)
        EG(I,K,J)=EG(I,J,K)
75      EBK(I,K,J)=EBK(I,J,K)
30      CONTINUE
C*******************************
C       FORM THE FORCE ELEMENTAL VECTORS
C       INPUT MASS ECCENTRICTY FOR EACH ELEMENT
        OPEN(UNIT=11,FILE='FORCE.DAT',TYPE='OLD')
C*******************************
        DO 610 I=1,IE
        READ (11,*) XL(I),XR(I),SL(I),SR(I)
```

```
      QE=(EM*((R(I)**2))*3.1415)/386.0
      QC(I,1)=((7./20.)*XL(I)*EL(I)+(3.0/20.)*XR(I)*EL(I))*QE
      QC(I,2)=((7./20.)*SL(I)*EL(I)+(3./20.)*SR(I)*EL(I))*QE
      QC(I,3)=((-1./20.)*SL(I)*(EL(I)**2)-(1./30.)*SR(I)*EL(I)**2)*QE
      QC(I,4)=((1./20.)*XL(I)*(EL(I)**2)+(1./30.)*XR(I)*EL(I)**2)*QE
      QC(I,5)=((3./20.)*XL(I)*EL(I)+(7./20.)*XR(I)*EL(I))*QE
      QC(I,6)=((3./20.)*SL(I)*EL(I)+(7./20.)*SR(I)*EL(I))*QE
      QC(I,7)=((1./30.)*SL(I)*EL(I)**2+(1./20.)*SR(I)*EL(I)**2)*QE
      QC(I,8)=(((-1./30.)*XL(I)*EL(I)**2)+(-1./20.)*XR(I)*EL(I)**2)*QE
      QS(I,1)=-QC(I,2)
      QS(I,2)=QC(I,1)
      QS(I,3)=-QC(I,4)
      QS(I,4)=QC(I,3)
      QS(I,5)=-QC(I,6)
      QS(I,6)=QC(I,5)
      QS(I,7)=-QC(I,8)
      QS(I,8)=QC(I,7)
610   CONTINUE
C     THE ELEMENTAL FORCE VECTOR ARE THUS FORMED
C*********************************
C     FORM THE GLOBAL FORCE VECTORS
C*********************************
C     GLOBAL FORCE MATRIX
      DO 642 I=1,I3
      QU1(I)=0.0
642   QU2(I)=0.0
      WRITE (15,*) (QU2(I1),I1=1,I3)
      I3=(IE*4)+4
C     INITIALIZE THE GLOBAL MATRICES
      DO 20 I=1,I3
      DO 20 J=1,I3
      GM(I,J)=0.0
      GG(I,J)=0.0
20    GK(I,J)=0.0
C     GLOBAL MAT SIZE
      I3=(IE*4)+4.
      J1=0
      K1=0
      DO 115 I=1,IE
      DO 111 J=1,8
      J1=J1+1
      DO 110 K=1,8
      K1=K1+1
      GM(J1,K1)=GM(J1,K1)+ETM(I,J,K)+ERM(I,J,K)
      GG(J1,K1)=GG(J1,K1)+EG(I,J,K)
      GK(J1,K1)=GK(J1,K1)+EBK(I,J,K)
110   CONTINUE
      K1=K1-8
111   CONTINUE
      K1=K1+4
      J1=J1-4
115   CONTINUE
```

```
C       FORCE GLOBAL ASSEMBLY
        K=0
        DO 626 I=1,IE
        DO 625 J=1,8
        K=K+1
        QU1(K)=QC(I,J)+QU1(K)
        QU2(K)=QS(I,J)+QU2(K)
625     CONTINUE
        K=K-4
626     CONTINUE
C       INPUT DISK NODES AND BRG NODES.
C*******************************
        READ (1,*) KD1,KD2
        READ (1,*) GM1,GM2,GM3,GM4,GG1,GG2
        READ (1,*) GM5,GM6,GM7,GM8,GG3,GG4
C*******************************
        K1=(KD1*4)-3
        K2=(KD2*4)-3
C       INPUT DISK ECCENTRICITY
C*******************************
        READ (11,*) PDX,PDY,PDX1,PDY1,PDX2,PDY2,PDX3,PDY3
        QU1(K1)=PDX+QU1(K1)
        QU1(K1+1)=PDY+QU1(K1+1)
        QU2(K1)=PDX1+QU2(K1)
        QU2(K1+1)=PDY1+QU2(K1+1)
        QU1(K2)=PDX2+QU1(K2)
        QU1(K2+1)=PDY2+QU1(K2+1)
        QU2(K2)=PDX3+QU2(K2)
        QU2(K2+1)=PDY3+QU2(K2+1)
C       DISK COEFICIENTS ADDITIONS
C*******************************
C       DISK #1
        GM(K1,K1)=GM1+GM(K1,K1)
        GM(K1+1,K1+1)=GM2+GM(K1+1,K1+1)
        GM(K1+2,K1+2)=GM3+GM(K1+2,K1+2)
        GM(K1+3,K1+3)=GM4+GM(K1+3,K1+3)
        GG(K1+2,K1+3)=GG1+GG(K1+2,K1+3)
        GG(K1+3,K1+2)=GG2+GG(K1+3,K1+2)
C       DISK NUMBER #2
        GM(K2,K2)=GM5+GM(K2,K2)
        GM(K2+1,K2+1)=GM6+GM(K2+1,K2+1)
        GM(K2+2,K2+2)=GM7+GM(K2+2,K2+2)
        GM(K2+3,K2+3)=GM8+GM(K2+3,K2+3)
        GG(K2+2,K2+3)=GG3+GG(K2+2,K2+3)
        GG(K2+3,K2+2)=GG4+GG(K2+3,K2+2)
C       BEARINGS AT THE ENDS
        OPEN(UNIT=39,FILE='DATA.DAT',TYPE='NEW')
        WRITE (39,*) I3
        WRITE (39,*) ((GM(I,J),J=1,I3),I=1,I3)
        WRITE (39,*) ((GK(I,J),J=1,I3),I=1,I3)
        WRITE (39,*) ((GG(I,J),J=1,I3),I=1,I3)
        WRITE (39,*) (QU1(K),K=1,I3)
```

```
WRITE (39,*) (QU2(K),K=1,I3)
PRINT *,'QU1',(QU1(I),I=1,I3)
PRINT *,'QU2',(QU2(I),I=1,I3)
STOP
END
```

```
      DYNAMIC MATRIC REDUCTION

C*******************************
C       THIS PROGRAM READ THE VALUES FROM P1.FOR PROG DATA FILE CO.DAT
C       AND CALCULATES THE SOMMERFELD NUMBER, READS BEARINGS COEFFICIENTS
C       FROM THE GRAPHS PERFORMS A REDUCTION GLOBAL MATRICES THE REDUCED
C       MATRICES ARE PRINTED ON KK.DAT FILE AND THE BRG COEFFICENTS FOR
C*******************************
      DIMENSION P1(12,12),P2(12,12),P3(16,16),P4(16,12),RKT(6)
      DIMENSION GM(28,28),GC(28,28),GK(28,28),GMS(16,12)
      DIMENSION GSS(16,16),GSSN(16,16),G(16,12),GM1(12,28)
      DIMENSION GK1(12,28),GC1(12,28),WKAREA(9000),B(2),EL(20)
      DIMENSION WA(50000),P5(12,12),GMK(12,12),GKN(28,28),WE(20)
      INTEGER LD(28),NM(20)
      DIMENSION A2(28,28),A5(28,28),QU1(28),QU2(28),QUR1(12),QUR2(12)
      DIMENSION GMM(28,28),GKK(28,28),GCC(28,28),GMN(28,28),R(28)
      DIMENSION GCN(28,28),TT(12,28),T(28,12),GKR(12,12),F8(12,28)
      REAL ATOP
      DIMENSION GMR5(12,12),GCR(12,12),F(28),FR(12),F6(16,16),F7(12,28)
      DIMENSION GMM1(28,28),GCC1(28,28),GMKC(24,24)
      DIMENSION GMKCI(24,24),QU(24),SS1(2),SS2(2),SS3(2)
      DIMENSION SS4(2),DD1(2),DD2(2),DD3(2),DD4(2),W(20)
      DIMENSION R1(24),BYPAR5(14)
      DIMENSION X(16),SYY(16),SYZ(16),SZY(16),SZZ(16)
      DIMENSION DYY(16),DYZ(16),DZY(16)
      DIMENSION DZZ(16),BYPAR1(16),BYPAR2(16),BYPAR3(16),BYPAR4(16)
      DIMENSION BYPAR6(16),BYPAR7(16),BYPAR8(16)
      DIMENSION C1(15,3),C2(15,3),C3(15,3)
      DIMENSION C4(15,3),C5(15,3),C6(15,3),C7(15,3),C8(15,3)
      DIMENSION S(2),S1(2),S2(2),S3(2),S4(2)
      DIMENSION D1(2),D2(2),D3(2),D4(2),QU11(28),QU22(28)
      COMPLEX WW5(3)
      DIMENSION TTQ(56,24),R20(56),R30(56),NLH(20),TW6(20),ANG(20)
C*******************************
      OPEN(UNIT=25,FILE='DATA.DAT',TYPE='OLD')
      OPEN(UNIT=5,FILE='RES.DAT',TYPE='NEW')
      OPEN(UNIT=21,FILE='KK.DAT',TYPE='NEW')
      OPEN(UNIT=3,FILE='PK1.DAT',TYPE='NEW')
      OPEN(UNIT=17,FILE='CO.DAT',TYPE='OLD')
      OPEN(UNIT=65,FILE='BRG.DAT',TYPE='NEW')
C     OPEN(UNIT=1,FILE='DISK.DAT',TYPE='OLD')
C*******************************
C       READ IN THE SLAVE AND MASTER DEGREE OF FREEDOM IN SEQUENCE
C       N5=16
C       IE=6
C       NSD=12
C       N1=28
C       N21=7
C*******************************
      OPEN(UNIT=74,FILE='MASTER.DAT',TYPE='OLD')
```

```
C       SLAVE AND MASTERS
        READ (74,*) N5,IE,NSD,N1,N21
        IN=IE+1
        READ (25,*) I3
        KLM=I3
        READ (25,*) ((GMM1(I,J),J=1,I3),I=1,I3)
        READ (25,*) ((GKK(I,J),J=1,I3),I=1,I3)
        READ (25,*) ((GCC1(I,J),J=1,I3),I=1,I3)
        READ (25,*) (QU11(K),K=1,I3)
        READ (25,*) (QU22(K),K=1,I3)
        PRINT *,'QU11',(QU11(K),K=1,I3)
        PRINT *,'QU22',(QU22(K),K=1,I3)
C*******************************
        OPEN(UNIT=10,FILE='T1.DAT',TYPE ='OLD')
        OPEN(UNIT=20,FILE='SOM.DAT',TYPE='NEW')
C*******************************
C       CALCULATE THE SOMMERFELD NUMBER FOR THE ROTOR
C*******************************
C       READ IN THE ELEMENTAL WEIGHT
        READ (10,*) EM,E
C       READ IN THE NUMBER OF ELEMENT
        READ (10,*) IE
        DO 470 I=1,IE
        READ (10,*) EL(I),R(I)
        PRINT *,'R*****',R(I)
        RKT(I)=R(I)
470     CONTINUE
C       CALCULATE ELEMENT WEIGHT
        DO 480 I=1,IE
        U=(3.14*(R(I)**2))*EM
480     WE(I)=EL(I)*U
C       ELEMENT WT ARE CALCULATED
C       CALCULATE ROTOR WEIGHT/TOTAL LENGTH
        READ (10,*) NB11,NB22
        READ (10,*) KD11,KD22,WD1,WD2
        TWR=0.0
        EL1=0.0
        DO 490 I=1,IE
        TWR=WE(I)+TWR
490     EL1=EL(I)+EL1
        RW=TWR+(WD1)+(WD2)
        PRINT *,'WEIGHT OF TH ROTOR',RW
        PRINT *,'LENGTH',EL1
C       INPUT BEARING NODES
C       READ (10,*) NB11,NB22
        IF (NB11.EQ.1) GOTO 30
        NB1=NB11-1
        NB2=NB22-1
        GOTO 50
30      NB1=NB11
        NB2=NB22-1
C       DETERMINE LOADING AT THE ENDS
```

```
C       FOR LHS
50      EMB=0.0
        I1=0
        DO 495 I=1,IE
        EL2=0.0
        DO 496 J=1,I
496     EL2=EL(J)+EL2
        IF (I.NE.1) GOTO 498
        EL2=EL2/2.0
        GOTO 499
498     EL2=EL2-(EL(I)/2.0)
499     EMB=(WE(I)*EL2)+EMB
495     CONTINUE
        KD1=KD11-1
        KD2=KD22-1
        EL3=0.0
        DO 475 I=1,KD1
475     EL3=EL(I)+EL3
        EMB3=EL3*WD1
        PRINT *,'MOMENT DUE TO DISK LMS',EMB3
        EL4=0.0
        DO 476 I=1,KD2
476     EL4=EL(I)+EL4
        EMB4=EL4*WD2
C       ADD DISK MOMENT TO TOTAL MOMENT
        EMB=EMB+EMB3+EMB4
C       PRINT *,'MOMENT TOTAL LHS',EMB
C       WEIGHT AT THE RHS
        P2=EMB/EL1
        P1=RW-P2
        P2=RW/2.0
        P1=P2
        EL5=0.0
        DO 477 I=1,NB1
477     EL5=EL(I)+EL5
        EL6=0.0
        DO 478 I=1,NB2
478     EL6=EL(I)+EL6
        B(2)=ABS((P1*EL5)-(P2*EL1))/EL6
        B(1)=RW-B(2)
        B(2)=P2
        B(1)=P1
        WRITE (20,*) 'BRG1',B(1),'BRG2',B(2)
C       BEARING CLEARANCE .0025
C*******************************
        RNB1=R(NB1)+.0025
        RNB2=R(NB2)+.0025
        SN1=((1.0E-6*2.0*(RNB1)*2.0*R(NB1))/B(1))*((RNB1/.0025)**2)
        SN2=((1.0E-6*2.0*RNB2*2.0*R(NB2))/B(2))*((RNB2/.0025)**2)
C       DETERMINE BEARING COEFFICIENTS FROM THE GRAPH
C*******************************
C       READ IN THE NUMBER OF POINTS FOR CURVE
```

```
      M8=2
C     READ IN CRITICAL  DAMPING SPEEDS
      OPEN(UNIT=29,FILE='SPEED.DAT',TYPE='OLD')
C     READ NUMBER FOR CRITICALS
      READ (29,*) ICS
      PRINT *,'ICS',ICS
      READ (29,*) (W(I),I=1,ICS)
C*******************************
      OPEN(UNIT=16,FILE='DAMP.DAT',TYPE='OLD')
C*******************************
C     READ IN THE NUMBER OF POINTS FOR CURVE
      READ (16,*) IB
      READ (16,*) (X(I),I=1,IB)
      READ (16,*) (SYY(I),I=1,IB)
      READ (16,*) (SYZ(I),I=1,IB)
      READ (16,*) (SZY(I),I=1,IB)
      READ (16,*) (SZZ(I),I=1,IB)
      READ (16,*) (DYY(I),I=1,IB)
      READ (16,*) (DYZ(I),I=1,IB)
      READ (16,*) (DZY(I),I=1,IB)
      READ (16,*) (DZZ(I),I=1,IB)
      READ (17,*) IC
      READ (17,*) ((C1(I,J),J=1,3),I=1,IC)
      READ (17,*) ((C2(I,J),J=1,3),I=1,IC)
      READ (17,*) ((C3(I,J),J=1,3),I=1,IC)
      READ (17,*) ((C4(I,J),J=1,3),I=1,IC)
      READ (17,*) ((C5(I,J),J=1,3),I=1,IC)
      READ (17,*) ((C6(I,J),J=1,3),I=1,IC)
      READ (17,*) ((C7(I,J),J=1,3),I=1,IC)
      READ (17,*) ((C8(I,J),J=1,3),I=1,IC)
C     VARIABLE SPEED LOOP (CPS.)
      WRITE (65,*) ICS
C*******************************
C     TRIAL WEIGHT ADDITION
C*******************************
      OPEN(UNIT=61,FILE='TW.DAT',TYPE='OLD')
C     INPUT ANGLE,TRIAL WEIGHT IBS.,AVAIL. PLANES
      READ (61,*) WT2,NK10,AL,THETA1
      F1C=0.0
      F1S=0.0
      F2C=0.0
      F2S=0.0
      F5C=0.0
      F5S=0.0
      F6C=0.0
      F6S=0.0
207   PRINT *,'IF BALANCE RUN INPUT 1'
      READ *,LM5
      IF (LM5.NE.1) GOTO 1000
      OPEN(UNIT=71,FILE='TW3.DAT',TYPE='OLD')
      L4=1
      GOTO 1001
```

```
1000    DO 999 L4=1,ICS
        IF (L4.EQ.1) GOTO 629
C       TRIAL WEIGHT ADDITIONS TO THE FORCING FUNCTION
C*******************************
C       INPUT ELEMENT NUMBER OF TRIAL WEIGHT
C       DISTANCE FROM THE LHS.
C         WEIGHT OF THE TRIAL WEIGHT
        READ (61,*) ITW
        PRINT *,'ITW***',ITW
        THETA=(2.0*3.1415*THETA1)/360.0
        WTW=WT2/386.0
C       DETERMINE NODES EFFECTED BY THE TRIAL WEIGHT
        K10=(ITW*4)-3
        K11=K10+1
        K12=K10+4
        K13=K10+5
        PRINT *,'K10',K10,'K11',K11,'K12',K12,'K13',K13
        IF (ITW.NE.7) GOTO 1231
        ITW=ITW-1
1231    STW=WTW*RKT(ITW)*SIN(THETA)
        CTW=WTW*RKT(ITW)*COS(THETA)
        SLH=(1.0-(3.0*(AL**2)/(EL(ITW)**2))+(2.0*(AL**3)/(EL(ITW)**3)))
        SRH=((3.0*(AL**2)/(EL(ITW)**2))-(2.0*(AL**3)/(EL(ITW)**3)))
        PRINT *,'EL',EL(ITW),'AL',AL,'WTW',WTW,'R',RKT(ITW),'THETA',THETA
        F1C=STW*SLH
        F1S=CTW*SLH
        F2C=CTW*SLH
        F2S=-STW*SLH
        F5C=STW*SRH
        F5S=CTW*SRH
        F6C=CTW*SRH
        F6S=-STW*SRH
        PRINT *,'F1C',F1C,'F1S',F1S,'F2C',F2C,'F2S',F2S
        PRINT *,'F5C',F5C,'F5S',F5S,'F6C',F6C,'F6S',F6S
        QU11(K10)=QU11(K10)+F1C
        QU22(K10)=QU22(K10)+F1S
        QU11(K11)=QU11(K11)+F2C
        QU22(K11)=QU22(K11)+F2S
        QU11(K12)=QU11(K12)+F5C
        QU22(K12)=QU22(K12)+F5S
        QU11(K13)=QU11(K13)+F6C
        QU22(K13)=QU22(K13)+F6S
        PRINT *,'QU11**',(QU11(K),K=1,I3)
        PRINT *,'QU22**',(QU22(K),K=1,I3)
C       THE TRIAL WEIGHTS HAVE BEEN ADDED TO THE FORCING FUNCTION
C*******************************
        GOTO 629
C       BALANCE RUN
C       NUMBER OF PLANES
1001    READ (71,*) NP1
C       ELEMENT NUMBER OF BALANCE WEIGHT PLANES
        PRINT *,'INPUT THREE BALANCE WEIGHT ELEMENTS STARTING FROM LEFT'
```

```
      DO 1004 I=1,NP1
1004  READ *, NLH(I)
C     BALANCE WEIGHTS
      READ (71,*) (WW5(I),I=1,NP1)
      DO 1002 I=1,NP1
      AL=0.0
      WTW1=AIMAG(WW5(I))/386.0
      WTW2=REAL(WW5(I))/386.0
      ITW=NLH(I)
C     DETERMINE NODES EFFECTED BY THE TRIAL WEIGHT
      K10=(ITW*4)-3
      K11=K10+1
      PRINT *,'K10',K10,'K11',K11
      STW=WTW1*RKT(ITW)
      CTW=WTW2*RKT(ITW)
      SLH=1.0
      PRINT *,'EL',EL(ITW),'AL',AL,'WTW',WTW,'R',RKT(ITW),'THETA',THETA
      F1C=STW*SLH
      F1S=CTW*SLH
      F2C=CTW*SLH
      F2S=-STW*SLH
      PRINT *,'F1C',F1C,'F1S',F1S,'F2C',F2C,'F2S',F2S
      QU11(K10)=QU11(K10)+F1C
      QU22(K10)=QU22(K10)+F1S
      QU11(K11)=QU11(K11)+F2C
      QU22(K11)=QU22(K11)+F2S
      PRINT *,'QU11',QU11(K10),'QU22',QU22(K10)
      PRINT *,'QU11',QU11(K11),'QU22',QU22(K11)
      PRINT *,'QU11***',(QU11(K),K=1,I3)
      PRINT *,'QU22***',(QU22(K),K=1,I3)
1002  CONTINUE
      PRINT *,'IF NOT FIRST BALANCE RUN INPUT 1'
      READ *,PP6
      IF (PP6.EQ.1.0) GOTO 207
C     THE TRIAL WEIGHTS HAVE BEEN ADDED TO THE FORCING FUNCTION
629   S(1)=SN1*W(L4)
      S(2)=SN2*W(L4)
C     PRINT *,'SOMMERFELD NUMBER','S1',S(1),'S2',S(2)
C     BEARING COEFFICENTS
      NX=IB
      IC=IB-1
      M8=2
      CALL ICSEVU (X,SYY,NX,C1,IC,S,SS1,M8,IER)
      CALL ICSEVU (X,SYZ,NX,C2,IC,S,SS2,M8,IER)
      CALL ICSEVU (X,SZY,NX,C3,IC,S,SS3,M8,IER)
      CALL ICSEVU (X,SZZ,NX,C4,IC,S,SS4,M8,IER)
      CALL ICSEVU (X,DYY,NX,C5,IC,S,DD1,M8,IER)
      CALL ICSEVU (X,DYZ,NX,C6,IC,S,DD2,M8,IER)
      CALL ICSEVU (X,DZY,NX,C7,IC,S,DD3,M8,IER)
      CALL ICSEVU (X,DZZ,NX,C8,IC,S,DD4,M8,IER)
      PI=3.1415*2.0*W(L4)
      C=.0025
```

```
      DO 405 I=1,2
      S1(I)=((SS1(I)*B(I))/C)
      S2(I)=((SS2(I)*B(I))/C)
      S3(I)=((SS3(I)*B(I))/C)
      S4(I)=((SS4(I)*B(I))/C)
      D1(I)=((DD1(I)*B(I))/(PI*C))
      D2(I)=((DD2(I)*B(I))/(PI*C))
      D3(I)=((DD3(I)*B(I))/(PI*C))
      D4(I)=((DD4(I)*B(I))/(PI*C))
405   CONTINUE
C*******************************
      WRITE (65,*) (S1(I),I=1,2)
      WRITE (65,*) (S2(I),I=1,2)
      WRITE (65,*) (S3(I),I=1,2)
      WRITE (65,*) (S4(I),I=1,2)
      WRITE (65,*) (D1(I),I=1,2)
      WRITE (65,*) (D2(I),I=1,2)
      WRITE (65,*) (D3(I),I=1,2)
      WRITE (65,*) (D4(I),I=1,2)
      I3=KLM
C     MULTIPLY MATRICES WITH FREQUENCY VALUES
C*******************************
      DO 420 I=1,I3
      DO 420 J=1,I3
      GMM(I,J)=GMM1(I,J)
420   GCC(I,J)=-W(L4)*GCC1(I,J)
C     INPUT THE BEARING NODES
C     READ(78,*) NB11,NB22
      NB1=(NB11*4)-3
      NB2=(NB22*4)-3
      GKK(NB1,NB1)=GKK(NB1,NB1)+S1(1)
      GCC(NB1,NB1)=GCC(NB1,NB1)+(D1(1))
      GKK(NB1,NB1+1)=GKK(NB1,NB1+1)+S2(1)
      GCC(NB1,NB1+1)=GCC(NB1,NB1+1)+D2(1)
      GKK(NB1+1,NB1)=GKK(NB1+1,NB1)+S3(1)
      GCC(NB1+1,NB1)=GCC(NB1+1,NB1)+(D3(1))
      GKK(NB1+1,NB1+1)=GKK(NB1+1,NB1+1)+S4(1)
      GCC(NB1+1,NB1+1)=GCC(NB1+1,NB1+1)+(D4(1))
      GKK(NB2,NB2)=GKK(NB2,NB2)+S1(2)
      GCC(NB2,NB2)=GCC(NB2,NB2)+(D1(2))
      GKK(NB2,NB2+1)=GKK(NB2,NB2+1)+S2(2)
      GCC(NB2,NB2+1)=GCC(NB2,NB2+1)+(D2(2))
      GKK(NB2+1,NB2)=GKK(NB2+1,NB2)+S3(2)
      GCC(NB2+1,NB2)=GCC(NB2+1,NB2)+(D3(2))
      GKK(NB2+1,NB2+1)=GKK(NB2+1,NB2+1)+S4(2)
      GCC(NB2+1,NB2+1)=GCC(NB2+1,NB2+1)+(D4(2))
      IF (L4.NE.1) GOTO 1033
C*******************************
      WRITE (3,*) I3
      WRITE (3,*) ((GMM(I,J),J=1,I3),I=1,I3)
      WRITE (3,*) ((GKK(I,J),J=1,I3),I=1,I3)
      WRITE (3,*) ((GCC(I,J),J=1,I3),I=1,I3)
```

```
C*********************************
1033    I3=KLM
        DO 100 I=1,I3
100     LD(I)=I
        DO 110 I=1,I3
110     R(I)=GMM(I,I)/GKK(I,I)
        PRINT *,(R(I),I=1,I3)
        DO 116 I=1,I3
        I1=I+1
        DO 115 J=I1,I3
        IF (R(I).GE.R(J)) GOTO 115
        LO=LD(I)
        LN=LD(J)
        LD(I)=LN
        LD(J)=LO
        RN=R(I)
        R(I)=R(J)
        R(J)=RN
115     CONTINUE
116     CONTINUE
        PRINT *,'LD(I)*****',(LD(I),I=1,I3)
        I3=KLM
        DO 205 I=1,I3
        I1=LD(I)
        DO 206 J=1,I3
        GM(I,J)=GMM(I1,J)
        GK(I,J)=GKK(I1,J)
        GC(I,J)=GCC(I1,J)
206     CONTINUE
205     CONTINUE
        DO 214 I=1,I3
        I1=LD(I)
        QU1(I)=QU11(I1)
        QU2(I)=QU22(I1)
214     CONTINUE
        DO 210 J=1,I3
        J1=LD(J)
        DO 215 I=1,I3
        GMN(I,J)=GM(I,J1)
        GKN(I,J)=GK(I,J1)
215     GCN(I,J)=GC(I,J1)
210     CONTINUE
C       FORM [GMS]  [GSS]
        I1=0
        J1=0
        DO 220 I=(N5+1),I3
        I1=I1+1
        DO 225 J=1,N5
        J1=J1+1
225     GMS(I1,J1)=GKN(I,J)
        J1=0
220     CONTINUE
```

```
      I3=KLM
      I1=0
      J1=0
      DO 230 I=(N5+1),I3
      I1=I1+1
      DO 235 J=(N5+1),I3
      J1=J1+1
235   GSS(I1,J1)=GKN(I,J)
      J1=0
230   CONTINUE
C*******************************
C     FORMATION OF THE TRANSFORMATION MATRIX
C*******************************
      DO 240 I=1,I3
      DO 240 J=1,N5
240   T(I,J)=0.0
C     MULTIPLICATION OF -[KSS] [KMS]
      CALL LINV2F(GSS,NSD,NSD,GSSN,4,WKAREA,IER)
      DO 245 I=1,NSD
      DO 245 J=1,NSD
245   GSSN(I,J)=-1.0*(GSSN(I,J))
      CALL VMULFP(GSSN,GMS,NSD,NSD,N5,NSD,NSD,G,NSD,IER)
C     FORMATION OF THE TRANSFORMATION MATRIX [T]
      DO 250 J=1,N5
250   T(J,J)=1.0
      I1=0
      J1=0
      DO 255 I=(N5+1),I3
      I1=I1+1
      DO 257 J=1,N5
      J1=J1+1
257   T(I,J)=G(I1,J1)
      J1=0
255   CONTINUE
C     THE TRANSFORMATION MATRIX IS THUS FORMED
C*******************************
C     TRANSPOSE [TT]
      DO 260 I=1,I3
      DO 260 J=1,N5
260   TT(J,I)=T(I,J)
C     MULTLIPLICATION OF THE SYSTEM MATRICES
      I3=KLM
      CALL VMULFP(TT,GMN,N5,I3,I3,N5,I3,GM1,N5,IER)
      CALL VMULFP(GM1,T,N5,I3,N5,N5,I3,GMR5,N5,IER)
      CALL VMULFP(TT,GKN,N5,I3,I3,N5,I3,GK1,N5,IER)
      CALL VMULFP(GK1,T,N5,I3,N5,N5,I3,GKR,N5,IER)
      CALL VMULFP(TT,GCN,N5,I3,I3,N5,I3,GC1,N5,IER)
      CALL VMULFP(GC1,T,N5,I3,N5,N5,I3,GCR,N5,IER)
      I3=KLM
      CALL VMULFP(TT,QU1,N5,I3,1,N5,I3,QUR1,N5,IER)
      CALL VMULFP(TT,QU2,N5,I3,1,N5,I3,QUR2,N5,IER)
C*******************************
```

```
      WRITE (21,*) N5
      WRITE (21,*) ((GMR5(I,J),J=1,N5),I=1,N5)
      WRITE (21,*) ((GKR(I,J),J=1,N5),I=1,N5)
      WRITE (21,*)  ((GCR(I,J),J=1,N5),I=1,N5)
      WRITE (21,*) (QUR1(I),I=1,N5)
      WRITE (21,*) (QUR2(I),I=1,N5)
      WRITE (21,*) I3
      WRITE (21,*) (LD(I),I=1,I3)
      WRITE (21,*) ((T(I,J),J=1,N5),I=1,I3)
C*******************************
C     MATRIX ADDITIONS
      DO 450 I=1,N5
      DO 450 J=1,N5
450   GMK(I,J)=GMR5(I,J)+GKR(I,J)
      N6=N5*2
      I3=KLM
      N71=I3*2
      DO 455 I=1,N5
      I1=I+N5
      DO 456 J=1,N5
      J1=J+N5
      GMKC(I,J)=GMK(I,J)
      GMKC(I1,J1)=GMK(I,J)
      GMKC(I1,J)=-1.0*(GCR(I,J))
      GMKC(I,J1)=GCR(I,J)
456   CONTINUE
455   CONTINUE
C     TAKE THE INVERSE OF THE GMKC MATRIX
      CALL LINV1F (GMKC,N6,N6,GMKCI,4,WKAREA,IER)
C     ASSEMBLE THE FORCING FUNCTION
      DO 460 I=1,N5
      I1=I+N5
      QU(I)=QU1(I)
460   QU(I1)=QU2(I)
C     MULTIPLY [GMKCI] WITH [QU] FOR RESPONSE
      CALL VMULFF (GMKCI,QU,N6,N6,1,N6,N6,R1,N6,IER)
      DO 500 I=1,I3
      I1=I+I3
      DO 510 J=1,N5
      J1=J+N5
      TTQ(I,J)=0.0
      TTQ(I1,J)=0.0
      TTQ(I,J1)=0.0
      TTQ(I1,J1)=0.0
      TTQ(I,J)=T(I,J)
510   TTQ(I1,J1)=T(I,J)
500   CONTINUE
      CALL VMULFF(TTQ,R1,N71,N6,1,N71,N6,R20,N71,IER)
      DO 520 I=1,I3
      I1=LD(I)
      I2=I+I3
      DO 530 J=1,I3
```

```
      IF (I.EQ.LD(J)) GOTO 540
530   CONTINUE
540   R30(I)=R20(LD(J))
      R30(I2)=R20(LD(J)+I3)
520   CONTINUE
      WRITE (5,*) 'RESPONSE',(R30(I),I=1,N71)
      PRINT *,'******I3**',I3,'N5',N5
      QU11(K10)=QU11(K10)-F1C
      QU22(K10)=QU22(K10)-F1S
      QU11(K11)=QU11(K11)-F2C
      QU22(K11)=QU22(K11)-F2S
      QU11(K12)=QU11(K12)-F5C
      QU22(K12)=QU22(K12)-F5S
      QU11(K13)=QU11(K13)-F6C
      QU22(K13)=QU22(K13)-F6S
C     THE TRIAL WEIGHTS HAVE BEEN SUBTRACTED FROM FORCING FUNCTION
      PRINT *,'NB1',NB1,'NB2',NB2
      GKK(NB1,NB1)=GKK(NB1,NB1)-S1(1)
      GCC(NB1,NB1)=GCC(NB1,NB1)-(D1(1))
      GKK(NB1,NB1+1)=GKK(NB1,NB1+1)-S2(1)
      GCC(NB1,NB1+1)=GCC(NB1,NB1+1)-D2(1)
      GKK(NB1+1,NB1)=GKK(NB1+1,NB1)-S3(1)
      GCC(NB1+1,NB1)=GCC(NB1+1,NB1)-(D3(1))
      GKK(NB1+1,NB1+1)=GKK(NB1+1,NB1+1)-S4(1)
      GCC(NB1+1,NB1+1)=GCC(NB1+1,NB1+1)-(D4(1))
      GKK(NB2,NB2)=GKK(NB2,NB2)-S1(2)
      GCC(NB2,NB2)=GCC(NB2,NB2)-(D1(2))
      GKK(NB2,NB2+1)=GKK(NB2,NB2+1)-S2(2)
      GCC(NB2,NB2+1)=GCC(NB2,NB2+1)-(D2(2))
      GKK(NB2+1,NB2)=GKK(NB2+1,NB2)-S3(2)
      GCC(NB2+1,NB2)=GCC(NB2+1,NB2)-(D3(2))
      GKK(NB2+1,NB2+1)=GKK(NB2+1,NB2+1)-S4(2)
      GCC(NB2+1,NB2+1)=GCC(NB2+1,NB2+1)-(D4(2))
999   CONTINUE
      STOP
      END
```

```
      MODAL ANALYSIS

C*********************************
C     THIS PROGRAM DOES THE MODAL RESPONSE ANALYSIS
C     DIAGIONALIZATION OF MATRICES
C*********************************
      IMPLICIT REAL*8(A-H,O-Z)
      DIMENSION GM(16,16),GK(16,16),GMT(16,16),GKT(16,16),GCT(16,16)
      DIMENSION GKKT(32,32),GMM(32,32),GKK(32,32)
      DIMENSION GKKI(32,32),GMMT(32,32)
      DIMENSION EV(32),EV3(32),TK(32),GKN(32,32),TR(32),LP(32),TI(32)
      DIMENSION WK(30000),GKKTI(32,32),GC(16,16)
      DIMENSION WK1(30000),WK2(30000)
      DIMENSION GMP(32,32),BETA(32),T8(32,32),TC(32,32),WK3(30000)
      COMPLEX*16 ALFA(32),T(32,32),T1(32,32),TT(32,32)
      COMPLEX*16  GME(32,32),GTM(32,32)
      COMPLEX*16 EV1(32),EV2(32),T9(32,32),TCT(32,32)
      COMPLEX*16 GMMC(32,32),GKKC(32,32)
      COMPLEX*16 E19(28),E20(28)
      COMPLEX*16 GTMC(32,32),PPK(32,32),C1,C2(32)
      COMPLEX*16 GKE(32,32),GTK(32,32)
      DIMENSION W(32),TN(28,16),QUR1(16),QUR2(16),ATAP(20)
      COMPLEX*16 Q11(32),Q22(32),QSS(32),QCS(32)
      COMPLEX*16 GMK1(32),GMK2(32),E3(32)
      COMPLEX*16 E4(32),E5(32),E6(32),TQ,TQ2
      COMPLEX*16 E1(32),E2(32),GMN1(32),W2
      DIMENSION VR(16),VI(16),WR(16),WI(16),YMA(6),YMI(6),LD(28)
      COMPLEX*16 TAN(6),EN10(28),EN9(28),TN1(28,16),E9(28),E10(28)
      COMPLEX*16 T2(32,32),C3(32),Z,ZI(32,32),W3
C*********************************
      OPEN(UNIT=9,FILE='ELL.DAT',TYPE='NEW')
      OPEN(UNIT=5,FILE='M.DAT',TYPE='NEW')
      OPEN(UNIT=2,FILE='KK.DAT',TYPE='OLD')
      OPEN(UNIT=29,FILE='SPEED.DAT',TYPE='OLD')
      OPEN(UNIT=60,FILE='TW1.DAT',TYPE='NEW')
C*********************************
      READ (29,*) ICS
      READ (29,*) (W(I),I=1,ICS)
      PRINT *,'IF BALANCE RUN INPUT 1 '
C*********************************
      READ *,LT5
      IF (LT5.NE.1) GOTO 1000
      ICS=1
1000  DO 999 L4=1,ICS
C*********************************
      READ(2,*) I3
      READ (2,*) ((GM(I,J),J=1,I3),I=1,I3)
      READ (2,*) ((GK(I,J),J=1,I3),I=1,I3)
      READ (2,*) ((GC(I,J),J=1,I3),I=1,I3)
      READ (2,*) (QUR1(I),I=1,I3)
```

```
      READ (2,*) (QUR2(I),I=1,I3)
      READ (2,*) IT
      READ (2,*) (LD(I),I=1,IT)
      READ (2,*) ((TN(I,J),J=1,I3),I=1,IT)
C*********************************
      I4=2*I3
      DO 8 I=1,I3
      DO 8 J=1,I3
      GMT(J,I)=GM(I,J)
      GKT(J,I)=GK(I,J)
8     GCT(J,I)=GC(I,J)
      DO 10 I=1,I4
      DO 10 J=1,I4
      GKKT(I,J)=0.0D+1
      GMMT(I,J)=0.0D+1
      GMM(I,J)=0.0D+1
10    GKK(I,J)=0.0D+1
      DO 15 I=1,I3
      I1=I+I3
      DO 16 J=1,I3
      J1=J+I3
      GMM(I,J1)=GM(I,J)
      GMM(I1,J)=GM(I,J)
      GMM(I1,J1)=GC(I,J)
      GKK(I,J)=-GM(I,J)
      GKK(I1,J1)=GK(I,J)
      GKKT(I,J)=-GMT(I,J)
      GMMT(I,J1)=GMT(I,J)
      GMMT(I1,J)=GMT(I,J)
      GMMT(I1,J1)=GCT(I,J)
      GKKT(I1,J1)=GKT(I,J)
16    CONTINUE
15    CONTINUE
      DO 886 I=1,I4
      DO 886 J=1,I4
886   GKN(I,J)=GKK(I,J)
      CALL LINV1F(GKK,I4,I4,GKKI,4,WK,IER)
      CALL VMULFF(GKKI,GMM,I4,I4,I4,I4,I4,TC,I4,IER)
      DO 60 I=1,I4
      DO 60 J=1,I4
60    TCT(I,J)=DCMPLX(TC(I,J),0.0D+1)
      IJOB=2
      CALL EIGCC(TCT,I4,I4,IJOB,EV1,T,I4,WK1,IER)
      DO 995 I=1,I4
      C1=DCMPLX(1.0D+0,0.0D+1)
      IF (EV1(I).EQ.0.0D+1) GOTO 995
      C2(I)=C1/EV1(I)
995   CONTINUE
      CALL LINV1F(GKKT,I4,I4,GKKTI,4,WK2,IER)
      CALL VMULFF(GKKTI,GMMT,I4,I4,I4,I4,I4,T8,I4,IER)
      DO 65 I=1,I4
      DO 65 J=1,I4
```

```
65      T9(I,J)=DCMPLX(T8(I,J),0.0D+1)
        IJOB=2
        CALL EIGCC(T9,I4,I4,IJOB,EV2,T1,I4,WK3,IER)
        DO 941 I=1,I4
941     C3(I)=C1/EV2(I)
        DO 521 I=1,I4
        LP(I)=I
        DO 522 J=1,I4
        A1=DREAL(C2(I))
        A2=DIMAG(C2(I))
        S1=DSQRT((A1**2)+(A2**2))
        B1=DREAL(C3(J))
        B2=DIMAG(C3(J))
        S2=DSQRT((B1**2)+(B2**2))
        DEL1=DABS(((A1-B1)/A1)*100.0D+0)
        IF (A2.EQ.0.0D+0) GOTO 721
        DEL2=DABS(((A2-B2)/A2)*100.0D+0)
721     DEL3=DABS(((S1-S2)/S1)*100.0D+0)
        IF ((DABS(A2)).LT.(1.0D-8)) GOTO 523
        GOTO 527
523     IF ((DABS(B2)).LT.(1.0D-8)) GOTO 528
        IF (A2.EQ.0.0D+1) GOTO 528
527     IF (DEL2.GT.0.5D+0) GOTO 522
528     IF (DEL3.GT.0.5D+0) GOTO 522
        IF (DEL1.GT.0.5D+0) GOTO 522
        LP1=LP(I)
        LP(I)=J
522     CONTINUE
521     CONTINUE
        K=1
559     DO 558 I=1,I4
        T2(I,K)=T1(I,LP(K))
558     CONTINUE
        K=K+1
        IF (K.LE.I4) GOTO 559
        DO 401 I=1,14
401     PRINT *,'EIGEN VALUES',I,' ',C3(LP(I))
C*********************************
        DO 30 I=1,I4
        DO 30 J=1,I4
30      TT(I,J)=T2(J,I)
        DO 50 I=1,I4
        DO 50 J=1,I4
        GMMC(I,J)=DCMPLX(GMM(I,J),0.0D+1)
        GKKC(I,J)=DCMPLX(GKN(I,J),0.0D+1)
        GTK(I,J)=DCMPLX(0.0D+1,0.0D+1)
        GTM(I,J)=DCMPLX(0.0D+1,0.0D+1)
        GKE(I,J)=DCMPLX(0.0D+1,0.0D+1)
50      GME(I,J)=DCMPLX(0.0D+1,0.0D+1)
        DO 38 I=1,I4
        DO 41 J=1,I4
        DO 40 K=1,I4
```

```
        GTK(I,J)=TT(I,K)*GKKC(K,J)+GTK(I,J)
40      GTM(I,J)=TT(I,K)*GMMC(K,J)+GTM(I,J)
41      CONTINUE
38      CONTINUE
        DO 45 I=1,I4
        DO 47 J=1,I4
        DO 48 K=1,I4
        GKE(I,J)=GTK(I,K)*T(K,J)+GKE(I,J)
48      GME(I,J)=GTM(I,K)*T(K,J)+GME(I,J)
47      CONTINUE
45      CONTINUE
C*********************************
        OPEN(UNIT=20,FILE='M1.DAT',TYPE='NEW')
C*********************************
        WRITE (5,*) 'GKE',(GKE(I,I),I=1,I4)
C       FORMATION OF THE FORCING VECTOR
        W2=DCMPLX(W(L4),0.0D+1)
        DO 965 I=1,I3
        Q11(I)=DCMPLX(0.0D+1,0.0D+1)
        Q22(I)=DCMPLX(0.0D+1,0.0D+1)
        Q11(I3+I)=DCMPLX(QUR1(I),0.0D+1)*(W2**2)
        Q22(I3+I)=DCMPLX(QUR2(I),0.0D+1)*(W2**2)
965     CONTINUE
        DO 66 I=1,I4
        QSS(I)=DCMPLX(0.0D+1,0.0D+1)
        QCS(I)=DCMPLX(0.0D+1,0.0D+1)
        DO 66 J=1,I4
        QSS(I)=TT(I,J)*Q22(J)+QSS(I)
66      QCS(I)=TT(I,J)*Q11(J)+QCS(I)
        DO 83 I=1,I4
        CI=(-1.0D+0)*DIMAG(GME(I,I))
        CR=(-1.0D+0)*DREAL(GME(I,I))
        GMK1(I)=DCMPLX(CI,DREAL(GME(I,I)))*W2
        W3=CMPLX(-1.0D+0,0.0D+1)
83      GMK2(I)=DCMPLX(DIMAG(GME(I,I)),CR)*(W2)
        TQ=DCMPLX(2.0D+0,0.0D+1)
        TQ2=DCMPLX(0.0D+1,2.0D+0)
        DO 81 I=1,I4
        E1(I)=QSS(I)/(TQ2)+QCS(I)/(TQ)
81      E2(I)=W3*(QSS(I))/(TQ2)+QCS(I)/(TQ)
        DO 84 I=1,I4
        E3(I)=E1(I)/(GMK1(I)+GKE(I,I))
84      E4(I)=E2(I)/(GMK2(I)+GKE(I,I))
        DO 79 I=1,IT
        DO 79 J=1,I3
79      TN1(I,J)=DCMPLX(TN(I,J),0.0D+0)
        DO 88 I=1,I4
        E5(I)=DCMPLX(0.0D+1,0.0D+1)
        E6(I)=DCMPLX(0.0D+1,0.0D+1)
        DO 88 J=1,I4
        E5(I)=T(I,J)*E3(J)+E5(I)
88      E6(I)=T(I,J)*E4(J)+E6(I)
```

```
C       RECOVERY OF THE SLAVES
        DO 89 I=1,IT
        EN9(I)=DCMPLX(0.0D+1,0.0D+1)
        EN10(I)=DCMPLX(0.0D+1,0.0D+1)
        DO 89 J=1,I3
        EN9(I)=TN1(I,J)*E5(J+I3)+EN9(I)
89      EN10(I)=TN1(I,J)*E6(J+I3)+EN10(I)
        DO 97 I=1,IT
        I1=LD(I)
        E19(I1)=EN9(I)
        E20(I1)=EN10(I)
97      CONTINUE
        PRINT *,'E19X',(E19(I),I=1,IT,4)
        PRINT *,'E19Y',(E19(I),I=2,IT,4)
        PRINT *,'E20X',(E20(I),I=1,IT,4)
        PRINT *,'E20Y',(E20(I),I=2,IT,4)
C       REARRANGE [E19],[E20]
        I41=IT/4
        I=0
        DO 894 I1=1,I41
        I=I+1
        VR(I1)=(DREAL(E19(I)))+(DREAL(E20(I)))
        VI(I1)=((-1.0D+0)*DIMAG(E19(I)))+DIMAG(E20(I))
        WR(I1)=DREAL(E19(I+1))+DREAL(E20(I+1))
        WI(I1)=((-1.0D+0)*DIMAG(E19(I+1)))+DIMAG(E20(I+1))
        PRINT *,'I',I,'I+1',I
        PRINT *,I1,'VR',VR(I1),'VI',VI(I1),'WR',WR(I1),'WI',WI(I1)
        I=I+3
894     CONTINUE
        I41=IT/4
        DO 796 I=1,I41
        PRINT *,VR(I),VI(I),WR(I),WI(I)
        Y=(VR(I)**2)+(VI(I)**2)+(WR(I)**2)+(WI(I)**2)
        Y1=(WR(I)**2-1.0D+0*(VI(I)**2)-1.0D+0*(VR(I)**2)+WI(I)**2)**2
        Y2=(4.0D+0)*((VR(I)*WR(I)+WI(I)*VI(I))**2)
        Y3=DSQRT(Y1+Y2)
        PRINT *,I,'Y',Y,'Y1',Y1,'Y2',Y2,'Y3',Y3
        YMA(I)=DSQRT((0.5D+0)*(Y+Y3))
        YMI(I)=DSQRT((0.5D+0)*ABS(Y3-Y))
        Y9=(VR(I)**2)-1.0D+0*(VI(I)**2)+(WR(I)**2)-1.0D+0*(WI(I)**2)
        PRINT *,'Y9',Y9
        T25=(2.0D+0*(VR(I)*VI(I)+WR(I)*WI(I)))/Y9
        TAN(I)=DATAN(T25)
        DELTA=DATAN((VR(I)-WI(I))/(WR(I)+VI(I)))
        ATAP(I)=(TAN(I)/2.0D+0)+DELTA
        ATAP1=ATAP(I)/W(L4)
        IF(T25.LT.0.0D+1) GOTO 659
        IF(Y9.LT.0.0D+1) GOTO 796
        ATAP(I)=ATAP(I)+3.1415D+0
        GOTO 796
659     IF(Y9.GT.0.0D+1) GOTO 796
        ATAP(I)=ATAP(I)+3.1415D+0
```

```
796     CONTINUE
        WRITE (9,*) 'SPEED RAD./SEC.',W(L4)
        DO 103 I=1,I41
C*******************************
103     WRITE (9,*) 'MAJOR AXIS',I,' ',YMA(I),'MINOR AXIS',I,' ',YMI(I)
        WRITE (60,*) I41
        WRITE (60,*) (ATAP(I),I=1,I41)
        WRITE (60,*) (YMA(I),I=1,I41)
C*******************************
999     CONTINUE
C*******************************
        OPEN(UNIT=59,FILE='BAL.DAT',TYPE='NEW')
        WRITE (59,*) I4
        WRITE (59,*) (E5(I),I=1,I4)
        WRITE (59,*) (E6(I),I=1,I4)
        WRITE (59,*) ((T(I,J),J=1,I4),I=1,I4)
C*******************************
        STOP
        END
```

```
        BALANCE WEIGHT CALCULATION

C*********************************
C       THIS PROGRAM CALCULATES THE BALANCE WEIGHTS
C       NECESSARY TO BALANCE THE ROTOR.
C*********************************
        IMPLICIT REAL*8(A-H,O-Z)
        DIMENSION WA(20000),TW4(10),ANG(10),TKK(10)
        DIMENSION TIM(7),TIM2(7)
        DIMENSION VR(7),VI(7),WR(7),WI(7),TIM3(10),YMA(7)
        COMPLEX*16 X10(28),X11(28),XI(7),X5(28),X6(28),XC(7,3)
        COMPLEX*16 CXC(7,3),CT(3,7),CL(3,3),TI(3,3),ZC(3,7),WC(3)
        COMPLEX*16 X1(7),TW3,PK(3,3),CLL(3,3)
C*********************************
        OPEN(UNIT=10,FILE='TW.DAT',TYPE='OLD')
        OPEN(UNIT=2,FILE='W6.DAT',TYPE='NEW')
        OPEN(UNIT=11,FILE='TW1.DAT',TYPE='OLD')
C*********************************
        READ (10,*) TW1,NP,DT1,DN1
        READ (11,*) I41
        READ (11,*) (TIM2(I),I=1,I41)
        READ (11,*) (YMA(I),I=1,I41)
C*********************************
        TW2=TW1
        TW3=DCMPLX(TW2,0.0D+1)
        DO 70 I=1,I41
        A10=YMA(I)*DCOS(TIM2(I))
        A11=YMA(I)*DSIN(TIM2(I))
70      XI(I)=DCMPLX(A10,A11)
        PRINT *,'XI',(XI(I),I=1,7)
        DO 10 I4=1,NP
        READ (10,*) L6
        READ (11,*) I41
        READ (11,*) (TIM(I),I=1,I41)
        READ (11,*) (YMA(I),I=1,I41)
C*********************************
C       CALCULATE THE INFLUENCE COEFFICIENTS
C*********************************
        DO 60 I=1,I41
        A5=YMA(I)*DCOS(TIM(I))
        A6=YMA(I)*DSIN(TIM(I))
60      X1(I)=DCMPLX(A5,A6)
        NT=I41
        DO 11 J=1,I41
        T10=TW1*DCOS((3.1415D+0/4.0D+0))
        T11=TW1*DSIN((3.1415D+0/4.0D+0))
        XC(J,I4)=(X1(J)-XI(J))/DCMPLX(T10,T11)
11      CONTINUE
10      CONTINUE
C       THE INFLUENCE COEFFICENTS ARE THUS CALCULATED
```

```
C*********************************
C       CONJUGATE INF MAT.
C*********************************
        DO 15 I=1,NT
        DO 15 J=1,NP
        C1=DREAL(XC(I,J))
        C2=-1.0D+0*DIMAG(XC(I,J))
15      CXC(I,J)=DCMPLX(C1,C2)
C       CONJUGATE INF MAT. ARE THUS FORMED
C*********************************
        DO 20 I=1,NT
        DO 20 J=1,NP
20      CT(J,I)=CXC(I,J)
C       TRANSPOSE OF THE CONJUGATE MAT.
C*********************************
        DO 25 I=1,NP
        DO 25 J=1,NP
        CL(I,J)=DCMPLX(0.0D+1,0.0D+1)
        DO 25 K=1,NT
25      CL(I,J)=CT(I,K)*XC(K,J)+CL(I,J)
C       INVERT THE COMPLEX MATRICES
C*********************************
        DO 30 I=1,NP
        DO 30 J=1,NP
        T10=DCMPLX(-1.0D+0,0.0D+1)
        TI(I,J)=DCMPLX(0.0D+1,0.0D+0)
30      TI(I,I)=DCMPLX(1.0D+0,0.0D+1)
        N=NP
        IA=NP
        M=NP
        IB=NP
        IJOB=0
        DO 120 I=1,NP
        DO 120 J=1,NP
120     CLL(I,J)=CL(I,J)
        CALL LEQT1C(CL,N,IA,TI,M,IB,IJOB,WA,IER)
        DO 100 I=1,NP
        DO 100 J=1,NP
        DO 100 K=1,NP
100     PK(I,J)=TI(I,K)*CLL(K,J)+PK(I,J)
        DO 35 I=1,NP
        DO 35 J=1,NP
35      TI(I,J)=TI(I,J)*T10
        DO 36 I=1,NP
        DO 36 J=1,NT
36      ZC(I,J)=DCMPLX(0.0D+1,0.0D+1)
        DO 40 I=1,NP
        DO 40 J=1,NT
        DO 40 K=1,NP
40      ZC(I,J)=TI(I,K)*CT(K,J)+ZC(I,J)
        DO 45 I=1,NP
45      WC(I)=DCMPLX(0.0D+1,0.0D+1)
```

```
      DO 46 I=1,NP
      DO 46 J=1,NT
46    WC(I)=ZC(I,J)*XI(J)+WC(I)
      DO 622 I=1,NP
622   PRINT *,'WC',WC(I)
C*******************************
      OPEN(UNIT=52,FILE='WEIGHT',TYPE='NEW')
      WRITE (52,*) 'WEIGHT',(WC(I),I=1,NP)
      OPEN(UNIT=11,FILE='TW3.DAT',TYPE='NEW')
C*******************************
      DO 130 I=1,NP
      D1=(DREAL(WC(I)))**2
      D2=(DIMAG(WC(I)))**2
      D12=DREAL(WC(I))
      D22=DIMAG(WC(I))
      TW4(I)=DSQRT(D1+D2)
130   ANG(I)=DATAN(D22/D12)
C*******************************
C     COMPLEX BALANCE WEIGHT
C*******************************
      WRITE (11,*) NP
      WRITE (11,*) (WC(I),I=1,NP)
C*******************************
      PRINT *,'BALANCE WEIGHT',(TW4(I),I=1,NP)
      DO 135 I=1,NP
      ALL=ANG(I)*360.0/(2.0*3.1415)
135   PRINT *,'ANGLE',ALL
      STOP
      END
```

APPENDIX-F

UNBALANCE RESPONSE CALCULATIONS OF THE SINGLE ROTOR DISK

In the present investigation, two rotor disks were mounted on a rotor shaft which was supported by the fluid-film bearing. Bhat et al. [22] used a single rotor mounted at the middle of a rotor shaft with fluid-film bearings one at each end of the shaft as shown in Fig. F.1. The details of this system are given in Table F.1.

The maximum unbalance response of this system obtained by the package developed in the present investigation and those obtained in [22] are shown in Fig. F.1. As can be seen in this figure the agreement between both the results is very good. It should be noted that the dynamic equation of motion developed in [22] were using the lumped-parameter method whereas, in the present investigation, they have been developed using the finite element method.

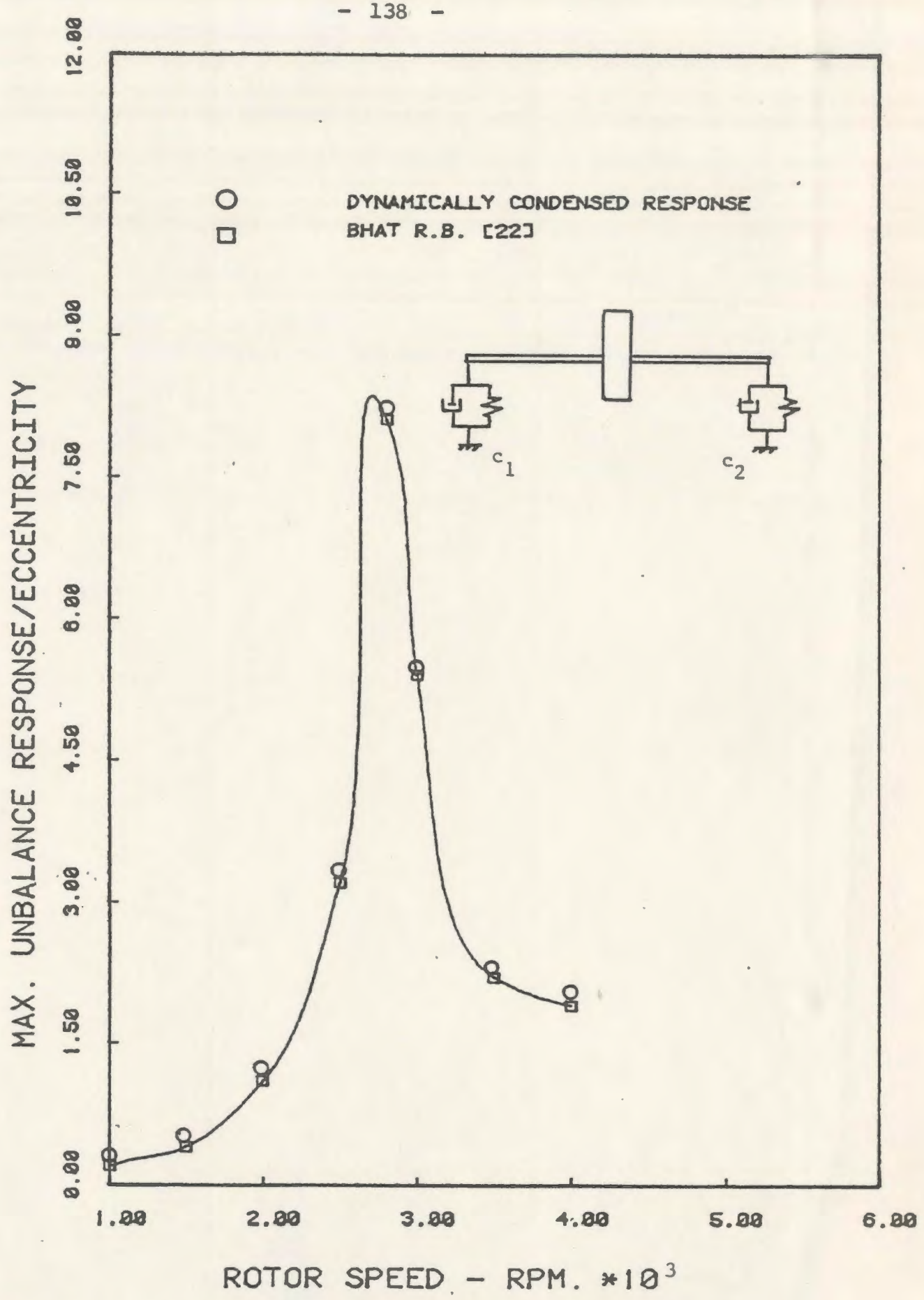

Fig. F. 1 The Unbalance Response of the Single Rotor Disk Mounted on Fluid-Film Bearings

Table F.1 Parameter Values of the Single Rotor Disk Bearing System

Disk Weight	116N
Type of Bearings	Plain Cylindrical
Bearing Diameter	0.0254 m
Bearing L/D Ratio	1
Viscosity of Oil at 25.5°C	0.0241 N.sec/m^2
Total Length of Rotor	0.5105 m
Modulus of Elasticity of Shaft	2.145×10^{11} N/m^2
Shaft Diameter	0.022 m
Disk Diameter	0.2032 m
Disk Eccentricity	1.084×10^{-4} Kg.m
Bearing Clearances	c_1=0.0000533m c_2=0.000188m